
Electronic Thesis and Dissertation Repository

7-31-2020 9:00 AM

Seeing the Invisible: An Integrated Remote Sensing Approach to Mapping Buried Architecture at Las Colmenas, Virú Valley, Peru

Kayla C. Golay Lausanne, *The University of Western Ontario*

Supervisor: Millaire, Jean-François, *The University of Western Ontario*

Joint Supervisor: Nelson, Andrew, *The University of Western Ontario*

A thesis submitted in partial fulfillment of the requirements for the Master of Arts degree in Anthropology

© Kayla C. Golay Lausanne 2020

Follow this and additional works at: <https://ir.lib.uwo.ca/etd>



Part of the [Archaeological Anthropology Commons](#), [Geographic Information Sciences Commons](#), and the [Remote Sensing Commons](#)

Recommended Citation

Golay Lausanne, Kayla C., "Seeing the Invisible: An Integrated Remote Sensing Approach to Mapping Buried Architecture at Las Colmenas, Virú Valley, Peru" (2020). *Electronic Thesis and Dissertation Repository*. 7244.

<https://ir.lib.uwo.ca/etd/7244>

This Dissertation/Thesis is brought to you for free and open access by Scholarship@Western. It has been accepted for inclusion in Electronic Thesis and Dissertation Repository by an authorized administrator of Scholarship@Western. For more information, please contact wlsadmin@uwo.ca.

Abstract

This thesis reports on the results of a survey project conducted in 2018 and 2019, intending to address two main research questions: (1) What remote sensing technique(s) worked best to identify buried features at Las Colmenas? (2) What combinations of techniques proved to be optimal for identifying buried features, and what are the benefits and limitations of the use of an integrated approach? This project incorporated two scales of analysis: macroscale optical and thermal Unmanned Aerial Vehicle (UAV) surveys and microscale Ground-Penetrating Radar (GPR), magnetic susceptibility, and magnetometry surveys. A side-by-side comparison proved the thermal UAV, GPR, and magnetic susceptibility surveys were most successful at Las Colmenas. However, by integrating these methods, we noted that a multi-faceted approach is indeed useful, but a small subset of these techniques can be used depending on funding, expertise, time available, environmental conditions, and goals of the project.

Keywords

Remote sensing, Archaeology, Integrated approach, Peru, Virú Valley, Gallinazo Group, Las Colmenas

Summary for Lay Audience

This research project employs five different remote sensing methods to assess the presence of buried structures without having to uncover them. The ancient urban settlement of Las Colmenas, on the north coast of Peru, is used as a case study. This project uses both thermal and optical drone surveys to assess the extent of the site and to document the ancient urban morphology of the settlement. Three geological survey methods are also used: Ground-Penetrating Radar (GPR), magnetic susceptibility, and magnetometry survey. These techniques identify buried structures based on physical differences caused by the composition of the features or past human activity. The first goal of this project is to assess which technique(s) were more successful at identifying buried structures at Las Colmenas. The second goal is to integrate the results of these techniques into a single cohesive dataset to determine which combination of techniques proved to be most optimal to identify buried features. As such, the benefits and limitations of an integrated approach are also addressed. By using a side-by-side comparison of the results from each technique, it is clear the thermal drone survey, GPR survey, and magnetic susceptibility surveys were the most successful in identifying buried architecture. By integrating the datasets into one single map, we noted that an approach that includes multiple techniques at once is advantageous, as it includes the different types of features each tool can identify. However, a smaller subset of techniques can be used depending on the goals of the project, as well as available funding and expertise, the portability of the equipment, the time available, and the environmental conditions of the survey area.

Acknowledgments

I would like to express my gratitude to my master thesis supervisors, Dr. Jean-François Millaire and Dr. Andrew Nelson. This project and my pursuit of Andean archaeology would not have been possible without Jean-François, whose undergraduate course showed me the beauty and wonders of Andean archaeology and led to my research in this area. His support and guidance throughout the creation, implementation, and writing of this project have been an invaluable asset. Andrew Nelson's feedback throughout this writing process has been insightful and thought provoking, which always challenged me to explore new avenues of thought.

This project would not have been possible without the funding and equipment provided through the Social Science and Humanities Research Council grant held by Dr. Millaire and equipment on loan from Sustainable Archaeology, London, Ontario. A big thank you to Lisa Hodgetts as well, for providing the magnetic susceptibility meter. Additionally, funding was also provided to me by the Social Science and Humanities Research Council and Ontario Graduate Scholarship. Funding from the Department of Anthropology at Western University was also most welcome.

Many people assisted with this project in 2018 and 2019, including Edward Eastaugh, Estuardo La Torre, Jeisen Navarro, Amedeo Sghinolfi, and Corey Hyland. More specifically, a huge thank you goes out to Edward Eastaugh for his consistent support with geophysical prospection. Ed's knowledge regarding geophysical surveys within an archaeological context was of critical importance to the success of this project. His help in the field and in the lab will always be appreciated. Estuardo La Torre and Jeisen Navarro's knowledge of the Peruvian landscape and archaeology was also critical for the interpretations of the results from this project.

Additionally, Amedeo Sghinolfi played an essential role in conducting these surveys at Las Colmenas, spending hours pulling the equipment on uneven terrain in the hot sun. Amedeo, who also shares a passion for Andean Archaeology, has always been a great source of guidance and second opinions both in the field and in Canada. Amedeo is

not only a colleague but also a great friend without whom I would not have been able to complete this thesis.

I cannot emphasize enough the importance of each member of the Department of Anthropology at Western played in the success of this project. Numerous members of the faculty and staff were instrumental in the completion of this thesis, special thanks to Laura Cousins, Edward Eastaugh, Lisa Hodgetts (as both a member of the department and as my project advisor), Jean-François Millaire, Andrew Nelson, and Christine Wall. Likewise, I would like to thank my examination committee members — Lisa Hodgetts, Peter Timmins, Mishal Pazner, and Randa Farah — for their constructive comments in my examination. Additionally, I would like to thank my friends in the department who always provided support, guidance, and fun times — Ricki-Lynn Achilles, Jillian Graves, Hilary Hager, Dallas Hauck, Alana Kehoe, and Amedeo Sghinolfi.

I would like to finish this acknowledgment by thanking my family, who have always supported my dream to become an archaeologist. Thank you to my parents, siblings, aunt and uncle, and grandparents, who have always encouraged me to explore my interests. This encouragement provided the foundation for my current accomplishments to date. Most notably, I would like to thank my partner, Asif Rajani, for his unconditional support through this project and over the last seven years. Thank you for your unwavering belief in my abilities and listening to my endless talks regarding dirt, rocks, and geophysics.

Table of Contents

Abstract.....	ii
Summary for Lay Audience.....	iii
Acknowledgments.....	iv
Table of Contents.....	vi
List of Tables.....	ix
List of Figures.....	x
List of Appendices.....	xvi
1 Introduction.....	1
1.1 Research Questions.....	4
1.2 Chapter Overview.....	5
2 Background.....	7
2.1 Virú Valley, the Gallinazo Group, and Las Colmenas.....	7
2.2 Previous research.....	11
2.2.1 Wendell Bennett.....	12
2.2.2 Gordon Willey.....	14
2.2.3 Heidy Fogel.....	15
2.2.4 Jean-François Millaire and team.....	15
2.3 Remote sensing.....	17
3 Aerial Surveys.....	20
3.1 Optical UAV Survey.....	23
3.1.1 Survey Workflow.....	24
3.1.2 Processing.....	27
3.1.3 Post-Processing.....	29

3.1.4	Ground-truthing	32
3.1.5	Trends	34
3.2	Thermal UAV Survey	36
3.2.1	Survey Workflow	40
3.2.2	Processing	41
3.2.3	Post-Processing	42
3.2.4	Ground-truthing	43
3.2.5	Trends	44
4	Ground-based remote sensing	46
4.1	Magnetic susceptibility	47
4.1.1	Survey Practice	51
4.1.2	Processing	53
4.1.3	Post-Processing	55
4.1.4	Ground-truthing	56
4.1.5	Trends	57
4.2	Magnetometer	59
4.2.1	Survey Workflow	61
4.2.2	Processing	63
4.2.3	Post-Processing	65
4.2.4	Ground-truthing	65
4.2.5	Trends	66
4.3	Ground-penetrating Radar	68
4.3.1	Survey Workflow	70
4.3.2	Processing	72
4.3.3	Post-Processing	75

4.3.4	Ground-truthing	76
4.3.5	Trends	77
5	Discussion	80
5.1	Individual technique assessment.....	80
5.2	Integrated technique assessment.....	90
5.2.1	Benefits and limitations of a multifaceted remote sensing approach	94
5.2.2	Conclusion	100
6	Conclusion	102
6.1	Future research.....	104
	References.....	106
	Appendices.....	113
	Curriculum Vitae	119

List of Tables

Table 5.1: Strengths and weaknesses of the remote sensing surveys techniques used in this project.....	87
Table 5.2: Type of features identified by each method	88
Table 5.3: Cost analysis of remote sensing techniques employed in this project.....	98
Table 5.4: Time to complete surveys for each remote sensing technique employed in this project	98
Table 5.5: Comparison of speed, cost and quality of results for each remote sensing technique employed in this project	99

List of Figures

Figure 1.1: Gallinazo Group (Millaire and Eastaugh 2011: 290)	3
Figure 1.2: Las Colmenas by Huaca Gallinazo (8°26'23.49"S 78°52'46.17"W).....	3
Figure 2.1: Virú Valley, Peru.....	7
Figure 2.2: Virú Valley and neighbouring valleys.....	8
Figure 2.3: Revised from Jordan Downey's (2014: 58) suggested period and their equivalent period names used by Virú Valley Project. Dates based on Millaire (2010), Quilter (2014), Willey (1953: 37), and Zoubek (1997).	9
Figure 2.4: Castillos in Virú Valley. Google Earth 2019	10
Figure 2.5: Virú polity region (Millaire et al. 2016).....	10
Figure 2.6: a Bennett's (1950: 51) map of Las Colmenas, A marks area of excavation; b Updated map of Las Colmenas, knolls labelled 1-7	12
Figure 2.7: Bennett's (1950: 52) excavation of Las Colmenas	13
Figure 2.8: Willey's (1953: 7) structure classification Revised	14
Figure 2.9: Electromagnetic spectrum (Revised from Campbell and Wynne 2011).....	18
Figure 3.1: World-View 3 image of Gallinazo Group and surrounding area	21
Figure 3.2: NDVI of the Gallinazo Group	22
Figure 3.3: NDVI of the Gallinazo Group reclassified.....	22
Figure 3.4: Visible range of electromagnetic radiation spectrum (Revised from Campbell and Wynne 2011).....	24
Figure 3.5: Drone survey plan (Revised from Casana et al. 2017).....	25

Figure 3.6: Vegetation comparison. (a) UAV survey 2018 - 9:30. (b) UAV survey 2019 – 14:30	26
Figure 3.7: (a) UAV survey prior to surface activity. (b) UAV survey post surface activity	27
Figure 3.8: Optical survey. Left - Orthomosaic; Right - derivative of the DEM	28
Figure 3.9: Optical orthomosaic overlaid on DEM	29
Figure 3.10: Digitized optical orthomosaic	30
Figure 3.11: False-colour orthomosaic	31
Figure 3.12: Crop mark comparison. Left - True colour; Right – False colour.....	31
Figure 3.13: Soil mark comparison. Left - True colour; Right- False Colour	32
Figure 3.14: Ground-truthed areas.....	33
Figure 3.15: HP-1. Left - Optical imagery; Right - Shovel shining results	33
Figure 3.16: HP-2. Left - Optical imagery; Right - Shovel shining results	34
Figure 3.17: Optical imagery walls in vegetation versus soil.....	35
Figure 3.18: Infrared section of electromagnetic radiation spectrum (Revised from Campbell and Wynne, 2011)	36
Figure 3.19: Electromagnetic radiation spectrum - Infrared region (Revised from Campbell and Wynne, 2011)	37
Figure 3.20: Thermal emission of adobe in sand matrix. Left - after sunrise; Right - after sunset. Revised from Casana et al. (2017).....	39
Figure 3.21: Thermal emission after sunrise of adobe in a sand matrix with topographic variations. Revised from Casana et al. (2017)	40

Figure 3.22: Thermal 1300 orthomosaic.....	42
Figure 3.23: Digitized thermal survey	43
Figure 3.24: HP-1. Left - Thermal survey; Right - Shovel shining results.....	44
Figure 3.25: HP-2. Left - Thermal survey; Right - Shovel shining results.....	44
Figure 4.1: Magnetic field direction variations (Revised from Wiltschko and Wiltschko 1995:2)	48
Figure 4.2: Magnetic oxides mineral conversion (Revised from Aspinall et al. 2009)....	50
Figure 4.3: Barrington MS3 susceptibility meter with an MS2D surface scanning probe. Photo by Edward Eastaugh.	51
Figure 4.4: Magnetic susceptibility broad-interval survey points at Las Colmenas.....	52
Figure 4.5: Magnetic susceptibility close-interval survey grids	53
Figure 4.6: Magnetic susceptibility broad-interval – (a) without clipping; (b) with clipping	54
Figure 4.7: Broad-interval magnetic susceptibility in classes – (a) outputted results; (b) cropped to site	55
Figure 4.8: Fine-interval magnetic susceptibility survey. Left - Results; Right - digitized	56
Figure 4.9: HP-1. Left - Magnetic susceptibility; Right - Shovel shining results	57
Figure 4.10: HP-2. Left - Magnetic susceptibility; Right - Shovel shining results	57
Figure 4.11: Low value walls with high value inside.	58
Figure 4.12: One feature (a) with high and low values.....	58

Figure 4.13: Magnetometer operational modes: (A) Single, (B), differential, (C) gradiometer (revised from Aspinall et al. 2009).....	61
Figure 4.14: Bartington Grad601-2 dual-sensor Fluxgate Gradiometer. Photo by Edward Eastaugh.....	61
Figure 4.15: Magnetometer grid system of survey area	62
Figure 4.16: Grids 2-5: (a) Prior to any editing; (b) after zero-mean traverse.....	63
Figure 4.17: Grids 2-5: (a) -1 to 1 Stand deviation; (b) -3 to 3 Stand deviation.....	64
Figure 4.18: Processed magnetometer grids	64
Figure 4.19: Digitized magnetometer results.....	65
Figure 4.20: HP-1. Left - Magnetometer features. Right - Shovel shining	66
Figure 4.21: HP-2. Left - Magnetometer features. Right - Shovel shining	66
Figure 4.22: Magnetometer results with features offset from urban grid.....	67
Figure 4.23: Potential hearths identified in magnetometer results; Left - Location on site, Right - Close up	68
Figure 4.24: Main components of ground-penetrating radar (adapted from Annan 2005).	69
Figure 4.25: Noggin 500® with a SmartTow configuration. Photo of Edward Eastaugh by Kayla Golay Lausanne.....	71
Figure 4.26: GPR Grid.....	72
Figure 4.27: GPR forward parallel survey; Transect always starts on Y axis and is parallel to X axis	72
Figure 4.28: GPR hyperbola formation (Adapted from Ristić et al. 2017)	73

Figure 4.29: (a) Unprocessed results; (b) Migration applied; (c) Dewow and envelope applied.....	74
Figure 4.30: Grid 12: (a) saturation 70%, contrast 20%; (b) saturation 40%, contrast 20%	74
Figure 4.31: Final processed images of GPR survey 0-10cm.....	75
Figure 4.32: Digitized GPR results.....	75
Figure 4.33: HP-1. Left - GPR results; Right - Shovel shining	76
Figure 4.34: HP-2. Left - GPR results; Right - Shovel shining	76
Figure 4.35: (a) GPR results from Huaca Gallinazo (Millaire and Eastaugh 2014); (b) GPR results from Las Colmenas.....	78
Figure 4.36: (a) area prior to vegetation removal (2018); (b) after vegetation removal (2019); (c) GPR results (2018)	79
Figure 5.1: (a) Optical UAV survey; (b) Thermal UAV survey.....	82
Figure 5.2: Aerial survey digitization comparison. (a) Optical UAV survey; (b) Thermal UAV survey	82
Figure 5.3: Aerial survey comparison, vegetation versus soil. (a) Optical UAV survey; (b) Thermal UAV survey.....	83
Figure 5.4: Comparison of ground-based remote sensing surveys.....	83
Figure 5.5: Comparison of all surveys over the same grid	85
Figure 5.6: Comparison of GPR, magnetic susceptibility, and thermal UAV survey results	86
Figure 5.7: Various integrations of remote sensing results.....	92

Figure 5.8: (a) Comparison of thermal with GPR results; (b) thermal with magnetic susceptibility results..... 93

List of Appendices

Appendix 1: Optical Survey 2018-14:20	113
Appendix 2: Optical Survey 2018-9:30	114
Appendix 3: Optical Survey 2019-14:30	115
Appendix 4: Crops growing along buried walls, HP-1	116
Appendix 5: Salt in the field beside Las Colmenas	116
Appendix 6: Thermal survey 2018-10:45	117
Appendix 7: Thermal survey 2018-13:00	118

1 Introduction

The use of remote sensing and geophysical prospection for surveying and mapping landscapes is becoming increasingly popular in archaeology. In Peru, these techniques have been instrumental in large scale surveys aimed at identifying archaeological sites, as well as small-scale analysis and architecture mapping projects. Various geophysical techniques, such as Ground-Penetrating Radar (GPR), magnetometer, magnetic susceptibility, and resistivity, have been implemented to map buried archaeological features in Peru and elsewhere around the world. These techniques have proven to be useful in the identification of such features, but also in diminishing the destructive impact of archaeology by reducing the need for excavation. Research projects often incorporate remote sensing techniques to create detailed maps of subterranean structures and identify the complex characteristics of buried urbanized sites. These maps provide information regarding the urban morphology of the sites or the form of human settlements and their formation and transformation processes through time (Nor and Noor 2014).

In recent years, archaeologists have begun to incorporate different methods of remote sensing within one context. Research has shown that comparative studies of different remote sensing techniques, which often include a side-by-side examination of the results, allow for informative comparisons (Clark 2003; Gaffney and Gater 2003; Weymouth 1986). Advances in Geographical Information Systems (GIS) have also offered archaeologists the ability to integrate multiple data sets into visually powerful displays. The use of integrated remote sensing approaches in archaeology has rapidly grown in the last 20 years, as archaeologists have started to see the potential of incorporating multi-scale and multi-sensor equipment (Capizzi et al. 2007; Casana, Herrmann and Fogel 2008; Drahor 2006; Drahor et al. 2009; Gaffney et al. 2004; Leucci, Giorgi and Scardozzi 2014). This combination of multiple techniques has proven useful for providing confirmatory, complementary or new information regarding subsurface features. The present work demonstrates the advantages of combining multiple remote sensing methods across different scales of analysis.

This project provides an opportunity to test the potential of different remote sensing techniques on a single archaeological site, advancing our understanding of remote sensing in archaeology. This project incorporates macro and micro level remote sensing — macro-level aerial surveys and micro-level geophysical surveys. This includes an optical Unmanned Aerial Vehicle (UAV) survey, a thermal UAV survey, a magnetic susceptibility survey, a magnetometer survey, and a GPR survey. Concurrently, these techniques help document early urbanism and land use as part of a minimally destructive investigation. This research project explores the potential of a multifaceted approach, which integrates a variety of remote sensing techniques to study urban life at the archaeological site of Las Colmenas. This information will enhance our knowledge of remote sensing techniques by documenting the benefits and limitations of each technique while assessing the efficacy of applying multiple techniques in the same area. I hypothesize that a multifaceted approach is required to obtain the maximum amount of information for many archaeological contexts. However, different projects will have different goals (e.g. rapid vs detailed assessment). Those goals will determine which techniques are best suited for the project.

In order to understand the need to use several remote sensing techniques to document a single site, this research project implemented five remote sensing techniques at an archaeological site on the north coast of Peru known to be an early center of urbanism. The earliest early urban centers in the Andes started to develop on the north coast of Peru in the 3rd century prior to the Common Era (Millaire 2020) and remained a prominent feature of lifeways in this region until the Spanish Conquest (Millaire and Eastaugh 2011). Work by Jean-François Millaire and his team from Western University has documented incipient urbanism in the Virú Valley, where the Virú culture spread across the entire valley floor. They have also examined the emergence of urban life at the polity's capital city, the Gallinazo Group, on the northern edge of the lower valley floor (Figure 1.1).

The Gallinazo Group is a large settlement believed to have been the capital of the Virú state, between 100 B.C. and 700 A.D. (Millaire and Eastaugh 2011). It consists of over 30 mounds, the largest of which is Huaca Gallinazo (V-59), where most of the

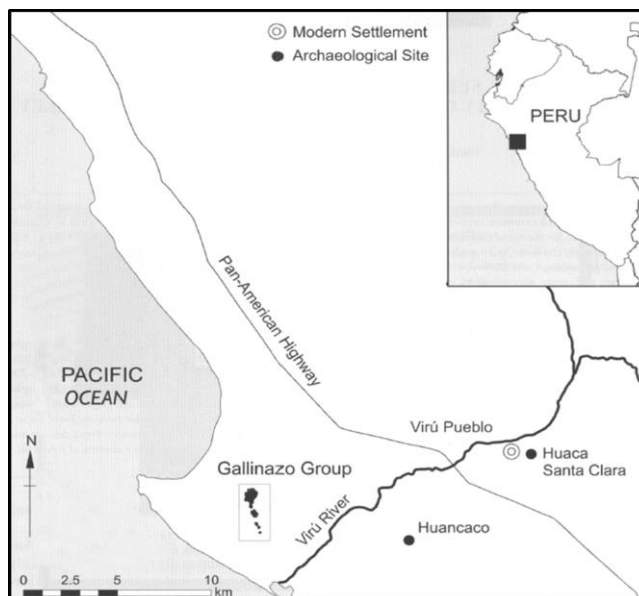


Figure 1.1: Gallinazo Group (Millaire and Eastaugh 2011: 290)

team's previous work was carried out. Huaca Gallinazo is surrounded by numerous smaller mounds, which likely consisted of physically detached neighbourhoods of the greater city. One of these mounds is a dwelling site known as Las Colmenas. Until now, this site has been referred to as V-157 following Willey's 1953 catalogue, but we have come to call this site Las Colmenas due to the presence of modern-day beehives on the site. V-157 is thus referred to as Las Colmenas throughout this paper. Apart from excavations by Bennett (Bennett 1950) in the area now covered in beehives, Las Colmenas is still intact, making it an exceptional area to study the urban layout of a neighbourhood through remote sensing.

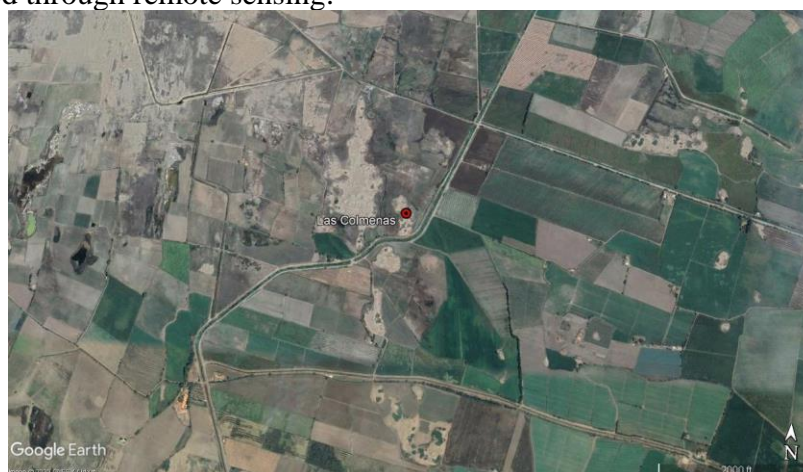


Figure 1.2: Las Colmenas by Huaca Gallinazo ($8^{\circ}26'23.49''S$ $78^{\circ}52'46.17''W$).

The Gallinazo Group has been the focus of intensive studies in the last decade by Jean-François Millaire and his team (Millaire and Eastaugh 2011, 2014; Millaire 2016). Millaire and his team have aimed to address the significant gap of information regarding the emergence of state and urban life on the northern coast of Peru during the Early Intermediate period (100 B.C.–A.D. 700) (Millaire and Eastaugh 2011). These projects have been primarily focused on Huaca Gallinazo, where a combination of remote sensing and excavation has been used to infer state organization, population size and urban design. This research project acts as a small component of this overall research scheme by providing results that can lead to a greater understanding of urbanization within the Gallinazo Group. The results of these surveys will document the urban design of a suspected neighbourhood of the large city and reveal any differences or similarities with the city's core, Huaca Gallinazo.

1.1 Research Questions

It has been well documented that multiple remote sensing surveys offer improved datasets and subsequent interpretations regarding subsurface archaeological structures (Capizzi et al. 2007; Gaffney and Gater 2003; Millaire and Eastaugh 2011, 2014). Van Leusen (2001: 575) argues when multiple archaeology surveys are integrated into a single dataset, “the whole... is larger than its constituent parts.” However, several studies of archaeological sites that have incorporated multiple remote sensing techniques present their datasets side-by-side, not as a single cohesive dataset. While this method is beneficial, there is more information available through the integration of datasets. The increase in popularity and streamlining of Geographic Information Systems (GIS) software has allowed the integration of multiple sets of remote sensing data into one combined dataset. This is a common but effort-intensive approach used by archaeologists (Gaffney et al. 2000; Buteux et al. 2000) to integrate diverse avenues of data collection. This project provides a broad integration of remote sensing datasets within one archaeological context, with the goal being to document the benefits of using a multifaceted approach. This research project uses widely known prospection methods, however incorporates a different way of visualizing remote sensing results to enhance our documentation of buried archaeological features.

This thesis reports on the results of a survey project conducted in 2018 and 2019, with the goal to address two main research questions: (1) What technique(s) worked best to identify buried features at Las Colmenas? (2) What combinations of techniques proved to be optimal for identifying buried features, and what are the benefits and limitations of the use of an integrated approach?

Each of the five remote sensing techniques employed in this research project offers specialized insight into the nature of the buried archaeology. However, some methods may not work as well as others in this sandy environment due to the varying environmental phenomena affecting the results of each method, and the physical requirements the methods require to document features. By providing the results of each method side-by-side, we can create a comparison to understand which techniques identified more features at Las Colmenas and can suggest which techniques would be best suited for future work on futures of this nature within a similar matrix. Subsequently, by integrating the datasets of each method, we can create a probable architectural plan, including structural characteristics and location of various occupational features at Las Colmenas. By integrating various sets of data, we can assess to what extent multiple techniques provide new information regarding the buried features at Las Colmenas. This integration of datasets will inform us of the benefits and limitations of a multifaceted remote sensing approach to archaeological fieldwork. In addition, future work using the results of this project can then shed new light on the use of urban space at this site.

1.2 Chapter Overview

The second chapter of this thesis provides an overview of the archaeological context of the Gallinazo Group, including previous archaeological work in the Virú Valley. Additionally, this chapter provides a brief background of remote sensing in archaeology. The third chapter addresses the aerial-based surveys used in this project, including optical and thermal UAV surveys. This chapter will cover the method of implementation, post-processing, and the results of the aerial surveys. Similarly, chapter 4 is an overview of all ground-based remote sensing surveys employed for this project, including the magnetic susceptibility, magnetometer and ground-penetrating radar

surveys. Each subsection will cover survey workflows, post-processing, and results. Chapter 5 uses the results of the five techniques to address the research goals of this project. Finally, Chapter 6 discusses final remarks and avenues for future research in remote sensing as well as at the Gallinazo Group.

2 Background

This chapter outlines the cultural and geographic context of Las Colmenas and provides an overview of the Virú Polity's settlement patterns. It also highlights previous work conducted at the Gallinazo Group and at Las Colmenas. Finally, this chapter presents a brief history of remote sensing work in archaeology.

2.1 Virú Valley, the Gallinazo Group, and Las Colmenas

The Virú Valley is a river valley oasis located on the coastal desert of northern Peru (Figure 2.1). The Virú Valley is situated south of the much larger Moche Valley, and north of Chao Valley (Figure 2.2). The Virú Valley stretches from the Pacific coastline to the Andean foothills, ranging from zero to ~ 130 meters above sea level (m.a.s.l.), before branching into two upper valleys – the Carabamba and Huacapongo valleys.

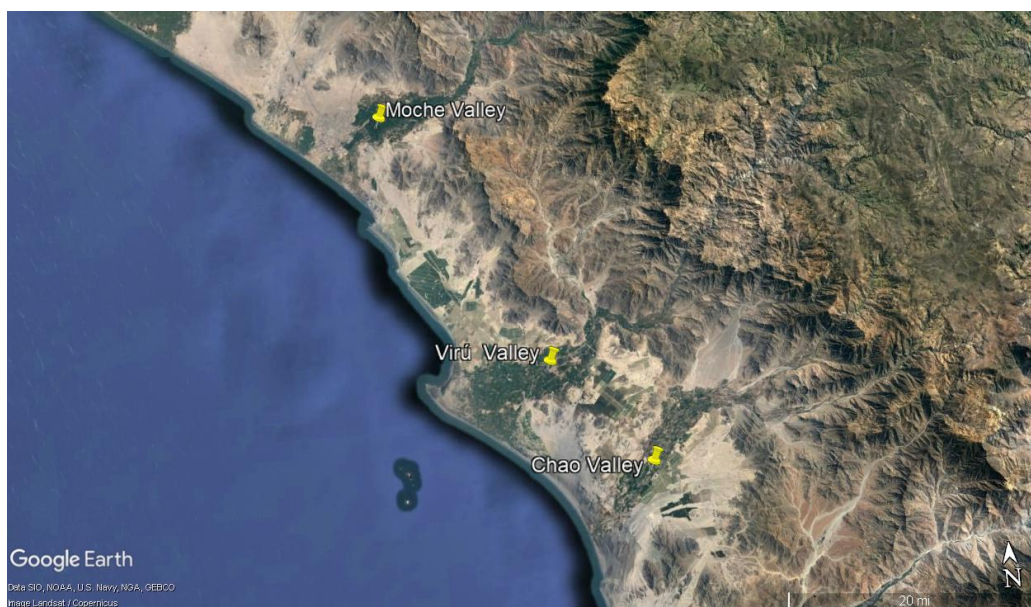


Figure 2.1: Virú Valley, Peru

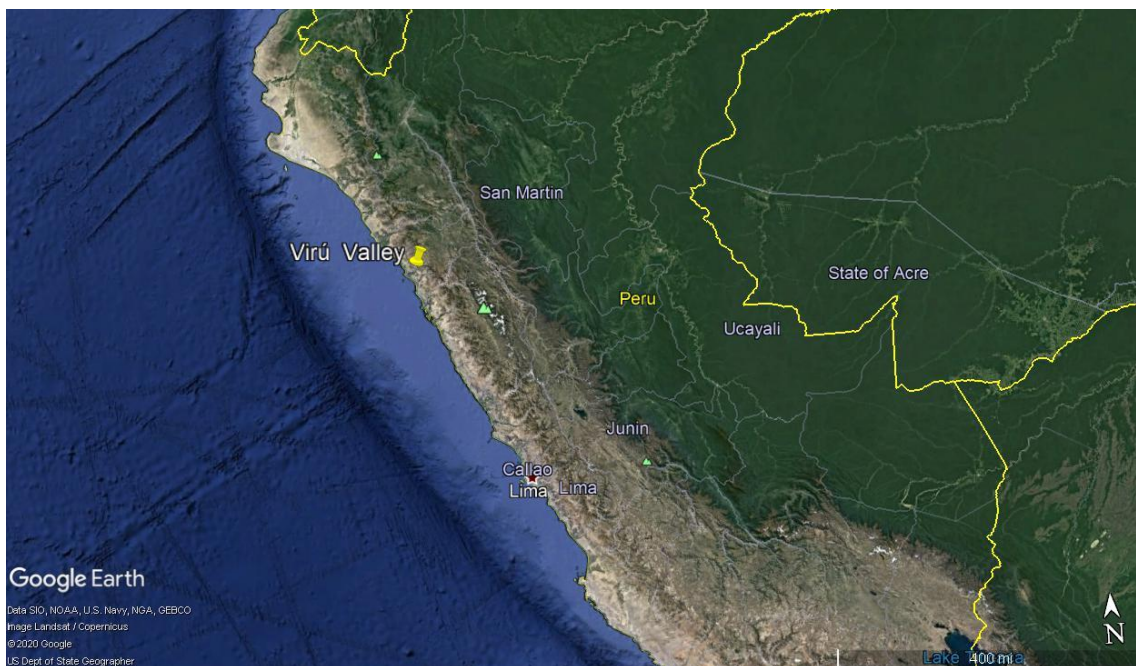


Figure 2.2: Virú Valley and neighbouring valleys

Due to the rich environment and relatively consistent access to water, the Virú Valley has a long history of occupation throughout Prehispanic times. During the Early Intermediate Period (EIP), the valley remained a focal point for the emergence of local traditions, coastal trends, urban development, statecraft, and expansionary dynamics. The primary focus of research within the EIP on the North Coast has been on the Moche Period (ca. A.D. 100-700), but research by Millaire (Millaire 2010) found the Virú period (ca. 200 B.C. - A.D 600) to represent a key moment for understanding the development of early urbanism and statecraft in the Andes (Downey 2014).

This research project is based on the updated Virú Valley ceramic sequence presented by Jordan Downey (2014). According to Downey, the Virú Valley was home to a state-level society, known as Virú, which occupied multiple settlements spread over the entire valley floor between 400 B.C. to A.D. 750 (Downey 2014). He argues that the Virú Polity occupied the territory during three phases of this period, originally believed to represent three distinct cultural manifestations. Indeed, Downey (2014) sees clear historical continuity from the Early Virú to the Middle and Late Virú phases (roughly

corresponding to the Puerto Morin, Gallinazo and Huancaco phase of earlier scholars (Figure 2.3) (Ford 1949; Ford and Willey 1949).

Period	VVP Equivalent	Approximate Date Range
Late Epoch	Estero	A.D. 1470 – 1532
	La Plata	A.D. 1100 – 1470
	Tomaval	A.D. 750 – 1100
Late Virú	Huancaco	A.D. 600 - 750
Middle Virú	Gallinazo/Virú	200 B.C. – A.D. 600
Early Virú	Puerto Morin	400 – 200 B.C.
Guañape	Guañape	1200 – 400 B.C.
Cerro Prieto	Cerro Prieto	? – 1200 B.C.

Figure 2.3: Revised from Jordan Downey’s (2014: 58) suggested period and their equivalent period names used by Virú Valley Project. Dates based on Millaire (2010), Quilter (2014), Willey (1953: 37), and Zoubek (1997).

The Virú Polity incorporated a large irrigation network, allowing for agriculture in an arid desert. This network is protected by large castle-like structures (*castillos*) located near the valley neck, believed to have served to defend the canal system and perhaps control the distribution of water in the coastal plain. The Virú Polity architectural schema includes large monumental structures and integrates public spaces within and beyond residential sectors. This Polity was most likely led by an elite group in control of the land and people, residing at the Gallinazo Group or at other major settlements.

The Virú Polity includes six *castillos* (Figure 2.4), located at the valley neck, likely built to control the water canal intakes. By considering the irrigated agriculture, and the large administrative architecture, Millaire suggests the Virú Polity was ruled by a highly centralized elite (Millaire 2010). Evidence of diagnostic ceramics from other valleys suggests the Virú Polity was an expansionist state, with outposts along the coast in the Moche and Chicama valleys (Millaire et al. 2016). According to Millaire and colleagues (2016), those outposts suggest that at one point, the Virú Polity could have controlled a substantial area of coastal desert in the region (Figure 2.5).

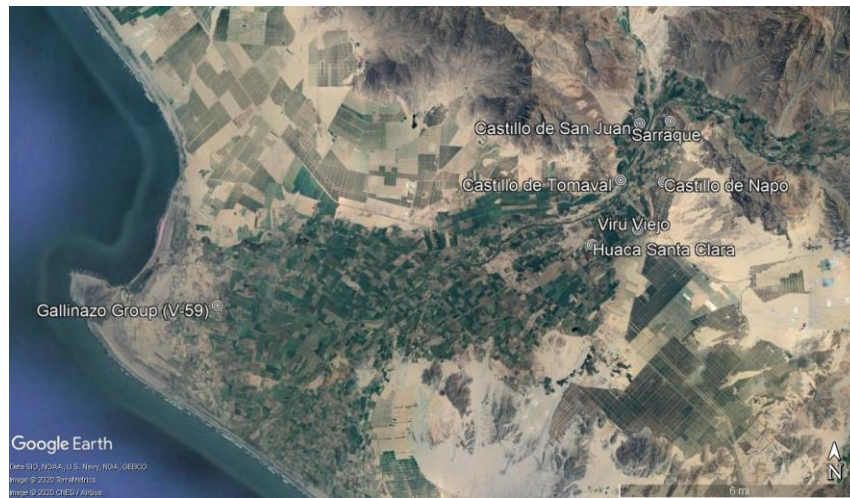


Figure 2.4: Castillos in Virú Valley. Google Earth 2019

The capital city of the Virú Polity was likely the Gallinazo Group (Figure 1.1), where Millaire and his team have conducted work over the past decade. This settlement dates from the Middle Virú phase and features some thirty architectural mounds spread across ~40 ha. The mounds are raised platforms from the accumulation and continuous superimposition of construction material and refuse, sitting on sand dunes (Millaire and Eastaugh 2011). The Gallinazo Group is estimated to have had a population ranging from 10,000-14,000 individuals (Millaire and Eastaugh, 2011). The largest and tallest mound of the group, believed to represent the city core, is Huaca Gallinazo. It features a large public space, a 25 m tall civic-ceremonial pyramid, and a large residential sector (Bennett

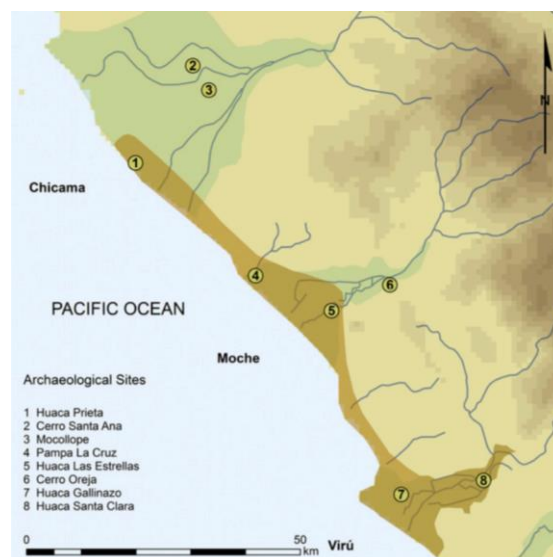


Figure 2.5: Virú polity region (Millaire et al. 2016)

1939; Millaire 2009; Millaire and Eastaugh 2011; Millaire 2010). The remaining architectural mounds in this group consist of smaller residential and/or civic-ceremonial sites. The Gallinazo Group relied on irrigation agriculture, traces of which are still visible in the field systems surrounding the mounds (Millaire and Eastaugh 2014)

This research project focused on a mound called Las Colmenas, located 50m away from Huaca Gallinazo. This site was previously labelled as V-157 (Bennett 1950) but was re-named Las Colmenas because of the presence of beehives (*colmenas* in Spanish) on a section of the mound. Las Colmenas measures ~179m in the N-S axis and ~88m in the E-W axis, with six knolls across the surface. These knolls are a mix of house-clusters and solid adobe platforms likely used for administrative or ceremonial purposes. Minimal work had previously been conducted at Las Colmenas, with only a small excavation done in the 1940s (Bennett 1950), making this an ideal site to pursue this research project.

2.2 Previous research

Prior to the 1930s, few research projects were carried out in the Virú Valley, but all this changed with Wendell Bennett, who undertook work in the lower valley in 1936 (Bennett 1939) and carried out excavations at Huaca Gallinazo. Some years later, other North American scholars pursued research in the region, a collaborative research program known as the Virú Valley Project. The key figures of the Virú Valley Project were James Ford, Gordon Willey, Wendell Bennett, Clifford Evans, William Strong, and Donald Collier. The goal of this multi-institution project was to analyze the cultural history and prehistory of the occupation of the valley (Bennett 1950; Collier 1955; Ford and Willey 1949; Strong and Evans 1952; Willey 1953). Subsequently, the Gallinazo Group site was left untouched until the 1990s, when Heidi Fogel undertook archaeological fieldwork at the Huaca Gallinazo. Jean-François Millaire and his team later revisited the site and spent over a decade studying Huaca Gallinazo (Millaire and Eastaugh 2011, 2014; Millaire, Golay Lausanne and Eastaugh 2018). In recent years, Millaire and his team surveyed other sites within the Gallinazo Group and elsewhere in the valley, as a means to understand the Virú occupation of the region.

2.2.1 Wendell Bennett

The earliest archaeological research at the Gallinazo Group was carried out by Wendell Bennett (Bennett 1939). The goal of Bennett's project was to identify and investigate mounds within the Gallinazo Group. Bennett conducted his survey in 1936 and 1946, studying twenty sites within the settlement. He produced topographic maps for twelve sites and carried out excavations at eight of those and test pits at four others. Outside these twelve sites, only one other had test pitting done, and the remaining seven only had the collection of surface ceramics (Bennett 1950). Bennett (1950) divided these twenty sites into three groups based on their morphology: (1) raised platforms, habitation knolls, and true pyramids, (2) platforms and habitation knolls, but not pyramids, and (3) earth mounds. Due to the presence of platforms and habitation knolls, Las Colmenas was classified into the first category. Bennett's drawing of the site indicates six knolls on the surface of the mound; however, they did not include one of the largest knolls on the site, which is located in the southeast corner of the mound (Figure 2.6a). The final count of knolls at Las Colmenas thus becomes seven (Figure 2.6b).

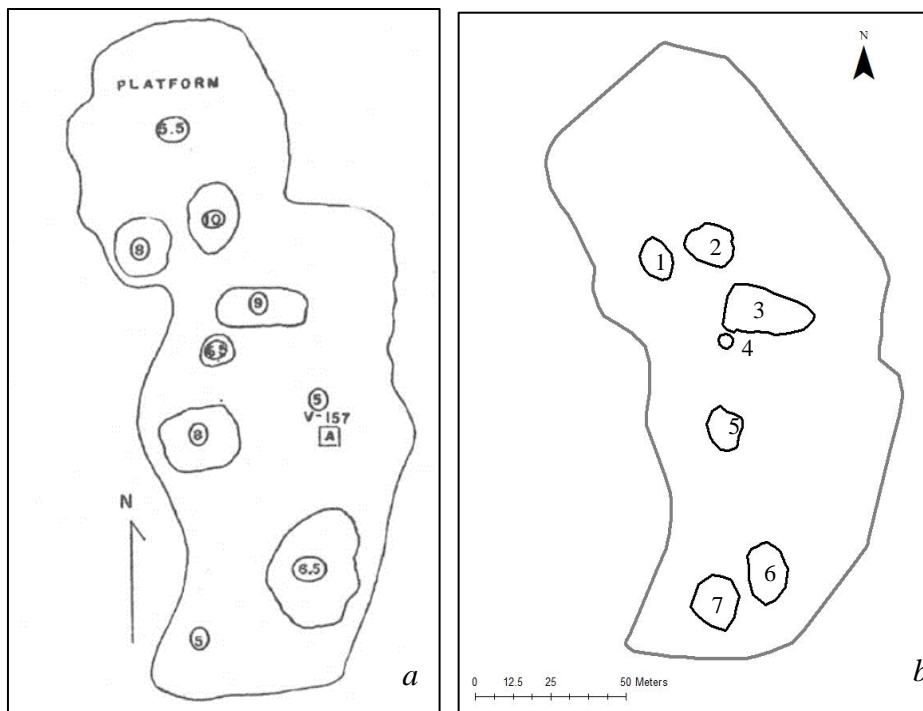


Figure 2.6: a Bennett's (1950: 51) map of Las Colmenas, A marks area of excavation; b Updated map of Las Colmenas, knolls labelled 1-7

Bennett conducted a 20 square meter excavation at Las Colmenas in a low-lying area of the site (Figure 2.6a, label A). The excavation revealed five floors of occupation, with numerous walls, rooms, and a gallery (Figure 2.7). A single child burial was found at the end of the gallery; this child was found inside an inverted jar (*olla*) with two other vessels, as well as gold pincers (Bennett 1950). The vessels featured Virú Negative decoration.

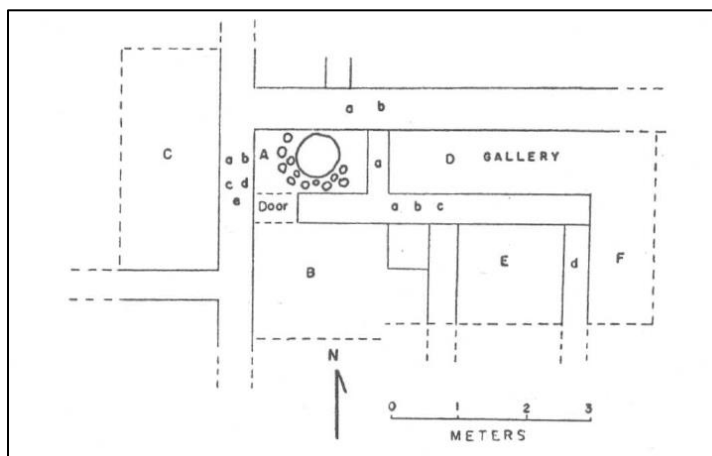


Figure 2.7: Bennett's (1950: 52) excavation of Las Colmenas

Bennett (1950) noted three different construction styles through time, defined as Gallinazo I, Gallinazo II, and Gallinazo III. Gallinazo I, the earliest, is characterized by the use of *tapia* walls. *Tapia* is the process of pouring clay into frames that were subsequently removed once the clay had dried, leaving a solid block of clay. These walls are often thick and built up over time. Gallinazo II period walls were made with conical-shape adobes, placed side by side, in alternating directions; clay was used to fill the gaps. The last phase, Gallinazo III, is characterized by cane marked adobe, which is the use of cane moulds to produce adobe bricks. Adobe bricks are made from clay and silt minerals (mud) most likely found here in riverbeds and irrigation canals. Along with the mud, adobes are often mixed with organic matter, such as hay, which acts as temper. Once the mud is pushed into a form, they are left to dry in the sun. According to Bennett (1950), this trend was consistent across Gallinazo Group sites, including Huaca Gallinazo and Las Colmenas.

2.2.2 Gordon Willey

As a member of the Virú Valley project, Gordon Willey provided a seminal study of settlement patterns in the Virú Valley (Willey 1953b). Willey's work provided the basis for many interpretations among north coast specialists. The goals of Willey's settlement pattern investigation were four-fold: to describe prehistoric sites with reference to geographic and chronological position, to reconstruct the development of the function and sequence of the sites, to reconstruct cultural institutions, and finally to compare the settlement patterns of the Virú valley with other regions in Peru (Willey 1953). Willey, alongside James Ford, visited 300 sites in the Virú Valley, where detailed maps of each site were made (Willey 1953). In addition, Willey used early military aerial photographs to identify 315 sites across the valley and map several of these (Willey 1953). Willey created a classification scheme based on the function of each site: 1) living sites, 2) community/ceremonial structures, 3) fortified strongholds or places of reuse, and 4) cemeteries (Willey 1953). Classifications one through four were subsequently broken down into subdivisions to provide a more detailed analysis of each site (Figure 2.8).

I.	Living sites:
	Scattered Small-House Village
	Agglutinated Villages:
	Irregular
	Regular
	Semi-isolated Large House
	Compound Village:
	Rectangular Enclosure
	Great Rectangular Enclosure
	Rambling Enclosure
II.	Community and ceremonial structures:
	Community Building
	Pyramid Mound
	Pyramid-Dwelling-Construction Complex
III.	Fortified strongholds or places of refuge
	Hilltop Redoubt
	Hilltop Platform
	Hilltop Village (Agglutinated)
	Castillo Fortification Complex
IV.	Cemeteries

Figure 2.8: Willey's (1953: 7) structure classification Revised

Following Bennett's classification, Willey lists Las Colmenas as a site with both community and ceremonial structures, more specifically as a pyramid-dwelling-

construction complex. Any site within the classification features dwellings or similar structures, in immediate association with a platform or pyramid structure. Willey (1953) notes that the platforms are generally created on top of old house structures or other rooms filled in to serve as the substructure. Fourteen mounds within the Gallinazo Group fall into this classification, including Huaca Gallinazo.

2.2.3 Heidi Fogel

As part of her doctoral dissertation work in the 1990s, Fogel (1993) studied the Virú occupation on the north coast of Peru, including the Gallinazo Group, through reanalysis of previous work done by the Virú Valley Project as well as an analysis of ceramics from the Moche, Virú, and Santa Valleys (Fogel 1993). Fogel examined the development of social complexity during Virú occupation, arguing the Virú Polity was the first Andean state to cover multiple valleys with the Gallinazo Group site as the urban capital (Fogel 1993). Fogel did not visit Las Colmenas but instead reexamined Bennett's (1939) analysis of the site. She argued the burial evidence suggests social differentiation, as the child was located with gold pincers and an abundance of vessels, which has been a consistent marker of socioeconomic status across Virú and Moche valley sites (Fogel 1993).

2.2.4 Jean-François Millaire and team

Throughout the latter half of the 2000s, Jean-François Millaire undertook field research on the Gallinazo Group. His work has supported the notion of a Virú Polity, including the expansionary dynamics of this polity (Millaire et al. 2016). Millaire's research at the Gallinazo Group has mainly focused on excavation and geophysical surveys of Huaca Gallinazo. Various surveys were carried out by Millaire and his team in 2008, 2009, and 2011. These surveys included excavations at Huaca Gallinazo, as well as using high-precision differential GPS to produce an accurate 3D model of the site. After clearing the top layer of sand (shovel shining) to reveal buried architecture, the GPS was used to document features to incorporate into the site map (Millaire and Eastaugh 2011). 2008 fieldwork included field walking, testing pitting, and the use of a core sampler with

the goal to identify if the urban city of Huaca Gallinazo continued beyond the boundaries of the raised mound, into the lower fields (Millaire and Eastaugh 2011). Fieldwalking and test pitting supported the idea that Huaca Gallinazo was confined to the mound.

Additionally, the core sampling appeared to confirm the urban settlement is isolated to the raised mound. However, a deeply buried settlement could not be ruled out (Millaire and Eastaugh 2011). In addition, the 2009 field season saw the use of a magnetometer to map buried archaeological features across Huaca Gallinazo, covering a total of 22,500 m² (Millaire and Eastaugh 2011). This survey was particularly successful at identifying large walls dividing individual compounds and some deeply buried walls. The survey did not locate all features when compared to excavation and shovel shining results, but the survey confirmed an abrupt end to the settlement at the edge of the mound, further supporting the results of test pitting, fieldwalking, and the coring survey. Based on a combination of excavation, shovel shining, and magnetometry, Millaire was able to argue the city once held a population of 10,000 to 14,400 people (Millaire and Eastaugh 2011).

During the 2008 and 2009 field seasons, radiocarbon samples were collected to understand the chronology of this site. This research proved that there was a long sequence of uninterrupted occupation of Huaca Gallinazo, in both the residential and civic sectors of the site (Millaire 2010). These radiocarbon dates placed Gallinazo Group's occupation from the beginning of the first century BC to the seventh century A.D. (100 B.C. - 700 A.D.) (Millaire and Eastaugh 2011).

In 2011, Millaire and his team employed a ground-penetrating radar (GPR) survey in areas previously surveyed by the magnetometer to assess the effectiveness of the techniques (Millaire and Eastaugh 2014). A total of 5,600 m² were surveyed. The GPR revealed the presence of numerous residential compounds with walls following similar orientation and bordered by thicker walls (Millaire and Eastaugh 2014). While the residential and civic structures followed a general north-south alignment, there is no clear evidence of centralized planning, leading Millaire to argue the construction and maintenance of individual compounds followed a semi-orthogonal block design, as previously described by Michael Smith (Smith 2007; Millaire and Eastaugh 2014). This urban design describes individual compounds abutting neighbouring compounds, creating

an urban design which is produced by the actions of individual builders making additions to previously existing rectangular houses (Millaire and Eastaugh 2014; Smith 2007)

Millaire's research has also included aerial surveys of Huaca Gallinazo, identifying numerous features across the surface of the site, well beyond the area previously surveyed (Millaire, Golay Lausanne and Eastaugh 2018). In recent years, Millaire and his team have moved beyond Huaca Gallinazo to use aerial surveys at other mounds within the Gallinazo Group. This included visual-spectrum and thermal-spectrum unmanned aerial vehicle (UAV) surveys of mounds V-153, V-152, V-154, V-163, V-303, V-155 and V-156. These surveys tested the benefits of using remotely sensed data, as well as provided information regarding neighbourhood and urban development throughout the Gallinazo Group.

2.3 Remote sensing

Remote sensing, as defined by Lillesand, Kiefer, and Chipman (2015: 1) is “the science and art of obtaining information about an object, area, or phenomenon through the analysis of data acquired by a device that is not in contact with the object, area, or phenomenon under investigation.” This is a sweeping definition that encompasses x-rays, the vision of the human eye, ultrasound, sonar, etc. Remote sensing targets numerous scales, from the Earth itself down to an individual cell. Remote sensing is a three-pronged project consisting of a target, a data acquisition technique, and the data analysis. The processes all vary depending on the technique used. Remote sensing works by measuring electromagnetic energy through sensors. These sensors are employed for data acquisition; sensors can be attached to an aircraft, satellite, balloon, and drone (UAV). But there are also non-photographic sensors, such as a radiometer, radar systems, electro-optical sensors, etc. The electromagnetic energy is reflected, transmitted, or emitted by the target and is recorded by the sensor(s). Remote sensing was first made possible with the creation of photography in 1839 (Myers and Myers 1995). Remote sensing works by measuring electromagnetic radiation (EMR). EMR is all energy that moves at the velocity of light in a wave pattern (Khorram et al. 2012). Visible light, microwaves, x-rays, ultraviolet, radio waves, infrared, and gamma rays complete the electromagnetic

spectrum (Figure 2.9). This spectrum comprises both frequency and wavelength- the different forms of EMR can be determined from these factors. When EMR interacts with matter, it can either be absorbed, reflected, scattered, emitted EMR by the matter, or transmitted EMR through the matter (Khorram et al. 2012). What allows remote sensing to work is that every object has a spectral signature, which is a particular emission and/or reflectance property. The sensors collect these signatures.



Figure 2.9: Electromagnetic spectrum (Revised from Campbell and Wynne 2011)

There are two different types of remote sensors: passive and active. Passive sensors, such as aerial imagery, record naturally occurring electromagnetic radiation reflected or emitted from the target (Khorram et al. 2012). Active sensors, such as a Ground-Penetrating Radar, create and emit electromagnetic radiation waves toward the target and record how much of it is reflected (Jensen 2005). Additionally, remotely sensed data can be described by resolution; the resolution is the maximum separation of the power of a measurement (Richards 2013). There are four types of resolution: spatial, spectral, temporal, and radiometric. Spatial is the fineness of an image, i.e. the pixel size. The spectral resolution is measured by the wavelength interval or the number of spectral bands (i.e. blue, red, green, etc.) (Richard 2013). Temporal resolution is the time it takes for the sensor to meet a target, and radiometric resolution is the brightness sensitivity of the sensor (Khorram et al. 2012). These resolutions are essential for understanding data selection and interpreting results. By combining resolution with a sampling frequency (how often data is collected), different types of remote sensing become possible.

Remote sensing is used to increase our visibility range — we can see much more, either at a large scale, an invisible spectral scale, or even buried features. Remote sensing has been used to monitor the stress of vegetation, environment quality, detect and identify catastrophic sites, crop production, water storage, water table levels, population growth, living conditions, and so much more. Remote sensing work is becoming increasingly

popular in archaeology. Around the beginning of the twentieth century, archaeologists adopted the use of aerial photography to visualize archaeological sites from a bird's eye view (Sever 1995). Archaeology during WWI experimented with aerial photography to document and locate archaeological sites, and in 1931 the first use of a photographic balloon was conducted to record an excavation (Myers and Myers 1995). From here, increased quality and greater detailed imaging became possible, including the creation of thermal imaging. As technology advanced, so did our ability to measure the entirety of the electromagnetic spectrum, thus giving archaeologists the ability to capture images of buried features.

Various remote sensing techniques have been employed across numerous archaeological contexts, and many projects incorporate multiple types of remote sensing methodology, just as Millaire and his team have done at Huaca Gallinazo. The last two decades have seen a rapid increase in the integration of multiple remote sensing techniques within a single context (Capizzi et al. 2007; Casana, Herrmann and Fogel 2008; Drahor 2006; Drahor et al. 2009; Gaffney et al. 2004; Leucci, Giorgi and Scardozzi 2014). Las Colmenas provides a unique opportunity to assess the capabilities of five different remote sensing techniques at a single site, which has had minimal impact from previous research or pedestrian activities. Previous remote sensing research has confirmed the capabilities of these techniques in the coastal desert environment of Peru.

3 Aerial Surveys

Archaeologists have traditionally been keen to adapt technologies developed in other fields of science to better understand ancient sites and landscapes and to strive for a genuinely sustainable archaeological science. Archaeological site stratigraphy, taphonomy, landscape survey, and radiocarbon dating are among the better-known techniques adapted to the field of archaeology from other fields, as is aerial archaeological survey, a technique adapted from aviation and geography. This section outlines the aerial surveys carried out as part of this project.

The last 100 years have seen a substantial increase in accessibility, precision, and expediency in the acquisition of aerial images. These images allow for the identification of large features that are often too large, discontinuous, or faint to be detected at ground level. Aerial survey is the method of acquiring imagery of a landscape by using an airborne vehicle, such as an Unmanned Aerial Vehicle, kite, balloon, airplane, or satellite, equipped with a camera (Mastelic et al. 2020). Depending on the camera used, the survey can target specific regions of the electromagnetic spectrum and thus produces different types of information.

As part of our aerial survey work, a multispectral survey was conducted over the entire surface of the Gallinazo Group site through the purchase of a satellite-derived dataset. Multispectral imaging is the process of capturing images within a specific wavelength range across the electromagnetic spectrum. This includes the visible spectrum and beyond to the infrared region (Brivio, Pepe and Tomasoni 2000). For the purpose of this project, the multispectral analysis analyzed the visible region (VIS), consisting of red, green and blue (RGB) wavelengths, and the near-infrared region (NIR). A single satellite-derived multispectral dataset (World-View 3) of the area encompassing the Gallinazo Group was acquired, which included the VIS and NIR bands (Figure 3.1). Multispectral analysis manipulates the spectral bands to produce new images; a popular



Figure 3.1: World-View 3 image of Gallinazo Group and surrounding area

manipulation process is a normalized difference vegetation index (NDVI). The NDVI measures the greenness or relative health of a plant. Plants absorb solar radiation and re-emit it within the near-infrared spectral region (Myneni et al. 1995). By using a ratio of near-infrared and red light recorded for each pixel, we can see if plants are stressed or dead. This stress would result in lower green value and an increase in yellow, which reflects significantly less in the near-infrared region (Myneni et al. 1995). This technique is useful in archaeology because of structures buried below the surface cause stress on overlaying plants, creating variations in the colour of surface plants or even an absence of vegetation. This stress and lack of vegetation can be mapped with the NDVI process.

By applying this process to the image of the Gallinazo Group, we are able to identify known archaeological sites as well as undocumented sites (Figure 3.2). Since the region has been irrigated, the majority of the land consists of agricultural fields. However, areas of archaeological interest are often raised features from hundreds of years of occupation, known as mounds, that are built on top of natural sand dunes (Millaire and Eastaugh 2011). In addition to being raised, these mounds have minimal vegetation and thus stand apart from the agricultural fields. Likewise, when there is vegetation, it is not

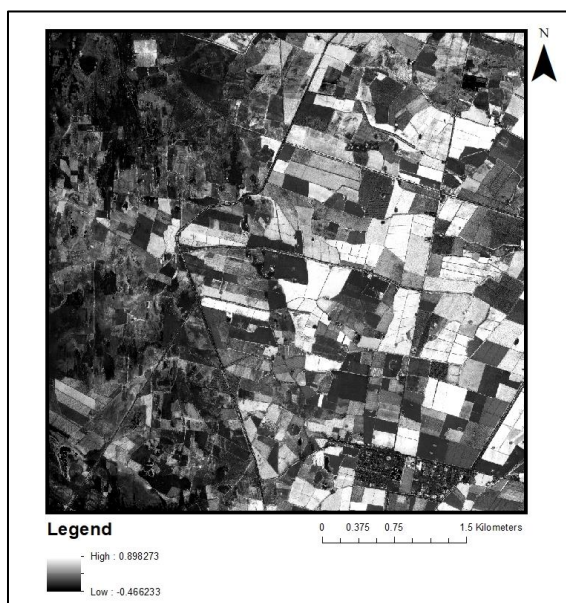


Figure 3.2: NDVI of the Gallinazo Group



Figure 3.3: NDVI of the Gallinazo Group reclassified

as abundant as the agricultural fields, and it often consists of bushes and smaller plants. In NDVI images, values from -1.0 to 0.01 represent ‘no vegetation,’ 0.1001 to 0.2 represents ‘sparse vegetation,’ and 0.2001 to 1.0 represents ‘high vegetation’ (Weier and Herring, 2000). By reclassifying these categories to generic values, such as 1 through 3, each class represents the entire range of values, making each category easily identified in the map (Figure 3.3). This does generalize the image and variations amongst the values; however, it allows us to pinpoint vegetation easily. By using this analysis, multiple potential sites are found, as well as sites previously noted by Wendell Bennett’s (Bennett 1950) survey of The Gallinazo Group. While multispectral image analysis holds great potential in archaeology (Powlesland et al. 2006; Winterbottom and Dawson 2005), the resolution of satellite-derived imagery is usually not good enough for urban archaeology. While multispectral cameras for Unmanned Aerial Vehicles (UAVs) existed when this study was carried out, none could be used for the survey at Las Colmenas.

Higher-resolution optical and thermal imagery were acquired through UAV surveys of the Las Colmenas site, as well as numerous other mounds within the Gallinazo Group. As previously mentioned, the different cameras used can impact the spectral information gathered; in this case, the optical cameras record information in the visible

range (VIS), whereas the thermal camera captures information in the far-infrared (FIR) region. This gave us two different datasets to document the architecture of Las Colmenas.

Both datasets require a form of post-processing known as photogrammetry. The American Society for Photogrammetry and Remote Sensing defines photogrammetry as “the science and technology of obtaining spatial measurements and other geometrically reliable derived products from photographs” (Lillesand, Kiefer and Chipman 2015: 146). Photogrammetry is the process of rebuilding a scene based on a series of overlapping photographs. This process requires the acquisition of successive individual images (orthoimages) of an object or landscape and the subsequent combination of these images to create one larger image (orthomosaic) of that object or landscape, either rendered in 2D or in 3D. While the processes associated with the optical and thermal surveys are similar, the cameras used and in-field workflows differ, which is why the surveys are discussed individually below.

3.1 Optical UAV Survey

The optical survey was conducted with a DJI Inspire 1 UAV, which can be fitted with different cameras. The optical camera employed for this survey came with the UAV; this is the Zenmuse X3, which has a 20 mm lens. The optical camera records the visible (VIS) light range of the electromagnetic spectrum (Figure 3.4). This is a relatively small portion of the spectrum but is essential to remote sensing. The visual spectrum camera is crucial in archaeology because the bird’s eye view makes soil and crop marks more prominent. Plant growth is not homogeneous above structures buried below the ground, producing what are known as crop marks. Where there is no vegetation, the structures often appear lighter than the surrounding soil, producing what are known as soil marks. These markings are what allow archaeologists to record the morphology of an ancient settlement without having to excavate it. That being said, not all below-ground features will be visible on the surface through crop or soil marks.



Figure 3.4: Visible range of electromagnetic radiation spectrum (Revised from Campbell and Wynne 2011)

3.1.1 Survey Workflow

The optical survey at Las Colmenas followed UAV workflows prescribed by Federman et al. (2017), Casana et al. (2017), and Nex and Remondion (2014):

- 1) The UAV should fly at 30 meters over the highest point of the site; likewise, the flight path should remain at one consistent elevation.
- 2) Flight paths should maintain a linear pattern with approximately 70% front overlap and 60% side overlap between images.
- 3) The UAV should take images at two different camera orientations: plan (90° downwards) and oblique (45° downwards) if a digital elevation model (DEM) is required.
- 4) UAV speed should not exceed 3-4m/s.

The UAV takes multiple successive images of a scene that are subsequently stitched together using software; in this case Agisoft Metashape Pro. This process relies heavily on how the survey was conducted, including speed, overlap, height, camera angle, number of transects, etc. (Figure 3.5). An essential characteristic to consider for determining the success of a survey during field application is resolution. The resolution of an image is based on the quantity and quality of the individual pixels - a large quantity and/or small pixels create a high-resolution image, whereas a small quantity and/or large

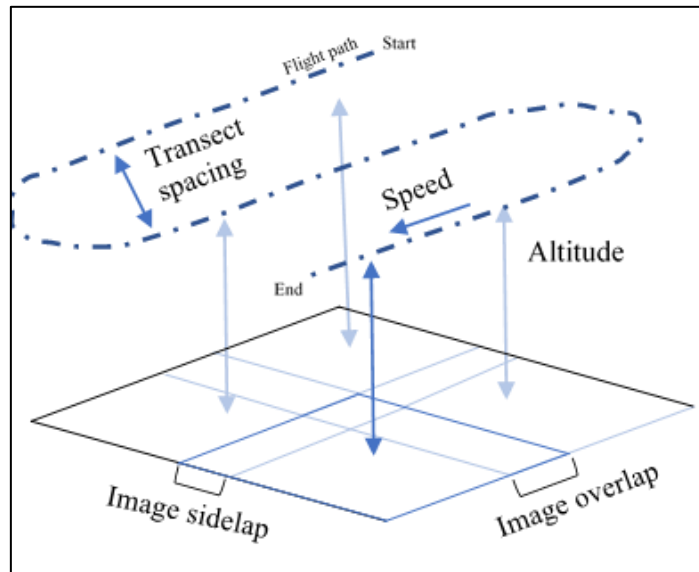


Figure 3.5: Drone survey plan (Revised from Casana et al. 2017)

pixels create a low or poor resolution image. By keeping the UAV height at 30m at 3-5.1m/s, we can capture high-resolution images at 1.3 cm (in other words, each pixel of the picture captured 1.3 cm of the site's surface). Another critical parameter is overlap; the individual images are 'stitched' together by having common points (called tie points) between successive images. The more tie points that exist, the better the accuracy of the image's 'stitch.' Agisoft recommends a minimum of 4,000 tie points; anything greater is ideal for small objects and increased accuracy. The photogrammetry processes produce 3-dimensional images of the area, which allow us to accurately assess the topography of a site in relation to architecture. This process is done by the creation of a digital elevation model (DEM). To create a DEM, the same survey area needs to be covered twice with a camera angle alternating from 90° to 45°. This captures the topography of the site, which allows the software to produce the 3D representation of the area. The optical UAV surveys conducted at Las Colmenas closely followed these survey parameters.

Prior to taking off, flight paths were created using Google Earth and DJI Go software to ensure consistent overlap, height, and site coverage. Due to varying weather conditions during the day, as well as the change in solar azimuth angle, two surveys were performed during the 2018 field season. These were done on two different days and times of day: 14:20 on day 1 (2018-14:20) (Appendix 1) and 9:30 on day 2 (2018-9:30) (Appendix 2). 2018-14:20 was chosen as it allowed ample time after the sun had risen and clouds cleared for the soil to heat up. 2018-9:30 was chosen to see the impact of

cloud cover on the optical imaging, as it was immediately after the sun had risen, when there was still cloud cover. While conducting other ground-based field surveys, vegetation was cleared off the surface of the site to allow the remote sensing equipment to pass uninterrupted. Due to this, a third survey was conducted in 2019, at 14:30 (2019-14:30), to see how vegetation growth over a year would influence crop and soil marks (Appendix 3). The short growth time for the vegetation enhanced the appearance of some vegetation marks in areas that were previously cleared; however, the vegetation growth was slower in other regions, making it nearly impossible to identify features (Figure 3.6). This made the results of the 2019-14:30 survey inconsistent and not very useful in mapping the architecture. The light conditions were ideal during the 2019-14:30 survey for the detection of crop marks. However, this also washed out the colour variations used to identify soil marks.

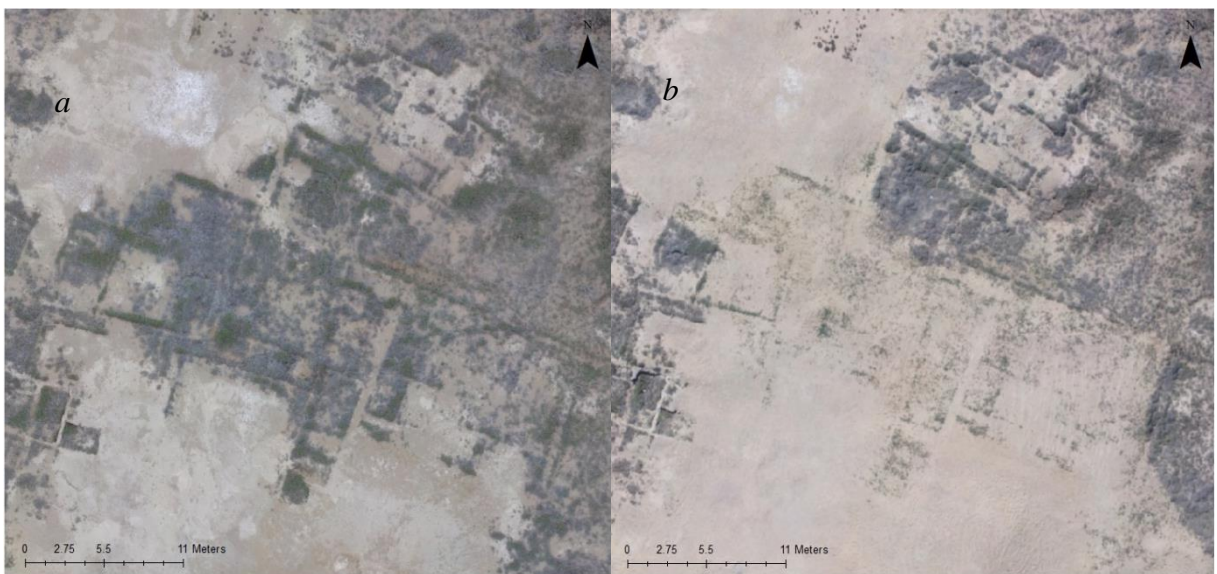


Figure 3.6: Vegetation comparison. (a) UAV survey 2018 - 9:30. (b) UAV survey 2019 – 14:30

Another noteworthy factor influencing the results of UAV surveys is pedestrian activity on the surface of the site, which we found greatly affected the visibility of soil marks. The 2019-14:30 survey was conducted after ground-based remote-sensing work took place, which resulted in increased soil movement and thus minimized our ability to see soil marks (Figure 3.7). Due to these conditions, the 2018-9:30 flight was used to

map the soil and crop marks of Las Colmenas, as it was captured prior to ground-based surveys, had no vegetation removal, and there was slight cloud cover allowing for increased visibility of soil marks.

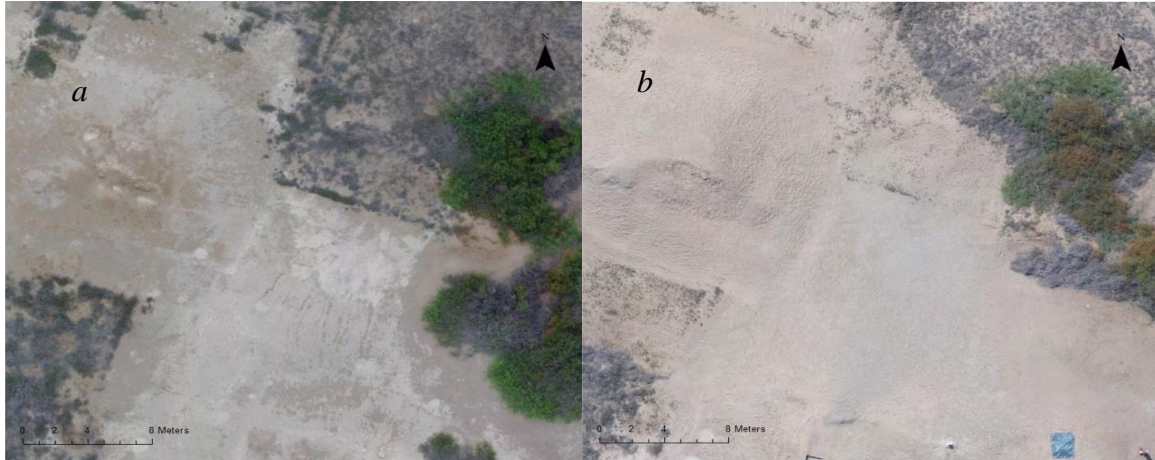


Figure 3.7: (a) UAV survey prior to surface activity. (b) UAV survey post surface activity

3.1.2 Processing

The following information is based on the use of the 2018-9:30 survey, as it proved to be ideal for mapping the buried architecture of Las Colmenas. The survey covered a total of 52,300 m² in 17:38 minutes, with a 1.3cm resolution, with the camera angle set to 90°. An additional survey was conducted over a 28,300m² area in 09:52 minutes, with the camera angle set at 45°. The total survey time then equals 27:30 minutes. A total of 363 photographs were obtained, which include 226 photos at 90° and 137 photos at a 45° angle from the ground surface. The images were processed through Agisoft Metashape Professional Edition v. 1.5.0 to produce an orthomosaic - a single rectified, georeferenced image, which is a conglomerate of the 360 individual orthoimages taken with the UAV. All image processing followed the workflow outlined by the Agisoft Metashape’s User Manual. The orthoimages were processed as a single group (chunk) to create a single orthomosaic. The first stage in creating an orthomosaic is known as “camera alignment”, in which the software searches for tie points between images and aligns the photos in their relative position. Subsequently, a “dense point cloud” is produced, which is a set of 3-D points that follow the shape and topography of

the site. The dense point cloud for this orthomosaic contained 1,298,984 tie points. Once the point cloud was made, two filtering processes called projection accuracy and reconstruction uncertainty were applied to the cloud to reduce errors. Projection accuracy errors occur when there is poor localization accuracy of a point projection, such as false matches. To filter out any projection accuracy errors, tie points with a projection value higher than one were removed. Reconstruction uncertainty occurs when points deviate from the object's surface; these occur more frequently on the edges of a set of images as there are fewer points in common. Any tie point with a reconstruction uncertainty greater than ten was filtered out. After these filter processes were applied, 276,526 tie points were left in the point cloud, subsequently being used to produce a three-dimensional image. The final orthomosaic and DEM were produced based on the tie points and the mesh (Figure 3.8). The orthomosaic and the DEM can be used together to produce 3D perspectives of the site. This is done by placing both images in ESRI's ArcScene software and 'draping' the orthomosaic on the DEM, which then renders the aerial imagery in 3D (Figure 3.9).

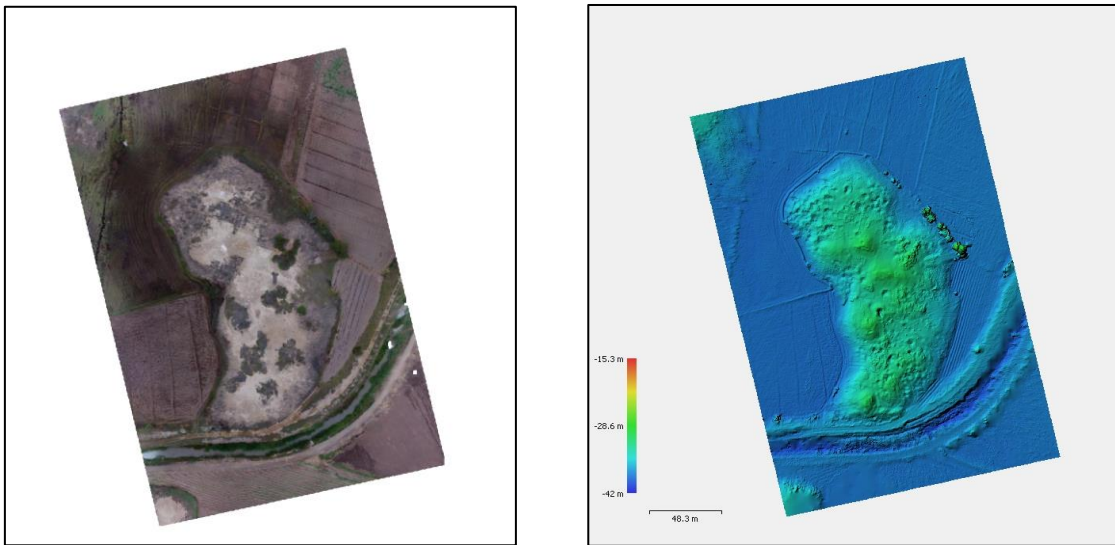


Figure 3.8: Optical survey. Left - Orthomosaic; Right - derivative of the DEM

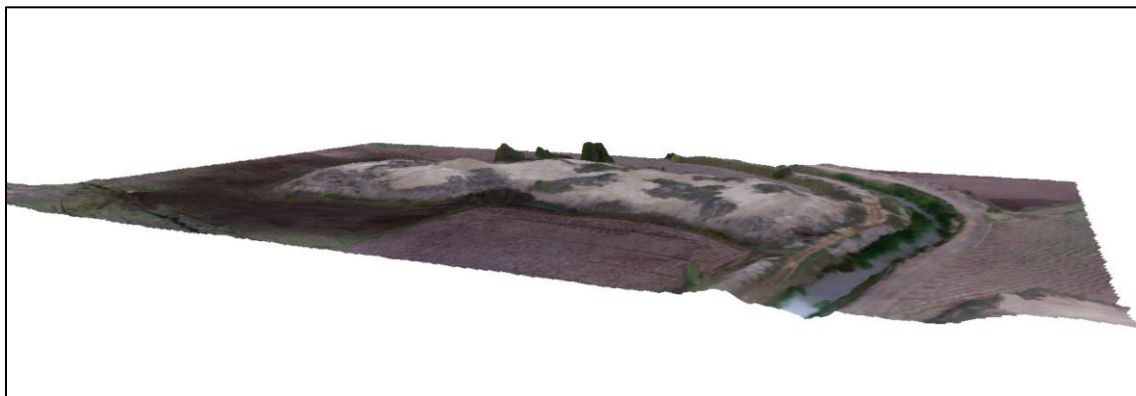


Figure 3.9: Optical orthomosaic overlaid on DEM

3.1.3 Post-Processing

Following the production of the orthomosaic, the crop and soil marks were digitized to produce an architectural map of the site. Digitization was carried out using ESRI's ArcMap v.10.4 software. The digitization focused on identifying walls buried below the site's surface by outlining walls with polylines (a connected sequence of line segments that denotes an individual object in ArcMap). Here, individual wall faces were outlined (walls were therefore represented by four polylines) to render each wall's thickness, which varied across the site. The following parameters were set for recording walls:

- 1) Differential growth of vegetation on the surface of Las Colmenas is mapped as walls, due to subsurface archaeological features.
- 2) Differential colours of soil on the surface of Las Colmenas are mapped as walls, due to subsurface archaeological features.
- 3) Walls visible on the surface of Las Colmenas are mapped as walls.

After following these steps, a final digitized map of the optical UAV survey was created (Figure 3.10). A benefit of working in a digital environment is the ability to manipulate images to produce additional products that aid in the process of identifying archaeological features.

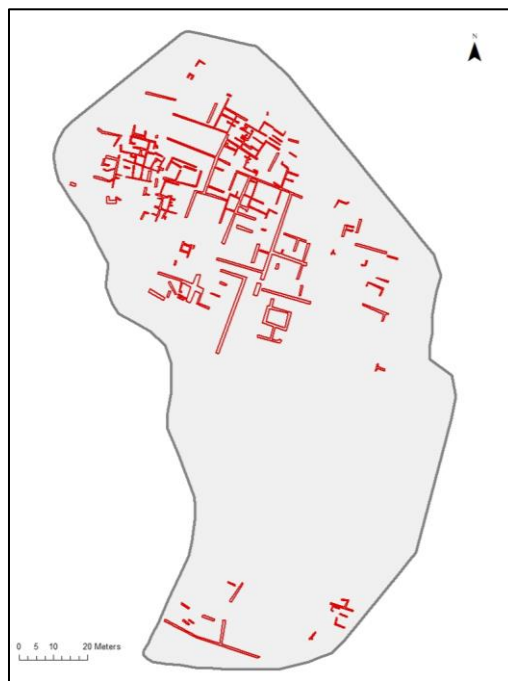


Figure 3.10: Digitized optical orthomosaic

After digitizing the optical UAV survey orthomosaic, the image was altered in ArcMap to produce false colour images in which the contrast, brightness, and/or the colour bands were changed to highlight certain features and aid in image interpretation. These images are produced by applying a ‘Stretch’ to the image; the stretch is where values of a single colour band are displayed across a ramp, or series of colours (for example, the red band in a visual image is displayed from white to deep red) (ESRI 2019). Instead of using the original red, green and blue bands of visual images, false colour images use other predefined ramps that better outline certain features within an image.

The false colour image found to be the most useful for the optical UAV imagery uses a stretched colour ramp across band 1, the red band. In this case, a linear stretch called “minimum-maximum’ is applied, which stretches a band based on the maximum and minimum pixel values for the given band, increasing the ability to see contrasts within the single dataset. The colours used for this ramp are yellow and purple (the values for the band go from deep yellow to white to deep purple), a contrast that proved to be the most useful in identifying archaeological features (Figure 3.11). In this case, areas of

vegetation are yellow, whereas soil areas are purple. Crop marks are highlighted as they appear as purple, greatly contrasting with the yellow vegetation. Compared with the original orthomosaic, the crop marks are more clearly visible on the false colour image (Figure 3.12), but the most remarkable differences are the soil marks, which are significantly more visible than on the original image (Figure 3.13). The final digitization for the optical UAV survey combined results from both the false colour and original orthomosaic. This created a map with the maximum number of features identified.

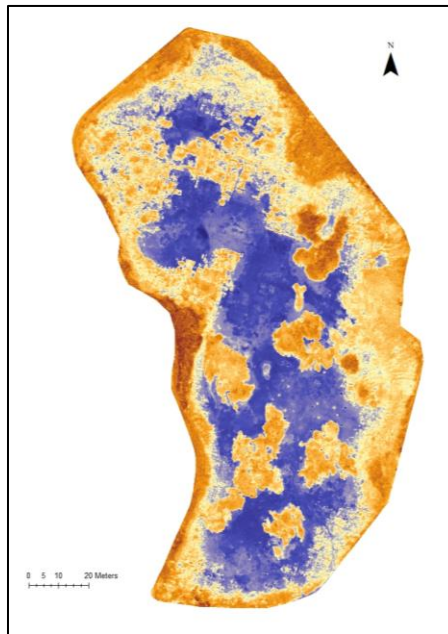


Figure 3.11: False-colour orthomosaic

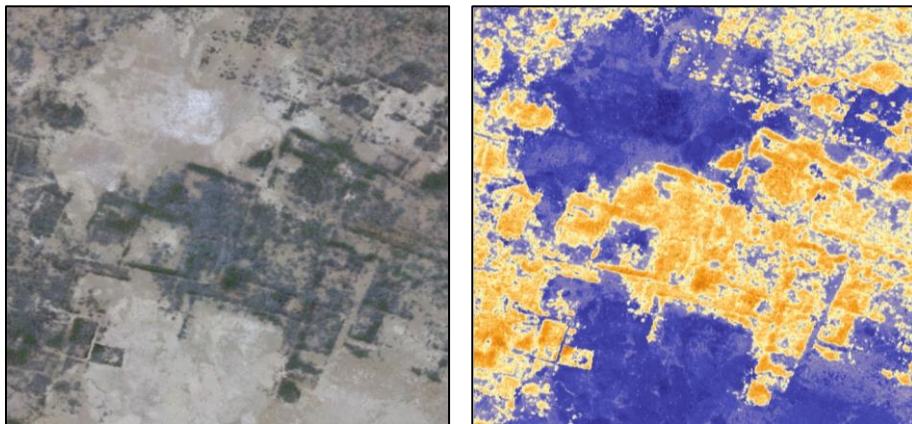


Figure 3.12: Crop mark comparison. Left - True colour; Right – False colour

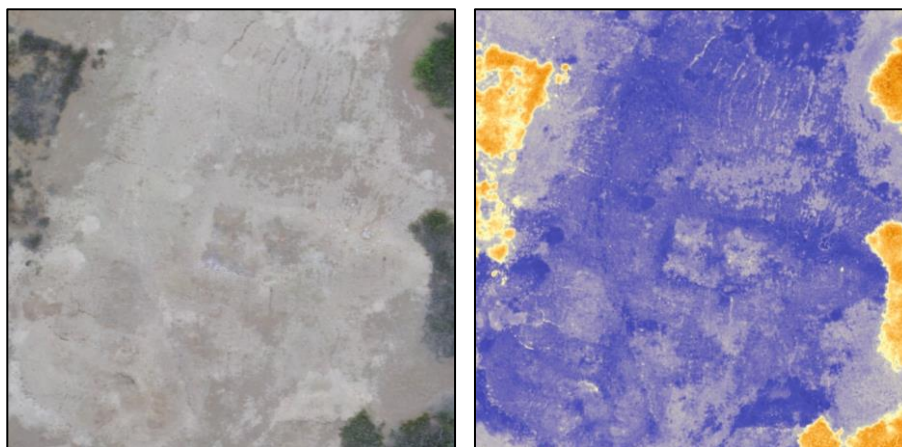


Figure 3.13: Soil mark comparison. Left - True colour; Right- False Colour

3.1.4 Ground-truthing

While the optical survey clearly identified numerous walls buried below the surface of Las Colmenas, ground-truthing was required to confirm the results. Ground truthing is the act of confirming remote sensing results by shovel shining or test pitting. Whereas test pitting is a small-scale excavation (often in 1m^2 areas), shovel shining is the practice of removing the top layer of soil or sand from an archaeological site to reveal the top of walls. Ground-truthing was carried out in two different areas of the site, called HP-1 and HP-2 (Figure 3.14). These are $4.5\text{-}5\text{m}^2$ areas in which shovel shining was conducted by removing the top $\sim 5\text{cm}$ of sand. Within these $4.5\text{-}5\text{m}^2$ areas, a 1m^2 test pit was excavated. These areas were selected because they appeared to be promising after different remote sensing techniques were tested at the site (see Chapter 4).

HP-1 is located on the northwesternmost mound, identified as a house-cluster from the optical imagery. By shovel shining a 5m^2 area, it became clear the optical imagery identified most of the buried architecture (Figure 3.15). The thicker walls making up a single room are identified in the optical imagery; however, thinner walls protruding from the larger room had not been identified. Shovel shining revealed vegetation following the perimeter of walls, supporting the use of crop marks as indicators for buried structures (Appendix 4). The test pit was conducted along the southernmost east-west wall of this room. The first floor was found 22cm below the top

of the wall. In this first 22cm, a few fragments of ceramic material were found. Below this floor, a 38cm thick layer was excavated, revealing an abundance of broken and often burned ceramic as part of a fill. In total, the test pit reached 60cm in depth.

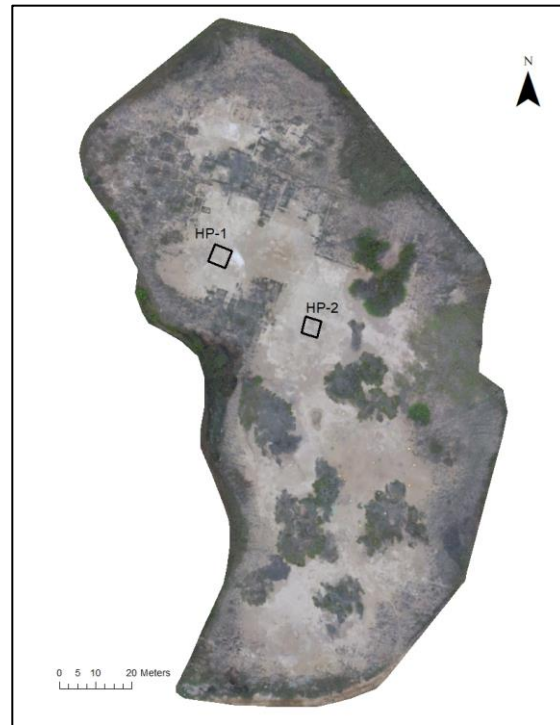


Figure 3.14: Ground-truthed areas

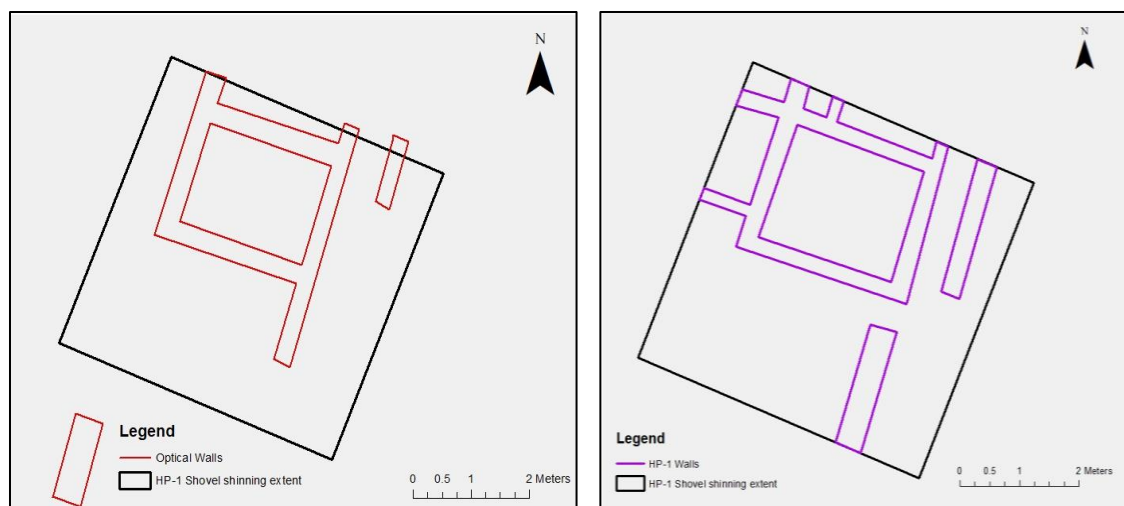


Figure 3.15: HP-1. Left - Optical imagery; Right - Shovel shining results

HP-2 is located on the longest mound found in the northeast part of the site. There were few walls visible in the optical imagery, but these walls do make up a larger room. A 4.5m² area above the room was shovel shined, revealing two long walls identified in the optical survey (Figure 3.16). However, as can be seen in Figure 3.16, one wall was missed by the optical survey. A test pit was excavated in this area down to the latest floor, located at a depth of 24cm. The fill above the floor contained ash and bones, with few ceramic fragments. Overall, ground-truthing confirmed the features identified in the optical survey. However, they also revealed that this technique did not identify all the buried features present. This is most likely due to the difficulty of mapping soil marks and the lack of consistent vegetation cover across the site. Additionally, if walls are deep enough, they may not produce any evidence on the surface.

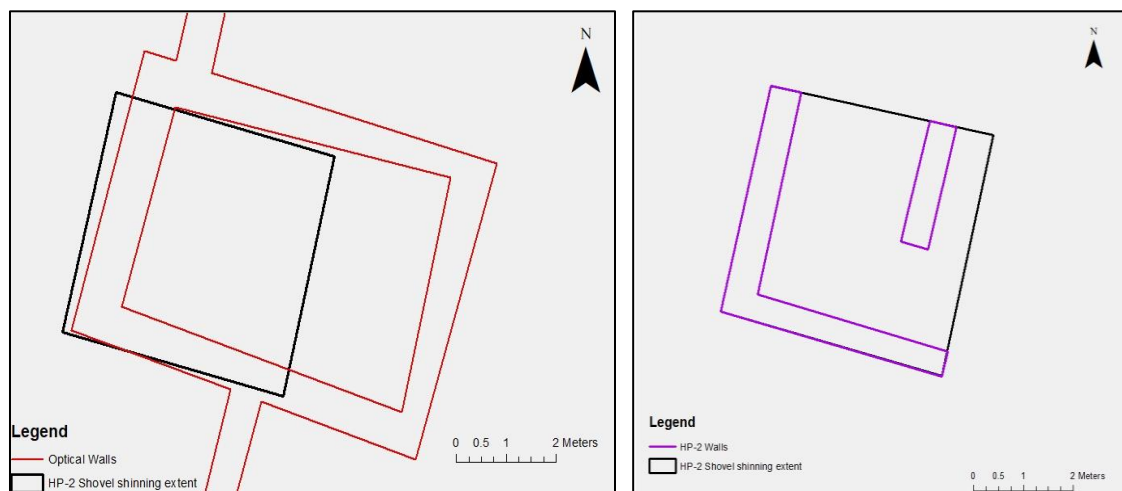


Figure 3.16: HP-2. Left - Optical imagery; Right - Shovel shining results

3.1.5 Trends

The most notable trend in this dataset is the concentration of architecture in the northernmost portion of the site. However, due to the placement of excavation in the 1940s by Wendell Bennet, we know there is architecture in the area covered with modern-day beehives (Figure 2.6a). The walls may not be appearing in the data due to recent disturbance associated with this activity, with modern looting, or because of an absence of vegetation. By following Willey's (Willey 1953a) suggestion of adobe

pyramids and the lack of architecture, it is reasonable to hypothesize that the mounds in the South are not house-clusters, but solid adobe platforms.

The DEM produced from the optical imagery (Figure 3.8), reveals new information about this site. Elevation differences between the walls and sand can be seen in the DEM, which produces a visualization of the walls prior to digitization. Additionally, the shape of the knolls becomes clearer; knoll 3 (Figure 2.6) is easily identified as a rectangular platform angling northeast towards Huaca Gallinazo, whereas knoll 7 and 6 do not have clearly defined exterior walls. This suggests knolls 7 and 6 are house clusters, where the boundaries of the houses are not as defined, whereas knoll 3 is an adobe platform with uniform and defined exterior walls.

There are notable trends with regard to what the optical UAV survey identified and what it did not pick up. The optical imagery picked up significantly more features in areas with vegetation cover (Figure 3.17). When taking into consideration the ground-truthing, it is clear that some walls were not detected. The areas where shovel shining took place (HP-1 and HP-2), had little to no vegetation on the surface. However, areas of high surface vegetation were not ground truth, thus we cannot know if walls are missing from those regions too.



Figure 3.17: Optical imagery walls in vegetation versus soil

The false-colour image(s) proved to be useful in altering brightness and contrast to increase the visibility of certain features. False-colour images increase feature identification in soil-covered areas, where they are difficult to identify otherwise. However, even with this modification of the images, there is still a substantial amount of space where no features were identified. The optical UAV surveys were useful for defining the limits of this site and identifying the region with an increased occupation, especially in a short time period. However, it is clear that large areas appear to lack any architecture and that some features are missed.

3.2 Thermal UAV Survey

The use of thermal imaging, also known as thermography, is the process of translating infrared radiation into pictures. Aerial thermography, or the use of airborne thermal sensors for remote sensing, has demonstrated its potential to reveal surface and subsurface archaeological features. Since the 1970s, aerial thermal imaging has been used by archaeologists to reveal a broad range of archaeological features, such as earthworks, roads, fields, and buried architecture (Casana et al. 2017). A thermal survey was conducted at Las Colmenas due to the popular use of this method in archaeology, and previous success in identifying buried features. The survey was carried out using a Zenmuse XT camera with a 9mm lens mounted on a DJI Inspire 1 UAV. This thermal camera records information from the infrared region of the electromagnetic spectrum

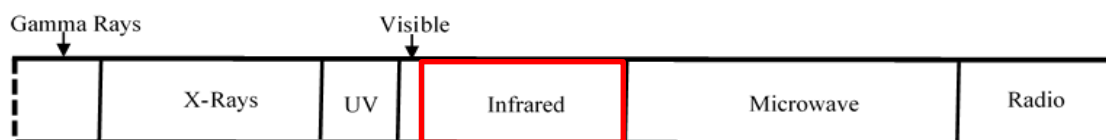


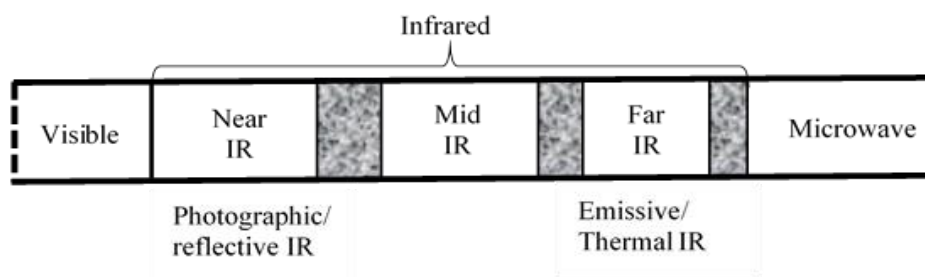
Figure 3.18: Infrared section of electromagnetic radiation spectrum (Revised from Campbell and Wynne, 2011)

(Figure 3.18).

Since the thermal camera operates within the infrared area of the spectrum, it includes any wavelength lower than the red portion of the visible light, but higher than microwave radiation. This area of the spectrum is much larger than the area of visible

light, and because of this, it incorporates a broader range of radiation with varying properties. This area is separated into three sub-regions: near-infrared (NIR), mid-infrared (MIR), and far-infrared (FIR) (Figure 3.19), the latter being the most useful for archaeological pursuits. While near-infrared radiation reveals how an object reflects solar energy, far-infrared radiations reflect variation in heat capacity (Campbell and Wynne 2011). This is helpful for archaeology because objects absorb, retain, and emit heat at different rates due to their composition, density, and moisture content. Thus, if a buried structure has a different composition, density, or moisture content than the surrounding soil, it should be visible in the far-infrared region of the spectrum. Architecture at Las Colmenas is made of sunbaked mudbricks, known as adobe. Adobe is primarily made of clay and silt material with a mixture of organics. The surrounding soil is primarily sand, with a mixture of eroded adobe from the buried structures and fill composed of domestic trash. Archaeological features can be identified by thermal imaging if:

- 1) There is substantial variation in thermal properties between the archaeological feature and the matrix.
- 2) The features are close enough to the surface to be impacted by heat variations.



- 3) The thermal imaging is gathered when the thermal differences are pronounced.

**Figure 3.19: Electromagnetic radiation spectrum - Infrared region
(Revised from Campbell and Wynne, 2011)**

There are four significant thermodynamic properties relevant to thermal imaging archaeological features: thermal conductivity, thermal inertia, volumetric heat capacity, and thermal emissivity. Thermal conductivity documents the ability of an object to transfer heat (Casana et al. 2017). Sand has a higher thermal conductivity, and thus the heat can penetrate deeper in the sand than with clay. Thermal inertia is the rate of this

heat transfer; this is important as different materials have different rates of change. Thus, certain times of the day will reveal different information (Casana et al. 2017). At sunrise, sand, which has higher inertia, will heat up before clay. Volumetric heat capacity is the amount of thermal energy required to raise the temperature of an object or soil matrix (Casana et al. 2017). The quality is primarily determined by the density and composition of the material. For instance, loose soil will have a lower heat capacity than dense clay. Thermal emissivity is the ability of the material to emit or reflect thermal radiation (Casana et al. 2017). In sum, thermal emissivity is the ratio of the difference between the two materials' ability to emit heat (sand and adobe both emit heat differently). When combined, these properties influence our ability to record features in an archaeological site such as Las Colmenas. The adobe bricks have a lower thermal conductivity, an increased volumetric heat capacity, and low thermal inertia. These properties greatly contrast to the loose sand of the surrounding ground at Las Colmenas, which has high thermal conductivity, low volumetric heat capacity, and high thermal inertia. In sum, the thermal emissivity between adobe and sand is substantially different, potentially allowing us to use this technique to identify buried architecture.

There are numerous other properties that influence the thermal conductivity, and subsequently thermal emission, of materials including salt concentration and water content. These two additives are essential to this research as both have the potential to affect thermal conductivity at Las Colmenas. The soil of the site has an abundance of salt, most likely from the nearby sea through groundwater transportation, which can be seen in the agricultural fields surrounding the site (Appendix 5). This could potentially decrease the thermal conductivity of the sand at the site (Abu-Hamdeh and Reeder 2000). By decreasing the estimate for thermal conductivity of the sand, the ratio of thermal emission between the sand and adobe lessens, minimizing the contrast between the two materials. Similarly, increased moisture will increase the thermal conductivity, thus conducting surveys during the rainy season would cause a higher contrast between wet sand and the relatively dry adobe (Abu-Hamdeh and Reeder 2000). During the field seasons at Las Colmenas, there was increased moisture during the morning due to occasional short rainfalls.

Aerial thermography is a technique used to detect subsurface architecture where archaeologists suspect substantial differences in thermal properties between the structure and the soil matrix. How deep the structures are from the surface is another important factor to consider. Ground-truthing revealed that features at Las Colmenas often occur within the top 5-10cm of soil. Thermal imaging has been argued to reach 50cm in depth (Casana et al. 2017), meaning that features at Las Colmenas are within reach for this remote sensing technique. Time of day is another essential parameter to consider (Casana et al. 2017). Temperatures will fluctuate throughout the year and across diurnal cycles, depending on the location of the survey site and its environment, which means that timing is a critical component of survey success. One of the most crucial aspects of thermal imaging research is the diurnal variation; after sunrise, the sand will heat faster than the adobe, and after sunset, the sand will rapidly lose heat while the adobe will retain the heat (Figure 3.20). Topographical features are also likely to be identified through thermal imaging as they have different properties than flat regions. These are also impacted by diurnal fluctuations since raised features will heat differently at sunrise, as the sun will heat the features obliquely (Figure 3.21). The timing of the thermal surveys will be discussed in the following section.

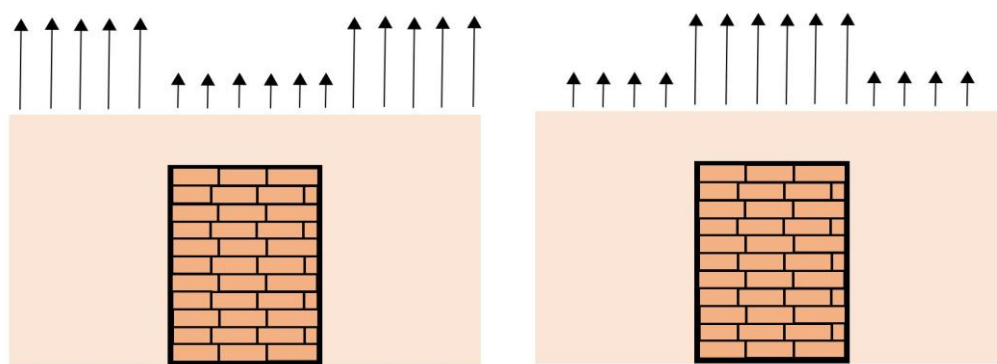


Figure 3.20: Thermal emission of adobe in sand matrix. Left - after sunrise; Right - after sunset. Revised from Casana et al. (2017)

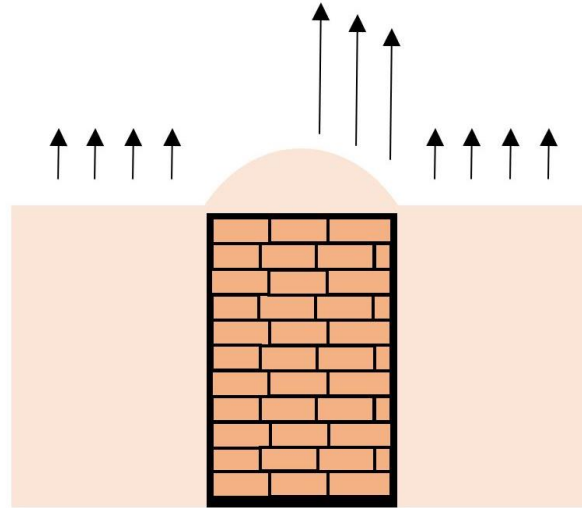


Figure 3.21: Thermal emission after sunrise of adobe in a sand matrix with topographic variations. Revised from Casana et al. (2017)

3.2.1 Survey Workflow

The thermal UAV survey at Las Colmenas was carried out following a workflow prescribed by Federman et al. (2017), Casana et al. (2017), and Nex and Remondion (2014):

- 1) The UAV should fly at 50 meters over the highest point of the site and the flight path should remain at one consistent elevation.
- 2) Flight paths should maintain a linear pattern with approximately 70% side overlap and 90% frontal overlap between images.
- 3) The UAV speed should not exceed 5-6 m/s.

There are two significant differences between the optical survey and thermal survey: the elevation and the absence of 45° images. Surveys conducted at 30-meter elevation result in numerous smaller images but a higher resolution, as seen in optical imaging (Chapter 3.1.1). This, combined with the monochromatic nature of thermal imaging, significantly reduced the number of tie points and resulted in numerous images falling out of alignment. To compensate, the UAV was flown at 50m, producing larger images, with a resolution to 9.4cm (each pixel corresponding to 9.4cm of site surface). In addition, 45°

images were not captured, as a DEM had already been produced using the optical survey imaging, which has a much better resolution.

Similar to the optical UAV surveys, multiple surveys were carried out to identify the optimal time of day for thermographic survey in this environment: the time of day when there is the most contrast in heat between the adobe and the sand. While scholars have argued the best time to conduct thermal surveys is at night (Casana et al. 2017), security and logistical reasons prevented us from conducting night surveys. In addition, previous work at Huaca Gallinazo proved that morning/early afternoon surveys showed more contrast between soil types than evening surveys (Millaire, Golay Lausanne and Eastaugh 2018). The morning surveys are also ideal for surveying regions with topographic variation as the raised features will heat differently at this time (Casana et al. 2017). Two thermal surveys were conducted, both on the same day in 2018. A survey was conducted at 10:45 (2018-10:45) (Appendix 6) and 13:00 (2018-13:00) (Appendix 7). The 2018-10:45 survey was conducted shortly after the cloud cover cleared up. However, there was not a significant amount of time for the sand to heat up, creating minimal heat variation. The 2018-13:00 survey took place approximately 3 hours after the cloud cover cleared up. This provided ample time for the sand to heat up, producing images that revealed buried features.

3.2.2 Processing

The following information is based on the 2018-13:00 survey. This survey captured 437 images while covering 24,200m² in 06:19 minutes. The images were processed in Agisoft Metascan Professional Edition v. 1.5.0, following the workflow outlined in the optical UAV survey section, including error reduction sequences listed by the Agisoft Metascan User Manual. A total of 108,316 tie points were created during photo alignment. However, after the error reduction filters were applied, only 20,149 tie points remained. A final orthomosaic was produced and used for post-processing (Figure 3.22).

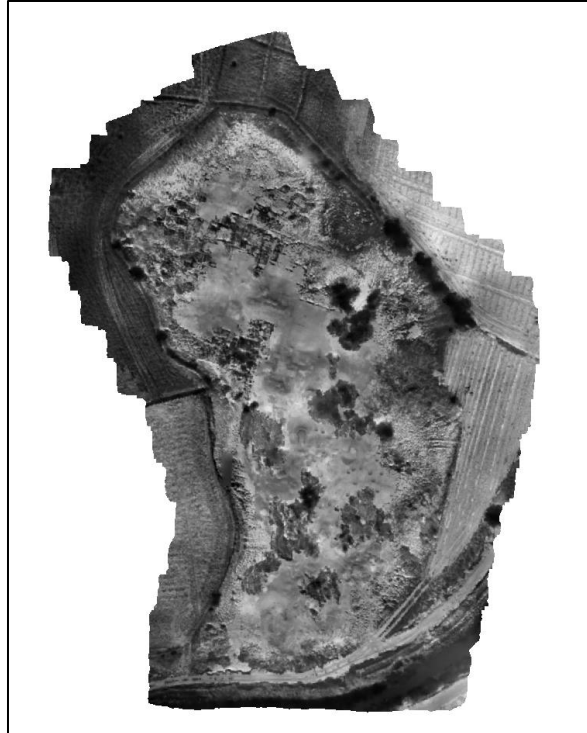


Figure 3.22: Thermal 1300 orthomosaic

3.2.3 Post-Processing

The digitization process was carried out using the workflow outlined in the optical UAV survey (Section 3.1.3), with a change in the criteria used to classify walls. While crop marks remain the same in thermal imaging, that is differential growth of vegetation over buried features, soil marks are no longer variations in surface soil colour but instead dark linear features in the soil as a result of cooler adobe walls contrasting with the warmer sand matrix. This alters the classification parameters set to digitize walls. In the thermal imaging, walls were recorded as:

- 1) Differential growth of vegetation due to subsurface archaeological features.
- 2) Dark grey-black linear features in a matrix of light grey soil due to subsurface archaeological features producing colder readings than the surrounding sand.
- 3) Walls visible on the surface of Las Colmenas.

The final digitized orthomosaic revealed a detailed map of the architectural structures buried below the surface of Las Colmenas (Figure 3.23).



Figure 3.23: Digitized thermal survey

3.2.4 Ground-truthing

To confirm the thermal UAV survey, the results were compared to the archaeological plan produced through shovel shining in the HP-1 and HP-2 test areas. Most walls identified in the HP-1 ground-truthing area were identified by the thermal UAV survey (Figure 3.24); only one narrow wall in the northeast most corner is missing. However, there are multiple walls in the thermal imaging that are not present in the ground-truthing. This could suggest the thermal imaging is picking up features that are buried deeper than the top 5cm of soil. Additionally, wall width is not consistent with the width of walls identified through ground-truthing. The ground-truthing of HP-2 yielded significantly fewer walls in the given area, as the walls and room in this area are larger than HP-1. However, similarly to HP-1, some internal walls were missed by the thermal imaging survey (Figure 3.25).



Figure 3.24: HP-1. Left - Thermal survey; Right - Shovel shining results



Figure 3.25: HP-2. Left - Thermal survey; Right - Shovel shining results

3.2.5 Trends

The thermal imaging picked up a significant number of walls across both vegetation and soil covered areas. Similar to the optical survey, it is clear from this survey that the vast majority of structures at Las Colmenas were clustered in the northern portion of the site. This further supports the notion of solid adobe structures in the South, rather than house-clusters. While the optical survey method failed to identify a large number of walls in soil covered areas of the site, the thermal image was successful and

identified numerous walls throughout, which can be explained by the heat variation between the soil and vegetation. An interesting trend is the thermal camera's ability to identify some walls over others. This is most likely due to the differential thermal emissivity of the adobe. The missing wall in HP-1 appears slightly thinner than the surrounding walls; this decreases the surface area, thereby increasing thermal inertia. In other words, the wall would heat faster than the surrounding sand, so when the survey was conducted 3 hours after sunrise it would already match the thermal emissivity of the sand matrix. However, thickness variation is not the case for the missing wall in HP-2. Factors such as different temper in the adobe, differential erosion, variations in manufacturing, decreased depth of the wall base, or wall lying closer to the surface, are but a few factors that could alter the thermal emissivity of the abode. As mentioned above, there are many properties that can cause a fluctuation in thermal emissivity, such as salt concentration or moisture content. An increase in either of these could, therefore, have caused increased thermal inertia for some walls (increasing the temperature faster) that would thus appear as warm as sand when the drone survey was conducted. Additionally, thermal inertia could increase if there is less wall to heat, in either width or depth, or even due to erosion. The two walls from HP-1 and HP-2 that were not picked up by this survey are found on the edge of a knoll, which could cause increased erosion and thus increase thermal inertia. Overall, there are many factors that could influence the appearance of some walls over others. Future work would benefit from further analysis of differential heat retention. However, overall the thermal imaging identified numerous walls across the northern portion of the site, producing a detailed architectural map of Las Colmenas.

4 Ground-based remote sensing

While the previous chapter covered the aerial surveys conducted at Las Colmenas, this chapter focuses on the use of ground-based remote sensing techniques employed in this research project. Ground-based remote sensing is the acquisition of remotely sensed data from the ground surface. The desire for effective and non-destructive methods of assessing archaeological features has led to the growth of ground-based remote sensing in archaeology. Many of the methods used were initially created for other fields, such as geology and engineering, but have now been adapted to archaeological research.

Ground-based remote sensing encompasses a wide range of geophysical techniques (techniques that use geophysical properties to assess buried features). Many geophysical techniques have been successfully applied to archaeology, such as electrical resistivity tomography (Fiandaca 2010), induced polarization (Slater and Lesmes 2002), ground-penetrating radar (Leucci et al. 2016), and magnetic surveys (Eppelbaum, Khesin and Itkis 2001). Despite years of use, the success or failure of individual geophysical techniques is heavily based on local conditions. Recent years have seen an integration of different geophysical techniques to limit the uncertainties and address the limitations of each technique. This project incorporates three geophysical surveys: magnetometry, magnetic susceptibility, and ground-penetrating radar. These are among the most widely used geophysical techniques in archaeology, as they have shown an extraordinary potential to locate buried archaeological features. However, few studies have incorporated these three techniques, as well as aerial surveys, in one setting to assess the benefits and limitations of each approach and the synergies of using them in combination.

All geophysical prospection works under the same principle: the identification of contrasts between features and surrounding materials. Magnetometry looks at changes in the Earth's magnetic field at a given point: the contrast between the feature and the magnetic field at that location. Magnetic susceptibility measures the ability of an object to become magnetized: archaeological features will have a different susceptibility than non-archaeological material or from each other. The ground-penetrating radar measures the contrast in velocity of microwaves between archaeological and non-archaeological

materials. These three techniques rely on measuring variations in the physical properties of archaeological features and their surrounding matrix to map subsurface remains.

While geophysical techniques have made strides towards large-scale mapping and site prospection, they are not without limitations. In fact, numerous environmental conditions affect the success of each technique. In addition, each technique requires specialized equipment, software, and knowledge. The following section covers the survey practices, processing, and trends seen in each dataset, including any limitations if encountered.

4.1 Magnetic susceptibility

Approximately 6% of the Earth's crust is made of iron, a ferrimagnetic mineral. Iron is distributed through rocks, clay, and soils as weakly magnetic minerals. Many studies (Fassbinder, Stanjek and Vali 1990; Tite 1972; Tite M. S. and Linington 1975; Tite M. S. and Mullins 1971; Weston 2002, 2004) have found that anthropogenic activity causes the redistribution and alteration of these chemical compounds, creating anomalies within the Earth's magnetic field. By studying these anomalies, we can identify archaeological patterns.

The Earth's magnetic field is created through a complex process known as the dynamo effect, where the convection of liquid iron within the Earth's outer core creates the magnetic field (Olsen 2016). The field is defined by the imagined North and South poles, where magnetic forces, known as flux lines, flow from and to. Since magnetic flux lines flow out of the Southern Hemisphere and into the Northern Hemisphere, the direction of the magnetic field trends at different angles across the surface of the Earth (Aspinall, Gaffney and Schmidt 2009). Figure 4.1 illustrates the various angles of the magnetic field around the globe. The magnitude of the flux, known as magnetic flux density, can be estimated at any given point on the surface of the Earth. This density is not influenced by the magnetic properties of the surface and thus remains relatively constant. However, the alternation of magnetic, chemical compounds in the soil (for example, burnt organic matter in a hearth) produces a magnetic fluctuation that differs

from the local field. Therefore, by measuring variations in the local magnetic field at a given point, we can identify sub-surface and surface anomalies. By having a clear understanding of what causes an anomaly, we can map buried archaeological features.

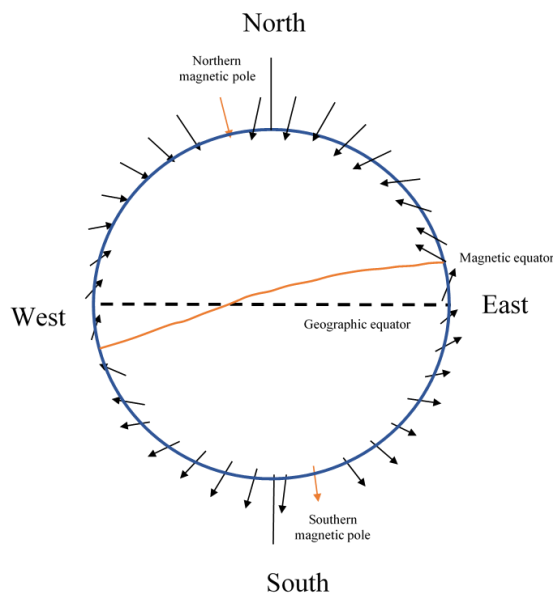


Figure 4.1: Magnetic field direction variations
(Revised from Wiltshko and Wiltshko 1995:2)

There are two types of magnetic anomalies: induced magnetism and permanent (remanent) magnetism. Permanent magnetism is displayed by an object which produces its own magnetic field, such as a bar magnet. Whereas induced magnetism is exhibited by an object which only becomes magnetized when placed into an existing magnetic field, such as paperclips becoming temporarily magnetic when coming into contact with a bar magnet (Aspinall, Gaffney and Schmidt 2009). Magnetic susceptibility assesses induced magnetism; it is called magnetic susceptibility as it gauges the ability of an object to become magnetized when placed into a magnetic field. Since Earth always has a magnetic field, we can always document the magnetic susceptibility of an object. In fact, all objects have a magnetic susceptibility; however, some objects will have an enhanced or decreased susceptibility. Anthropogenically influenced topsoil has a high concentration of magnetizable minerals known as iron oxides, which lead to enhanced magnetic susceptibility, which makes it possible to map buried features.

Iron oxides minerals are often referred to as ferrimagnetic minerals. The enhancement of topsoil by ferrimagnetic minerals was first described by Le Borgne (Le Borgne 1955, 1960). Ferrimagnetic minerals are the most prevalent magnetic minerals on Earth. They consist of various arrangements of iron and oxygen ions, with different crystal structures and ionic valence (Aspinall, Gaffney and Schmidt 2009). There are three iron oxides with the most archaeological significance: hematite (α - Fe_2O_3), magnetite (Fe_3O_4), and maghemite (γ - Fe_2O_3) (Fassbinder 2015). Hematite has fully oxidized iron, but has an overall weak susceptibility, whereas magnetite and maghemite are ~1,000 times higher in susceptibility (Aspinall, Gaffney and Schmidt 2009). The major difference between magnetite and maghemite is the level of iron oxidation; iron within magnetite is only partially oxidized, whereas the iron in maghemite is fully oxidized (Aspinall, Gaffney and Schmidt 2009). While hematite and maghemite have the same chemical makeup, they have different crystal arrangements, which result in different magnetic susceptibility. The most common iron oxide found in soil is hematite; thus, its conversion to a strongly magnetic oxide due to human habitation has seen increased studies (Graham and Scollar 1976; Tite 1972; Tite M. S. and Mullins 1971). A magnetic susceptibility meter identifies these strong magnetic oxides (magnetite and maghemite).

While an anomaly may occur, we must fully understand how human occupation can enhance magnetic susceptibility to map a site successfully. The conversion of hematite to strongly magnetic oxides is due to a sequence of reduction and oxidization reactions (Figure 4.2). Most commonly, this process is seen with the burning of the material. Burning vegetation or firing pottery, for example, result in a reducing environment due to loss of oxygen, which produces magnetite. The subsequent cooling and re-oxidation transform magnetite into the highly susceptible maghemite (Le Borgne 1955, 1960). However, this is not the only way maghemite can be formed. Magnetite within sediment or parent rock can become re-oxidized to produce maghemite (Fitzpatrick and Le Roux 1975). Lepidocrocite can dehydrate to maghemite, depending on particle size and temperature (Schwertmann and Taylor 1979). During a fire, the goethite within organic matter can become maghemite (Schwertmann and Fechter 1984). Lastly, when heated, siderite oxidizes to maghemite (Van der Marel 1951). The

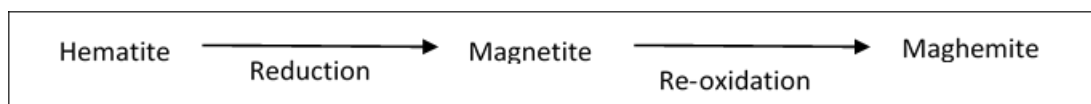


Figure 4.2: Magnetic oxides mineral conversion (Revised from Aspinall et al. 2009)

formation and transformation process of ferrimagnetic minerals is a complex process affected by geochemistry, weather conditions, climate, geology, and temperature. However, scholars have highlighted five pathways in which human occupation may alter hematite to maghemite. The first method of susceptibility enhancement is through burning, as previously explained. Whether cooking food, firing ceramic or firing bricks, intense heating and cooling results in magnetic susceptibility enhancement (Le Borgne 1960; Tite M. S. and Mullins 1971). Another path of enhancement is organic waste decomposition; the necessary conditions of waste decomposition (reduction and oxidization) produce the same environment in which magnetic minerals may be altered (Aspinall, Gaffney and Schmidt 2009; Linford 2004). The third process of enhancement involves magnetotactic bacteria: bacteria with micro-sized magnetite crystals in their bodies (Fassbinder, Stanjek and Vali 1990). These bacteria are found in decayed wood, and while the susceptibility signal is fairly weak when the mineral is magnetite, the susceptibility equipment can pick up these minute changes (Aspinall, Gaffney and Schmidt 2009). Decayed wood in post-moulds is one of the main areas where this is relevant to this project. The fourth form of enhancement is the addition of magnetic material to the soil, including pottery, bricks, metal, etc. which would be found in a midden or refuse left in rooms (Weston 2002). Lastly, the fifth form of enhancement is through pedogenesis (soil formation processes) (Maher and Taylor 1988). Evidence has shown the presence of magnetite in soil without any microorganisms, indicating the influence of soil formation processes. These processes all lead to an increase in magnetite, maghemite or a combination of the two iron oxides in archaeological features (Aspinall, Gaffney and Schmidt 2009). Whenever an archaeological feature is composed of or surrounded by magnetically enhanced minerals, the feature will be identifiable through magnetic susceptibility imaging.

A common trend within the Gallinazo Group is the burning of older material and waste prior to building a new floor (Bennett 1939). While the material is subsequently

buried by a new floor, the adobe walls undergo a reduction-oxidation event that alters the magnetic minerals in the clay. This causes an enhanced susceptibility in walls adjacent to areas of burning events. In addition, wooden posts were often used to hold up roofs within some rooms. These posts, if left, would decay and produce an enhanced magnetic susceptibility. Another aspect of enhanced magnetic susceptibility at Las Colmenas is the inclusion of magnetic material; there is an abundance of ceramic material across that site that increases susceptibility. If rooms are full of ceramic, the inside of the room may show an increased susceptibility compared to the walls of the room.

4.1.1 Survey Practice

The magnetic susceptibility survey was conducted with a Barrington MS3 susceptibility meter with an MS2D surface scanning probe (Figure 4.3). The MS2D loop probe is a 180mm diameter probe with a depth response of 50% at 15mm and 10% at 60mm. This tool is ideal for both archaeological assessments and environmental magnetic surveys as it records concentrations of ferromagnetic material in the soil. The readings collected by the MS3 meter were logged on a GPS enabled Trimble Nomad data collector with Bartsoft software. This tool records both the magnetic susceptibility readings and the location data, thus allowing for accurate spatial reference. In addition, GPS points were recorded for the gridded region to ensure accuracy. To collect readings, the probe was placed flat against the ground surface. This sensor operates on the principle of difference between the magnetic susceptibility of the air (magnetic field) and that of the sample taken. To account for any change in the susceptibility of the air, or what is known



Figure 4.3: Barrington MS3 susceptibility meter with an MS2D surface scanning probe. Photo by Edward Eastaugh.

as 'drift,' a zero-reference (or blank reading) of the air must be done periodically to calculate this 'drift', thus ensuring the accuracy and consistency of the results.

Two different magnetic surveys were conducted at Las Colmenas: a broad-interval survey and a close-interval survey. The goal of the broad-interval survey was to assess the limits of occupation by identifying areas of increased susceptibility. The goal of the close-interval survey was to identify specific areas of interest to determine the locations with increased burning, possibly indicating room use.

The broad-interval survey was conducted through a random-walk process. This is the act of walking across the site at random and collecting points. A total of 1426 readings were taken across the site (Figure 4.4). Zero-readings were taken after every ten samples to ensure accuracy. A benefit of using a broad-interval in a random-walk order is the ability to take readings in areas otherwise inaccessible. For example, the portion of the site occupied by modern-day beehives is not an easy location to survey systematically, but a random survey allowed for some data to be collected without interfering with the bees. Likewise, the southern portion of the site is covered with looters pits, which could nonetheless be broadly surveyed with the magnetic susceptibility sensor.

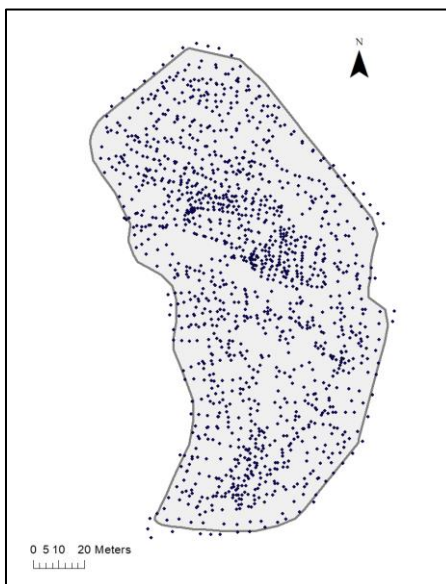


Figure 4.4: Magnetic susceptibility broad-interval survey points at Las Colmenas

The close-interval survey followed a grid system in which areas of the site were divided into survey areas based on the topography of the site; flat areas are preferred for conducting a fine-interval survey. The area surveyed is on the northern portion of the site, where the drone surveys identified increased occupation. This sector was also surveyed using the other ground-based remote sensing techniques. Six separate grids were surveyed, labelled A-F (Figure 4.5). Points were then collected sequentially on 1m transects with zero-readings occurring at the beginning and end of each line. In grid A, readings were collected every 1m, creating a 1x1m resolution, whereas, in grids, B-E readings were collected every 50cm, creating a 1x0.5m resolution.

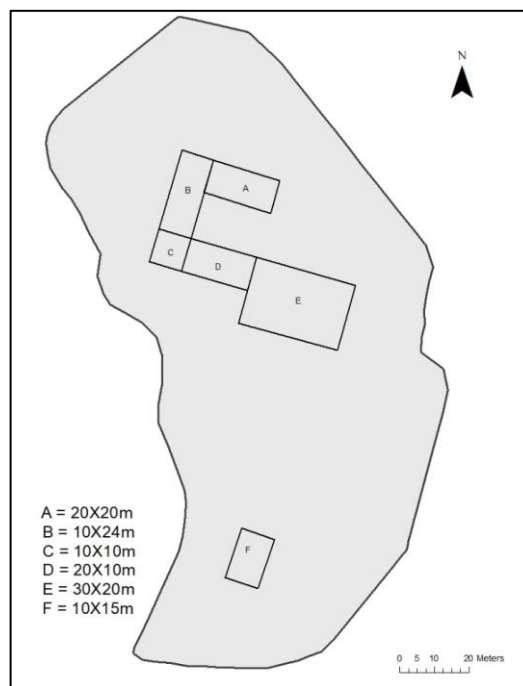


Figure 4.5: Magnetic susceptibility close-interval survey grids

4.1.2 Processing

Results processing was carried out using the Bartsoft for Windows CE software. The following protocol is a combination of BartSoft User manual recommendations and previous work by scholars (Hodgetts et al. 2016; Hodgetts, Dawson and Eastaugh 2011). The data initially output by the sensor is not normalized in reference to the zero-readings taken during the survey, which account for drift due to the nature of the machine. A drift

correction algorithm is applied to the data to take this drift into account. Since drift is considered linear over time, the algorithm measures the discrepancy between the first and last measurements. After this process was applied, the data is exported into a Text (tab-delimited) file (*.txt), which contains the XY data as well as the susceptibility value for each reading. The next step in preparing the data for analysis is called clipping: this is the removal of extremely strong and weak magnetic anomalies that resulted from modern-day objects. This removal is done to lessen their influence on the data (Figure 4.6). From here, the data is uploaded into ArcGIS to create a visualization of the results by using an interpolation process called Inverse Distance Weighting (IDW). This is the act of creating values for unknown pixels between known pixel values by using a linear weight combination of a set of known points. In this case, the weight is a function of inverse difference from each known point. In sum, points farther away have less effect on unknown points. The final interpolation maps (Figure 4.6a) are then used in ArcMap for post-processing. The values were classified into the maximum number of classes, at thirty-two, with a corresponding colour to visual illustrate the contrast between different values. The ranges are based on a quantile classification, where each range of values is placed into groups of equal size. This means each range may not be equal, but it covers

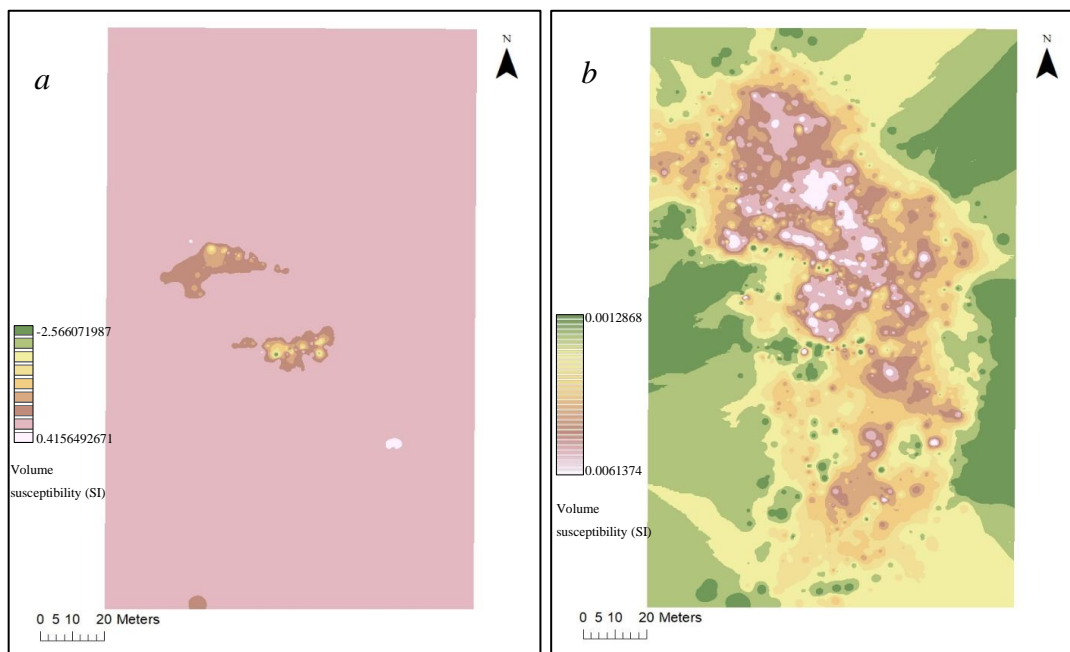


Figure 4.6: Magnetic susceptibility broad-interval – (a) without clipping; (b) with clipping

the same number of occurrences. This is calculated by dividing the number of readings by the number of classes (32). The benefit of this process is that each class is equally represented on the map. The previous process of clipping away extreme outliers becomes beneficial at this phase, as outliers can become over-represented in the data set. This is the final stage of processing, producing maps that identify variations in magnetic susceptibility across the site, which can provide information regarding anthropogenic activity (Figure 4.7).

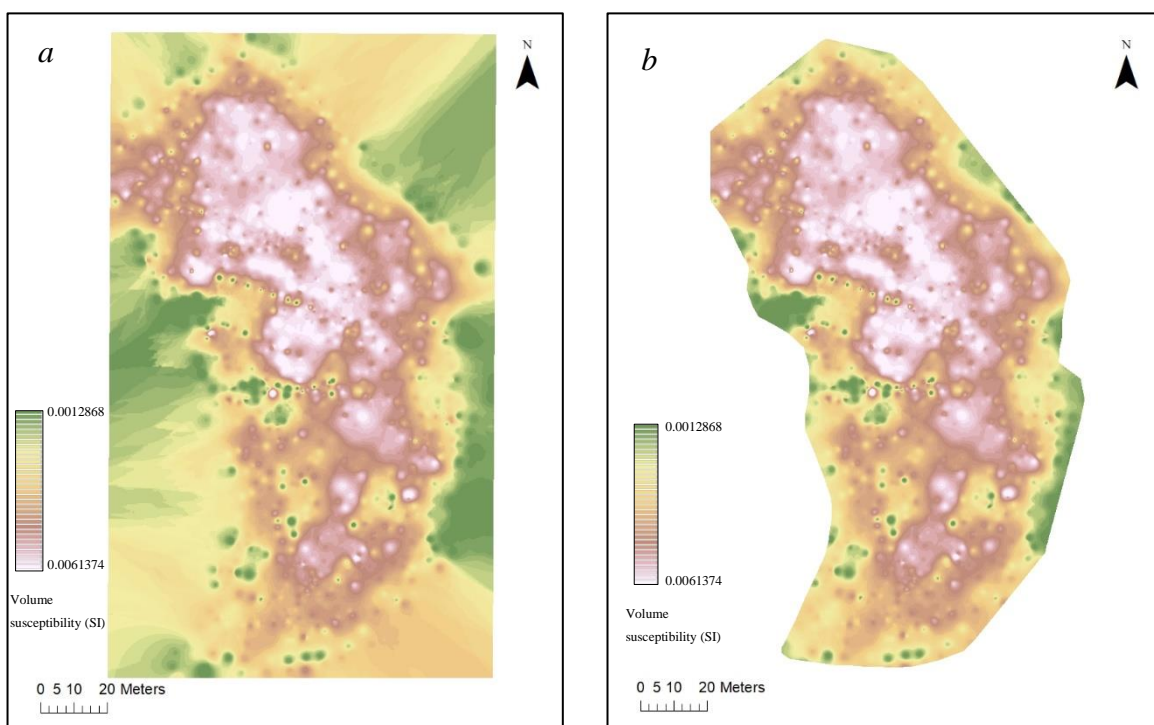


Figure 4.7: Broad-interval magnetic susceptibility in classes – (a) outputted results; (b) cropped to site

4.1.3 Post-Processing

The post-processing of the magnetic susceptibility survey results was conducted with the close-interval survey, where the goal was to identify archaeological features buried below the ground, such as clearly defined walls and rooms. There is an obvious contrast in susceptibility readings, which produces linear features that were mapped as walls (Figure 4.8, Left). This was done by using the polyline feature in ArcMap to mark

differences in susceptibility readings. A polyline was created along the center of the differences; this is different from the previous surveys where I outlined each feature. In the case of magnetic susceptibility, the width of features is interpolated through processing; thus, an accurate width cannot be given. Once mapping the susceptibility differences, a detailed map of features at Las Colmenas was created (Figure 4.8, Right).



Figure 4.8: Fine-interval magnetic susceptibility survey. Left - Results; Right - digitized

4.1.4 Ground-truthing

When comparing the HP-1 shovel shining results to the close-interval magnetic susceptibility survey results, it is clear the magnetic susceptibility identifies features in the general area in which they occur. However, the size and exact location are slightly offset (Figure 4.9). The magnetic susceptibility survey which covered the HP-1 was conducted at a broader interval (1x1m) than the other close-interval magnetic susceptibility surveys (1x0.5m). This creates a larger area where interpolation occurs, lessening the accuracy of the results. However, the survey did identify the large room and one wall coming off the larger room. The HP-2 survey area was conducted at 1x0.5m; the increased survey interval creates a more accurate location of features (Figure 4.10). Each

wall was identified through the HP-2 magnetic susceptibility survey, however not completely.

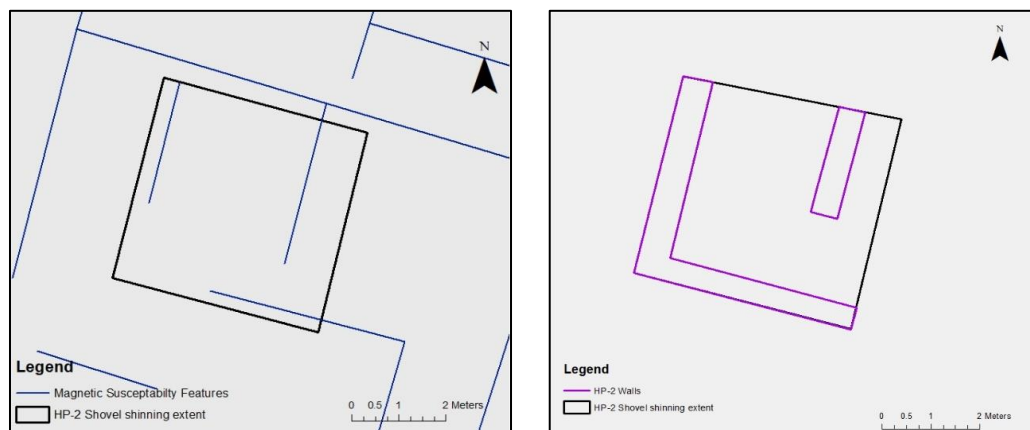


Figure 4.9: HP-1. Left - Magnetic susceptibility; Right - Shovel shinning results



Figure 4.10: HP-2. Left - Magnetic susceptibility; Right - Shovel shinning results

4.1.5 Trends

The broad-interval survey reveals high readings across the northern portion of the site, with low readings in the south (seen above in Figure 4.7*b*). The lack of high readings in the South potentially suggests increased occupation of the Northern portion of Las Colmenas. If this is the case, it supports the notion of raised platform mounds in the South. If the southern part of Las Colmenas saw heavy anthropogenic use, there would be increased magnetic susceptibility of soils, similar to the northern portion of the site.

However, this is not recognized, indicating minimal use of the southern area or perhaps the high values suggesting anthropogenic activity occur deeper than the equipment's ability to assess.

The most notable trend in the small-interval survey was the contrast between the magnetic susceptibility of ancient walls and the background soil. Indeed, at Las Colmenas, the magnetic susceptibility survey results helped identify numerous archaeological features whose properties differed from those of the surrounding matrix. Walls along areas of burning had an increased susceptibility likely due to the conversion of hematite to maghemite in the adobe walls. Similarly, space around non-burnt walls that were littered with highly magnetic artifacts, such as pottery, created a high susceptibility reading (Figure 4.11). Also, the large inverted 'L' shaped wall, labeled 'a' in Figure 4.12, revealed two different magnetic susceptibility values. The north-south wall appears to have a high value, contrasting with the surrounding lower values, whereas the east-west wall has a low value, contrasting with the high values surrounding it. There have been multiple instances where there are different magnetic susceptibilities of mud-brick due to the inclusion of different materials (Becker and Fassbinder, 1999). This confirms that the values themselves are not diagnostic of features per se, but instead the contrast between features and surrounding soil. Walls do not all have one specific

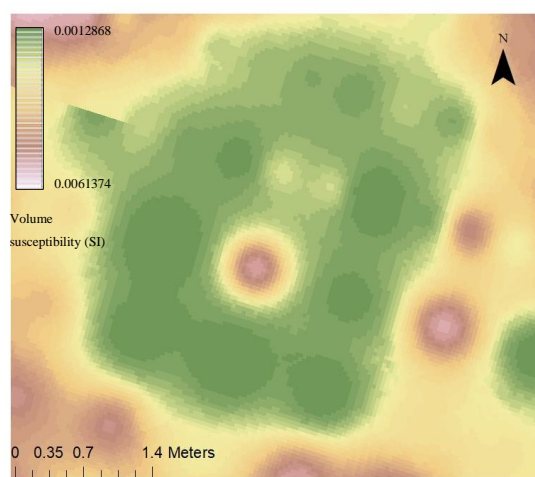


Figure 4.11: Low value walls with high value inside.

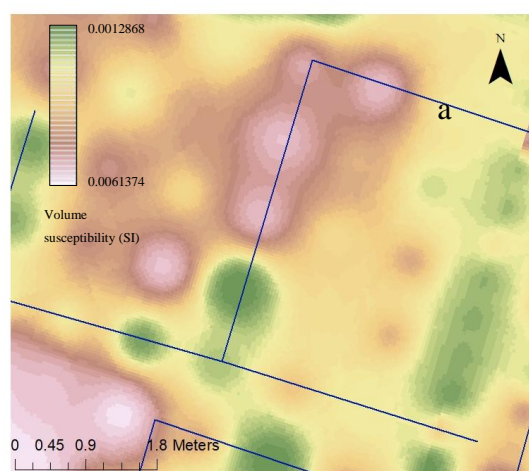


Figure 4.12: One feature (a) with high and low values

susceptibility value, but instead range from high to low. This is most likely due to the prevalence of burned walls and burnt fills across the site. Conversely, areas where vegetation had been removed during the previous field season, featured unusually low susceptibility, most likely due to the presence of roots beneath the surface.

4.2 Magnetometer

Magnetometry is one of the most popular geophysical prospection methods in archaeology. This is due to the natural and cultural processes which generate magnetic variations, as seen with the magnetic susceptibility. As previously mentioned, there are two types of magnetic anomalies: induced magnetism and permanent (remanent) magnetism. The magnetometer differs from magnetic susceptibility as it records both of these types of magnetism. Permanent (remanent) magnetism: the ancient magnetic field present at the time when the remanent magnetism was acquired (Aspinall, Gaffney and Schmidt 2009). The magnetometer records deviations in the strength of the magnetic field at a given point, which can be caused by both induced and remanent magnetism (Johnson et al. 2009). In some cases, a feature may have both induced and remanent magnetism, where both values contribute to the overall anomaly.

A remanent magnetization can be acquired by five main processes: thermoremanent magnetization (TRM), detrital remanent magnetization (DRM), chemical remanent magnetization (CRM), lightning-induced remanent magnetism (LIRM), and shock (shear) remanent magnetism (SRM) (Fassbinder 2015; Games 1977). TRM is the process of magnetization by exposing soil, rocks, or sediments to high temperatures (Fassbinder 2015). When minerals are heated above their curie temperatures, the materials lose their magnetic order and readily align with the ambient magnetic field at the time of firing (Aspinall, Gaffney and Schmidt 2009). The minerals then retain that alignment after they cool. DRM is caused by soils containing permanently magnetized oxide grains, subsequently deposited in water, such as a pit or ground depression. These grains orient their magnetic axis parallel to the magnetic field direction (Fassbinder 2015). CRM is any chemical alteration that may induce magnetism, such as low-temperature oxidation, exsolution, diagenesis, or dehydration (Opdyke and Channell

1996). LIRM is magnetization brought about through a lightning strike that magnetized the surrounding soils, rocks, and sediments (Maki 2005). SRM is the magnetization acquired as a shock wave from an impact passes through rock while in the presence of a magnetic field, the most common example of this is ceramic and adobe production (Nagata 1971; Tikoo et al. 2015).

The two most relevant forms of remanent magnetism at Las Colmenas are TRM and SRM. Due to the increased amount of burning with kilns and between occupations, there is an increased potential for TRM. Likewise, SRM is a significant form of remanent magnetization at Las Colmenas, as the adobe bricks used to make the walls acquire SRM. The pressure in which the clay undergoes when pushed into the brick moulds produces SRM (Games 1977). By conducting a magnetometer survey, we can identify areas where remanent and/or induced magnetism causes fluctuations in the strength of the magnetic field. These fluctuations are anthropogenic in nature.

Magnetometers can be classified into two categories: scalar and vector. The scalar instruments measure the total strength of an ambient magnetic field at a given point, whereas a vector instrument measures a portion of the field in a particular direction (Aspinall et al. 2009). Within these two categories, there are numerous different types of magnetometers which are used for different purposes. For archaeological purposes, fluxgate and SQUID vector magnetometers are used, and overhauser and alkali-vapour scalar are used (Aspinall et al. 2009). Magnetometers come in three different operational modes: single, differential, and gradiometer (Figure 4.13). A single-use magnetometer has one sensor and measures the direct field at the given point. A differential magnetometer uses two sensors: one sensor is kept at a fixed location to continually record the Earth's magnetic field, which is then subtracted from the second sensor used to measure the area of interest. The gradiometer has two sensors oriented vertically at a fixed distance from one another. The upper sensor records the Earth's magnetic field, whereas the lower records the magnetic field. These are then subtracted to find the specific deviation of the given area. This project used a fluxgate gradiometer, with two vertically aligned gradiometer sensors attached to a bar (Figure 4.14). This magnetometer can pick up data down to one meter below the ground but does not record the depth of

anomalies; the results, therefore, indicate that there is anomaly identified within the the first meter of soil below the ground.

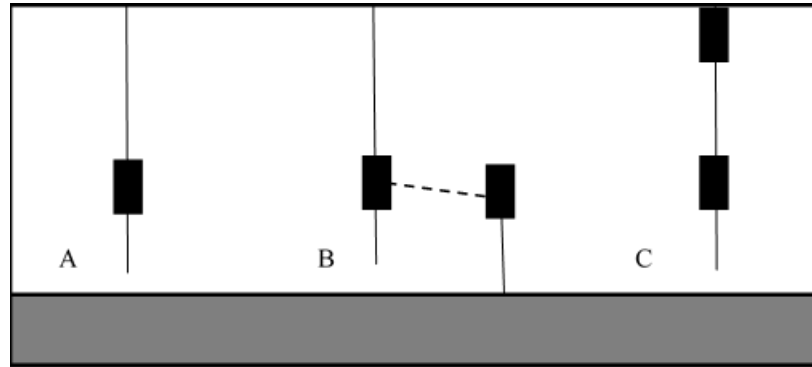


Figure 4.13: Magnetometer operational modes: (A) Single, (B), differential, (C) gradiometer (revised from Aspinall et al. 2009)



Figure 4.14: Bartington Grad601-2 dual-sensor Fluxgate Gradiometer. Photo by Edward Eastaugh.

4.2.1 Survey Workflow

The magnetometer survey used a Bartington Grad601-2 dual-sensor Fluxgate Gradiometer. This system consists of a data logger (DL602) and two Grad-01-1000L sensors mounted on a carrying bar. The dual sensor was employed as it doubled the speed of the surveys. Close-interval surveys were conducted in a grid format, similar to that of

the magnetic susceptibility close-interval survey. Seven grids were surveyed, each starting in the southwest corner, moving north (Figure 4.15). The survey was carried out at 25cm transects intervals with a sample interval collected every 12.5cm, resulting in a 25x12.5cm resolution. This survey employed parallel forward walking, where each line is completed south to north. The seven surveys covered a total of 2,080 m² and included the three northernmost mounds. The grids were created to find the best possible way to survey the area, given the topography of the site. In cases where there was a sudden drop or large looters pit at the end of a line, the transect was stopped early. Before conducting the primary survey, a reference point was collected. This is collected in a 2-3m space outside of the survey area with no interference from buried features; this is confirmed by ensuring any variation is within a range of $-2/+2nT$. Once a suitable space is found, the cardinal directions were laid out and remained in place for the entire surveying process. This space was then used prior to each survey to adjust sensor alignment and balance control. This included rotating the sensor in the cardinal directions and at various degrees of tilt as instructed by the magnetometer.

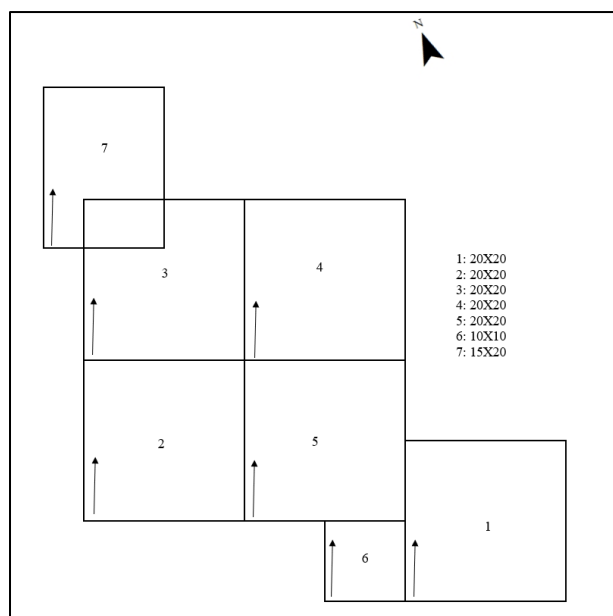


Figure 4.15: Magnetometer grid system of survey area

Each corner of the grids were recorded using a differential GPS to allow for georeferencing in ArcMap during post-processing. While each survey was conducted, the magnetometer recorded the data to be subsequently downloaded and processed.

4.2.2 Processing

The first step was to export the data from the magnetometer Data Logger. This was done through Grad601 software, which outputs the data in XYZ format. Subsequently, the data was uploaded and processed through Geoplot, a geospatial data visualization application. Based on the formatting of the software, grids are more easily processed individually. However, if the grids share one or more sides, they can be placed in a proper position within the software. Thus grids 2-5 were processed together, whereas the 1, 6, and 7 were processed individually (Figure 4.15).

The first stage of processing is largely concerned with resolving errors associated with the instrument used or resulting from field procedures. The primary algorithm applied is called zero-mean traversing (ZMT). ZMT is a protocol used to correct for baseline shifts when using a dual-sensor instrument, removing the stripping effect (Figure 4.16). To account for these differences, the mean value is calculated individually for each traverse and is subtracted from each data point along that line. This reduces the mean to zero, which is why it is called a zero-mean traverse. Once applied, the minimum and maximum standard deviation values used to shade the image can be changed to create an image with an ideal amount of contrast to reveal features. Figure 4.17 reveals the difference in changing the extent of the standard deviation between images. Too much contrast will highlight nearly everything in the image (4.17a), whereas a lower deviation

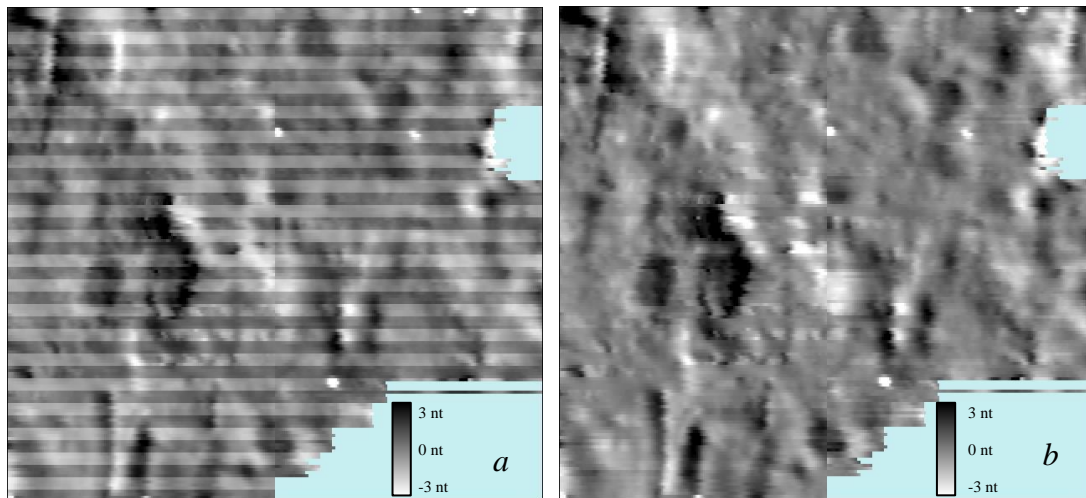


Figure 4.16: Grids 2-5: (a) Prior to any editing; (b) after zero-mean traverse

highlights extreme anomalies (4.17b). After adjusting each grid, the final grids are ready for post-processing (Figure 4.18).

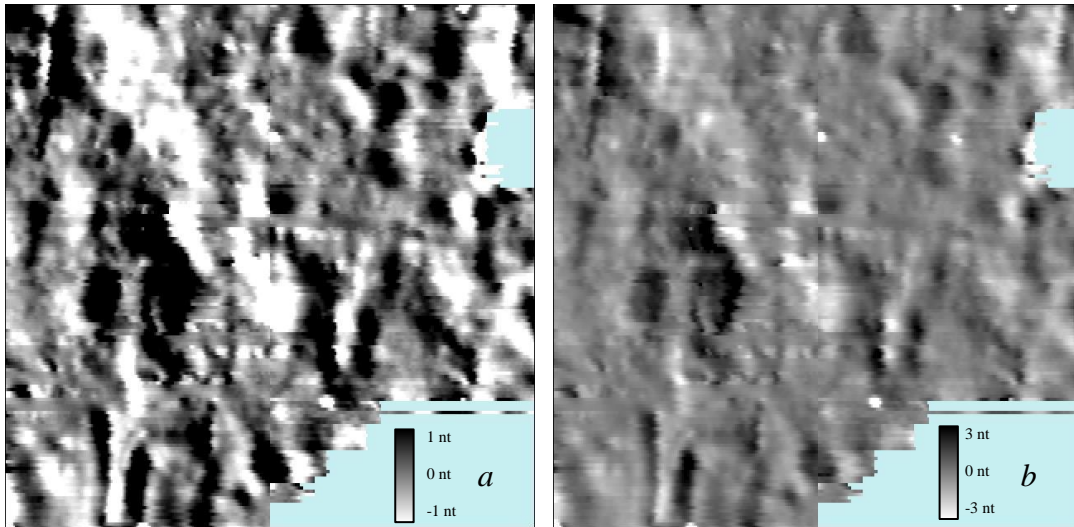


Figure 4.17: Grids 2-5: (a) -1 to 1 Stand deviation; (b) -3 to 3 Stand deviation

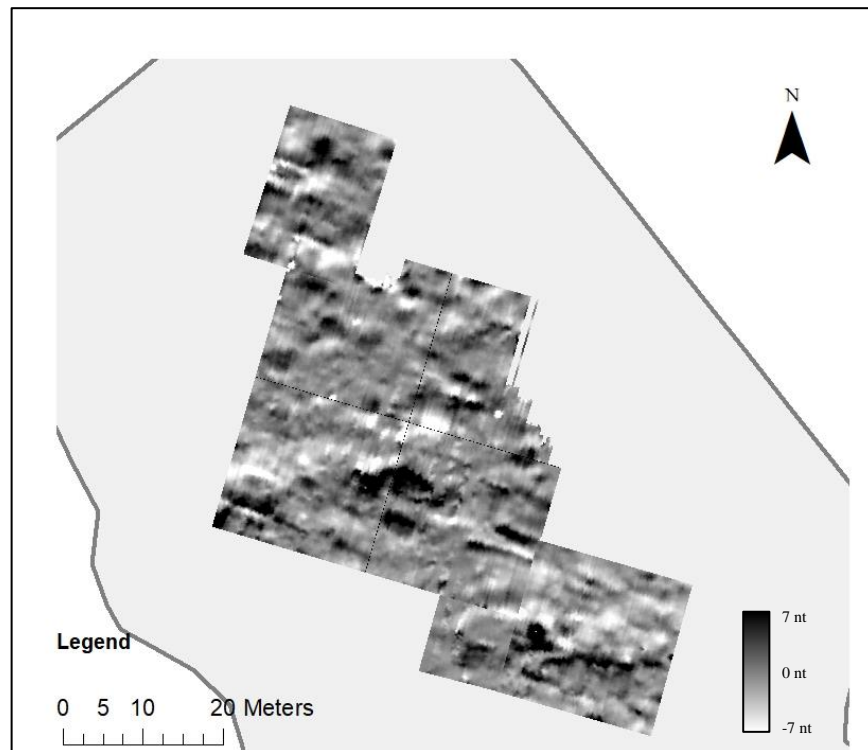


Figure 4.18: Processed magnetometer grids

4.2.3 Post-Processing

The corrected magnetometer data was then post-processed in ArcMap to identify features. Magnetometer feature identification works on a pattern-recognition approach, where patterns between magnetic anomalies are assessed and identified as potential features. Features in magnetometer data appear as either positive, negative, or bipolar anomalies. A positive feature is white, and a negative feature is dark-grey to black, and a bipolar feature has both a positive and negative component. Each type of feature was marked by placing a polyline down the center of each anomaly. In the case of nonlinear anomalies, a polygon was used to outline the extent of the feature. Following these parameters, a digitized model of the magnetometer results was created (Figure 4.19).

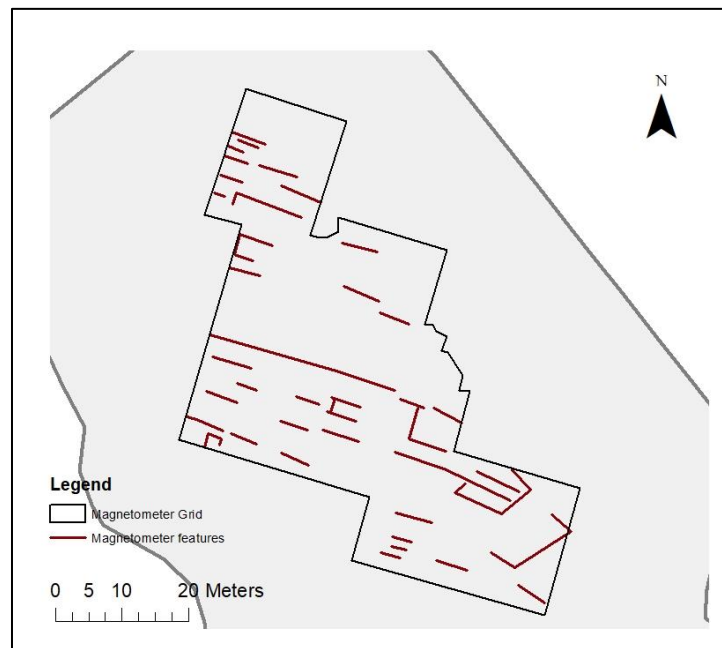


Figure 4.19: Digitized magnetometer results

4.2.4 Ground-truthing

By comparing the magnetometer results with HP-1 (Figure 4.20), it is clear the magnetometer missed a substantial number of features. In this case, only a single wall was identified. It is slightly offset from the walls found in ground-truthing, but it is unclear if this feature corresponds with a known wall, or in fact, is another wall buried

deeper, as only the top few centimetres of soil were cleared and the instrument can measure up to one meter in depth. The results of HP-2 are similarly lacklustre, with the identification of two walls, one which corresponds to a known wall (Figure 4.21). However, the other wall was not identified in ground-truthing. Indeed, this suggests it is likely a more deeply buried wall than the assessed area.

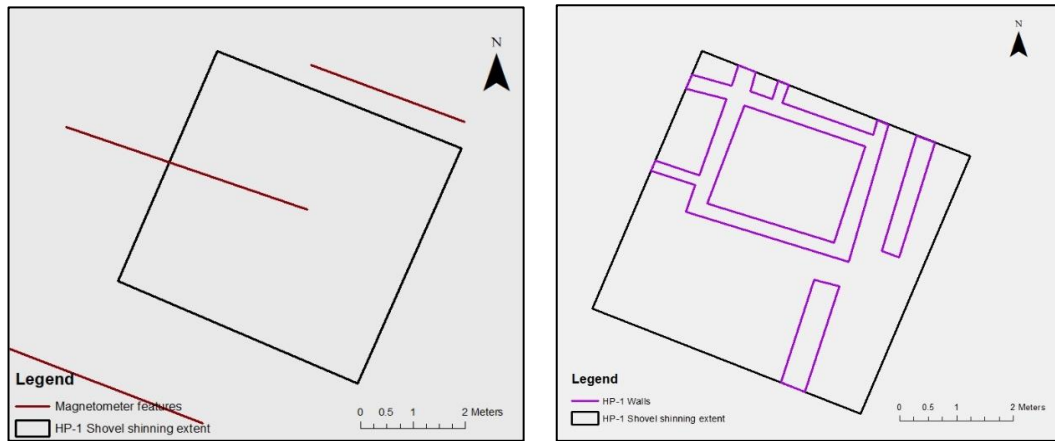


Figure 4.20: HP-1. Left - Magnetometer features. Right - Shovel shinning

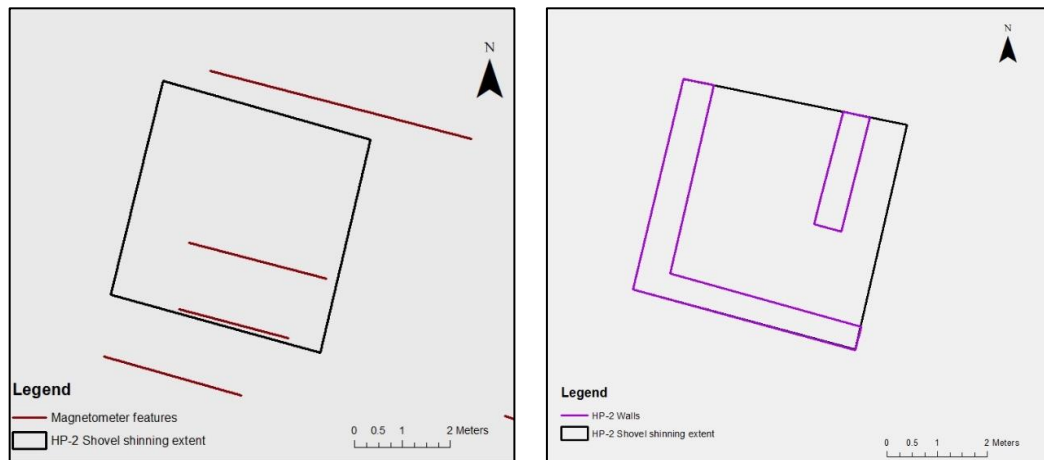


Figure 4.21: HP-2. Left - Magnetometer features. Right - Shovel shinning

4.2.5 Trends

The most notable trend within the magnetometer results is the lack of walls in the north-south direction. Recent studies (Fassbinder 2015) have shown that magnetometer surveys close to the geomagnetic equator are difficult to interpret and implement. At the

geomagnetic equator, anomalies with a north-south orientation are almost completely unidentifiable due to the minimal difference between the feature orientation and the orientation of the magnetic equator. However, studies show that by combining a dual-sensor gradiometer with a scalar magnetometer helps reveal north-south oriented features at the geomagnetic equator (Fassbinder and Gorka 2011). While this is an unfortunate discovery, the results still yield contributory information to this project.

In HP-2, a single wall is identified in the magnetometer that is not seen in shovel shining; this suggests deeper walls are being identified with the magnetometer than what was identified through shovel-shining. Likewise, when viewing the results, there are two sets of anomalies (Figure 4.22) that occur at a different angle than other known features at this site. This suggests a deeper set of walls, possibly of earlier occupation following a different urban grid orientation. However, the magnetometer only reaches one meter of depth, and previous excavation data by Bennett (1939) revealed consistent wall orientation throughout the excavated area, which reached more than 2 meters in depth. As such, the orientation modification might not be due to urban grid orientation changes over time, but could possibly instead be due to a pit or the accumulation of highly magnetic material at the base of the knoll adjacent to the features.

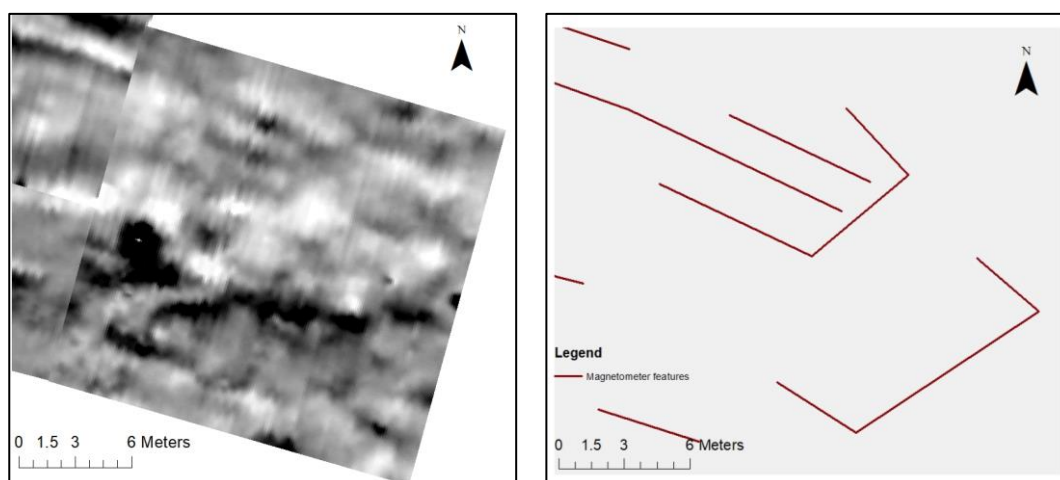


Figure 4.22: Magnetometer results with features offset from urban grid

One of the most significant results of this survey is the identification of hearth features. Previous work at Huaca Gallinazo with a Fluxgate gradiometer identified hearth features as circular, bipolar anomalies. Two of these anomalies were found within this data set (Figure 4.23), suggesting the presence of two hearths. This will eventually need to be confirmed through excavation.

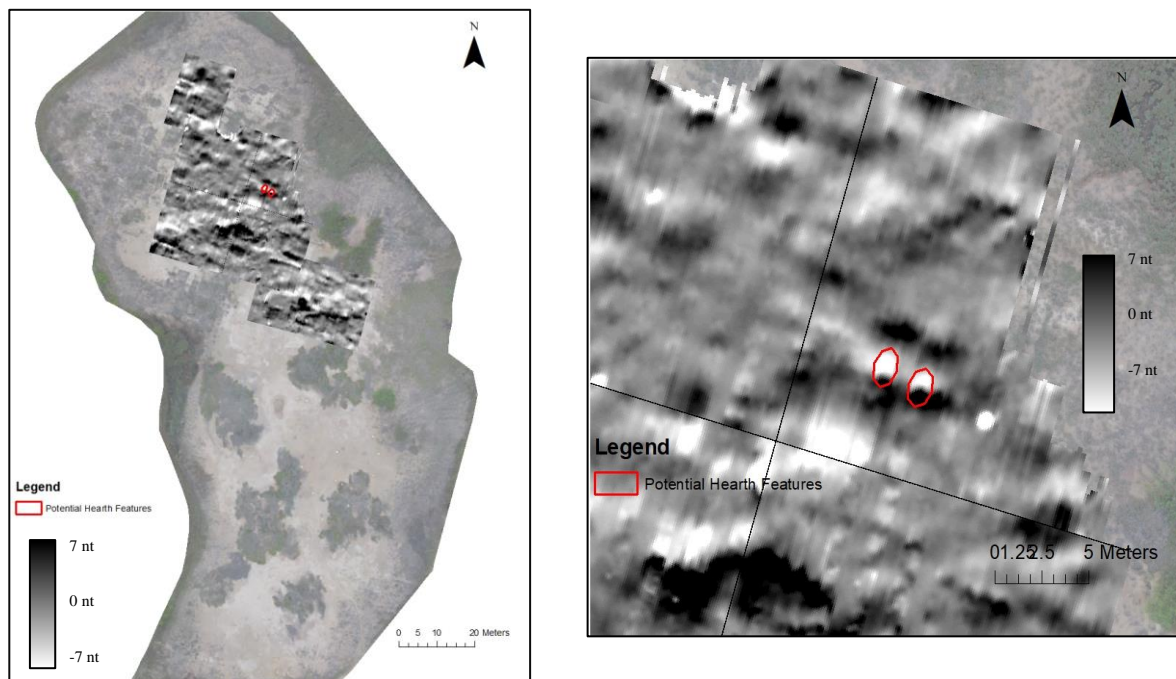


Figure 4.23: Potential hearths identified in magnetometer results; Left - Location on site, Right - Close up

4.3 Ground-penetrating Radar

The Ground-Penetrating Radar (GPR) has gained wide acceptance in archaeology over the last decades, as a method for rapidly locating buried archaeological features and artifacts. The GPR is a geophysical tool used to accurately map the spatial extent of subsurface objects or changes in soil and subsequently producing an image of the buried materials. The radar moves on the ground in linear transects, emitting radar waves that are propagated downward, in pulses, where they are reflected by buried features and eventually detected by a receiving antenna (Figure 4.24) (Annan 2005). The GPR consists of four main components; waveform generators, a transducer, a single processor, and a data storage and display unit. The waveform generator produces a radio wave that

is emitted and subsequently received by the transducer, which is also referred to as the antenna. The data is then processed and stored within the GPR to be exported later.

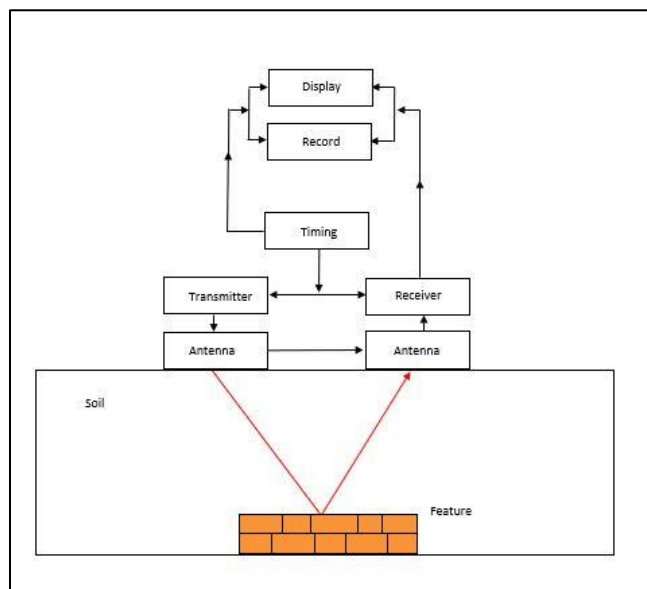


Figure 4.24: Main components of ground-penetrating radar (adapted from Annan 2005).

The GPR identifies different dielectric constants of materials through the use of radar waves. This is the ability of a material to store electrical energy; it is also referred to as relative permeability (Annan 2005). When the GPR emits a radio wave, the velocity of the wave is set for the dielectric constant of the matrix soil. Once the wave hits a medium with a different dielectric constant, it is reflected in the surface and received by the GPR's antenna. Changes in dielectric constants are due to differences in the physical and/or chemical properties of the material—specifically, changes in composition, density, and moisture content of the buried object. The strength of the reflection is determined by the contrast between dielectric constants. For instance, dry sand has a dielectric constant of 3-5, granite has a dielectric constant of 4-6, and clay has a dielectric constant of 5-40 (Annan 2005). If the radar wave propagates through a sand matrix and encounters a clay feature, the signal will be greater than the signal received from granite.

While reflections often occur from a change in soil type, they also happen where there is a discontinuity between the electrical properties of the sediment or soil, voids in the soil, changes in bedrock, variations in density, or change in water content (Conyers

2016). More importantly, reflections occur at interfaces between archaeological features and the surrounding sediment or soil due to changes in composition, density, and moisture content. For instance, the contrasting density between a limestone structure surrounded by clay loam will be identified and mapped by the GPR. While reflections can be caused by archaeological features, there are numerous other factors that can produce reflections that must be understood in order to identify archaeology features accurately.

A beneficial aspect of using a GPR that is not found in any other method used for this project is the ability to assess the depth of the identified features. By measuring the travel times of the energy pulses and their associated velocity through the ground, depth in the ground can be accurately measured to produce a 3-D model. The depth to which radar energy can penetrate and the quality of the results is in part controlled by the frequency of the radar transmitted (Conyers 2012). The frequency controls the wavelength of the propagating waves as well as the amount of weakening or attenuation of the waves in the ground (Conyers 2016). The GPR antennas control the frequency – there are numerous different frequencies used, often for different purposes; however, archaeology tends to use 10-1,200MHZ (Conyers 2016). Lower frequency radars (10-120 MHz) can reach up to 50m in depth penetration but can only identify large subsurface features, whereas high-frequency radars give up depth penetration with reaching only a couple meters. However, they can identify features within centimetres (Conyers 2016). This project used a high-frequency Noggin® 500 with 500mhz antenna, making it an ideal tool to locate near-surface archaeological features with centimetre accuracy.

4.3.1 Survey Workflow

The GPR survey covered a total of 2,191 m², between fourteen different grids surveyed with the Noggin 500® with a SmartTow configuration (Figure 4.25). The minimum grid size was 10m by 10m, and the maximum grid size was 20m by 10m. The grids were laid to account for the topography of the site. Prior to conducting the GPR surveys, grid areas were cleared of all vegetation. In most cases, this was minor plant

growth; however, in other areas, there was the complete removal of shrubs and medium-sized stumps. The GPR survey followed the following parameters:

- 1) Survey transects of 25cm
- 2) Step size set to 0.01m
- 3) The velocity of dry sand (0.12 m/s)
- 4) Depth set to 1.5m
- 5) The survey must use forward parallel transects

Depth was kept to 1.5m, as a sample survey revealed an abundance of 'noise' or interference afterwards, making it difficult to use the data. For each survey, the starting position (0,0) was chosen based on the topography of the site. For instance, in all cases, the GPR survey would go upslope to reduce sliding associated with surveying downslope. Each survey was recorded to keep track of directionality and area covered (Figure 4.26). The survey grids ranged in size, based on the terrain; areas were gridded together, which had similar topographic properties. For example, surveys were created around the knoll, and then across the knoll. Survey grids were also created around looters pits and the steep slope of the site edge. A forward parallel survey was used throughout this project, meaning the surveys always started on the Y-axis (Figure 4.27). This is important since a forward-reverse survey, or zig-zag survey has the potential for offsetting readings. The GPR features a wheel odometer to keep track of distance travelled. Prior to each survey, the odometer was calibrated to ensure data quality.



Figure 4.25: Noggin 500® with a SmartTow configuration.
Photo of Edward Eastaugh by Kayla Golay Lausanne.

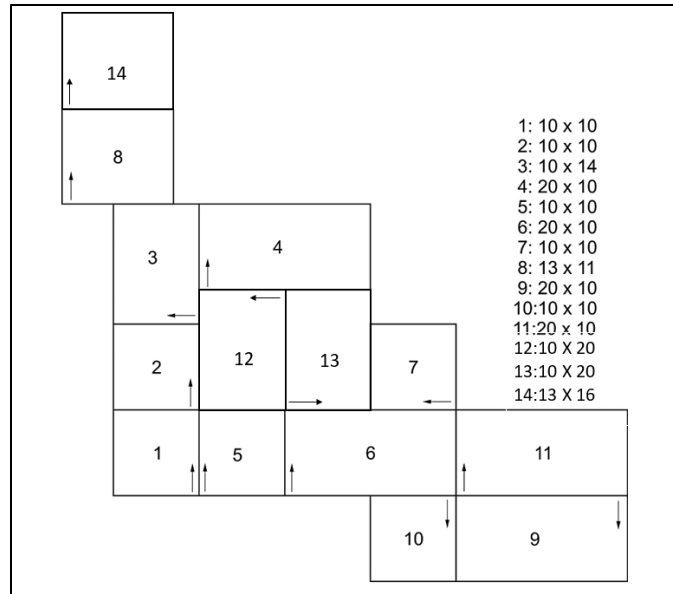


Figure 4.26: GPR Grid

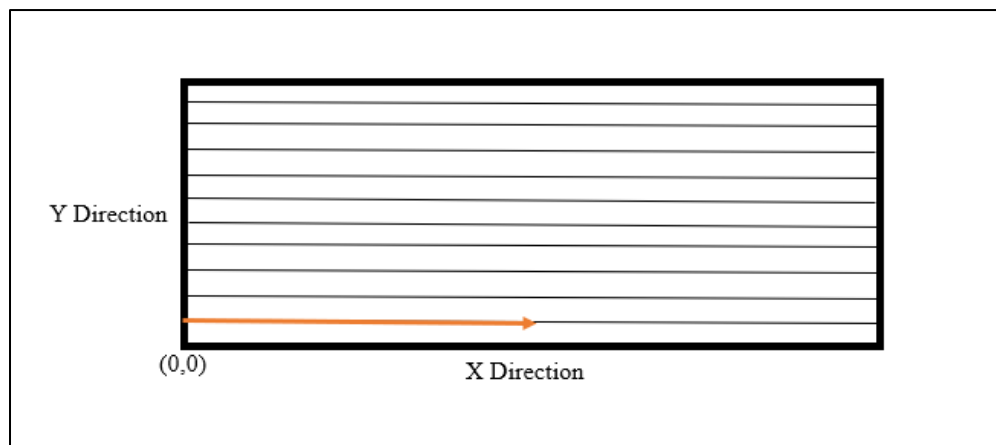


Figure 4.27: GPR forward parallel survey; Transect always starts on Y axis and is parallel to X axis

4.3.2 Processing

The GPR results are processed in EKKO_Project, a software used for the organization, processing, and display of GPR data. Each grid was processed individually to increase the quality of the results. Three filters were applied to each grid: migration envelope and Dewow. Migration is a 2D filter process that corrects for GPR based offsets in the data set (Sensors & Software Inc. 2015). Anomalies in GPR data sets appear as hyperbolas; this is because, as it moves along a transect, the GPR unit initially records the

buried object as it is travelling towards it, records the object again when it is above it, and finally records it as it moves away (Figure 4.28). The migration process collapses hyperbolic response into single points based on a given ground velocity; in this case, the velocity of radar waves propagating through dry sand (0.12m/s) (Figure 4.29b). The envelope process converts the oscillatory black and white (+/-) nature of the radar waves to a single of only positives, making the results easier to read. Dewow is a time- (i.e. Depth-) based filter that removes nonlinear noises, known as wow, which result from the antenna (Sensors & Software Inc. 2015). Dewow removes unwanted low frequencies while preserving high-frequency singles. This is done by applying a running average to each trace; the average value of all points is calculated and subtracted from the central point. This process then moves along each trace and repeated point by point (Figure 4.29c). Once these processes were completed, the gain and contrast were adjusted for each grid to create an image with clear features. The gain function is crucial as it increases the visualization of weak signals. Radar signals generally decrease with depth, thus applying the gain function enhances the appearance of weak signals at depth. Additionally, the contrast and saturation of each image can be adjusted to increase the visibility of features (Figure 4.30). Once this processing has been completed, a 3D model of each grid was created. From each model, the software allows the user to move through depth-slices. These are individual images that showed all anomalies within a specific depth range. In this case, all depth slices were set to 5cm deep.

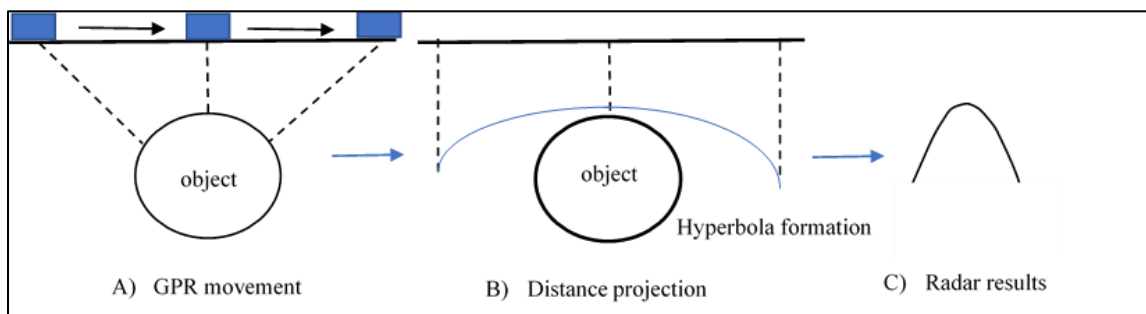


Figure 4.28: GPR hyperbola formation (Adapted from Ristić et al. 2017)

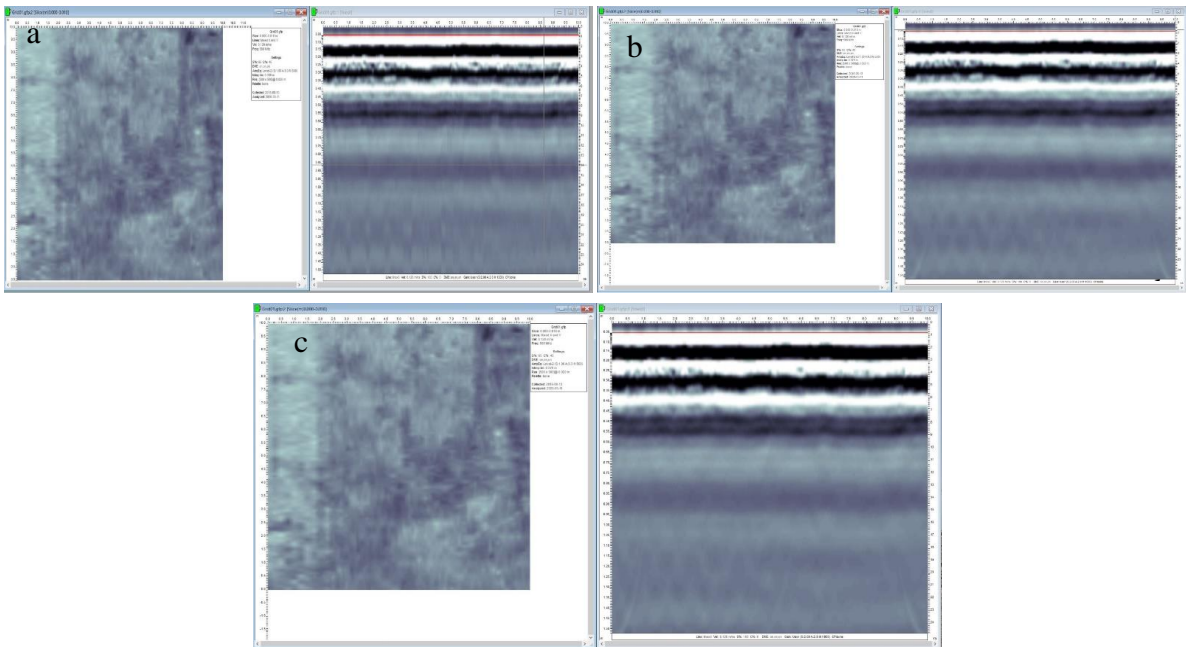


Figure 4.29: (a) Unprocessed results; (b) Migration applied; (c) Dewow and envelope applied

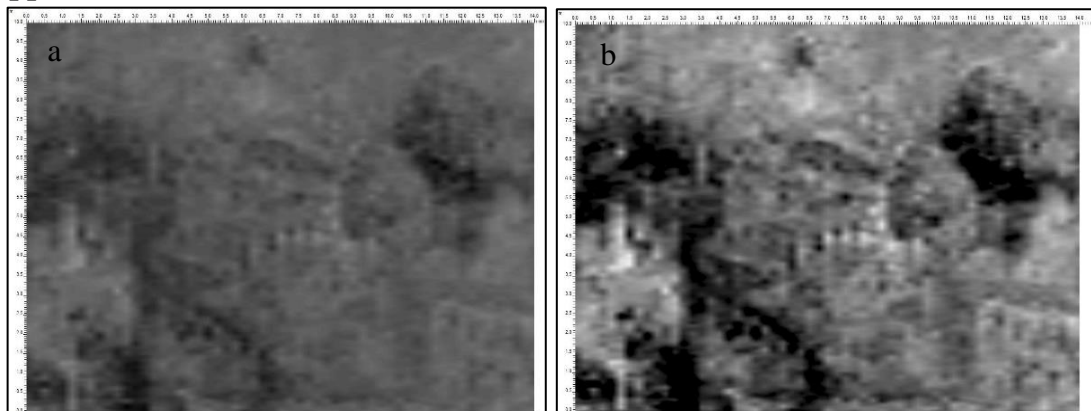


Figure 4.30: Grid 12: (a) saturation 70%, contrast 20%; (b) saturation 40%, contrast 20%

An image of each depth-slice was exported and used for digitization, producing a final processed GPR map of the survey area (Figure 4.31). Unfortunately, after approximately 25cm, there is a substantial amount of noise with no identifiable features.



Figure 4.31: Final processed images of GPR survey 0-10cm

4.3.3 Post-Processing

Processed results were uploaded into ArcMap, where they were georeferenced to the survey grids. Walls were digitized in the same way as for the aerial imagery; each wall face was marked with a polyline to document the width of each wall. Anomalies were digitized as walls if they were linear anomalies. The final digitized image of the GPR imagery identified numerous rooms (Figure 4.32).

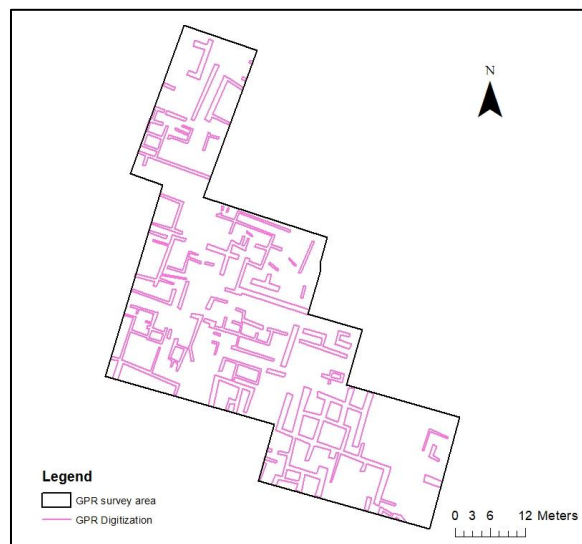


Figure 4.32: Digitized GPR results

4.3.4 Ground-truthing

The GPR results from HP-1 are nearly identical to ground-truthing results of the same area (Figure 4.33). All the walls in the northwest corner were identified except for one, possibly due to its small size, causing it to appear as part of another wall. Additionally, wall width appears to be slightly different from the known walls. This is most likely due to the minimal contrast between values within the results. HP-2 has similar results with the identification of each wall found through ground-truthing (Figure 4.34). The close alignment of GPR results with ground-truthing results confirms the ability of the GPR to pick up buried structures at Las Colmenas with accuracy.

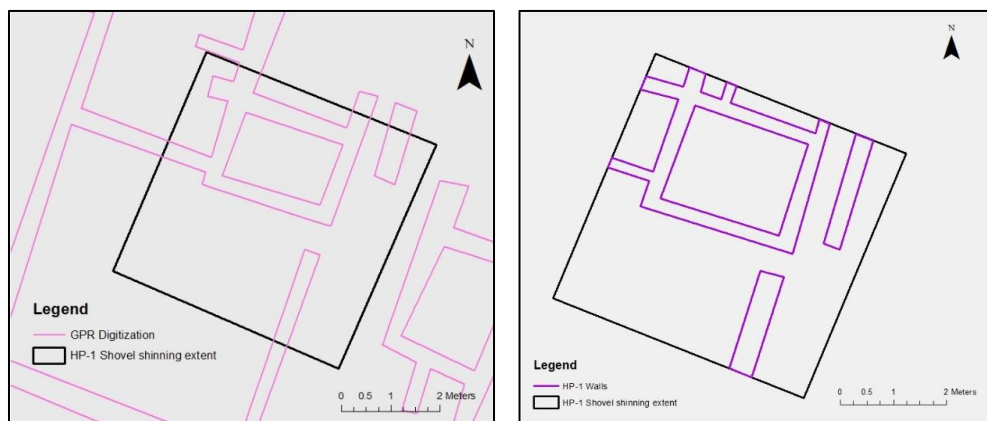


Figure 4.33: HP-1. Left - GPR results; Right - Shovel shinning



Figure 4.34: HP-2. Left - GPR results; Right - Shovel shinning

4.3.5 Trends

The first and most notable trend with the GPR data set is the lack of results below 25cm. While the GPR was set to record up to 1.5 meter in depth, results below the first 25cm were extremely noisy. This is most likely due to interference from conductive soils. The depth penetration of GPR radio waves is determined by the electrical conductivity of the materials being assessed (Daniels 2005). Having an increased electrical conductivity of the soils causes rapid attenuation of the radar energy, restricting the depth to which the waves can travel (Daniels 2005). Soils with heavy clay content, specifically soil rich in high cation-exchange capacity minerals such as smectite, have increased electrical conductivity (Saarenketo 1998). While the adobe at Las Colmenas and within the Gallinazo group did not undergo petrographic analysis, the mere presence of clay can cause increased attenuation. Another aspect affecting the electrical conductivity of soil is salt and moisture content. A high salinity context increases attenuation; since Las Colmenas is close to the ocean, there is an increased salt content in the soil resulting in high changes of attenuation. Increased moisture can also cause attenuation; clay grains have low porosity and thus high retention of moisture. If the soil is too wet, it will cause attenuation. This fieldwork was conducted during the 'wet' season in Peru. While this region of the country is arid, with minimal rain, there were occasions throughout the field season where there was light rain. Between the presence of clay, salt, and moisture, the electrical conductivity of the soil would have been high, resulting in the lack of depth penetration seen in this data set.

Another noteworthy factor is the lack of high contrast between adobe and matrix soil within this data set. Adobe erosion into the surrounding soil can decrease the dielectric constant difference between the sand and the adobe, causing a smaller variation to be assessed by the GPR. On the surface of Las Colmenas, there is a clear presence of eroded adobe in the soil, most likely affecting the appearance of the GPR results. This, combined with the issues discussed above, results in less-than-ideal environmental conditions for successful results. In addition, when comparing the results to the 2008 GPR conducted at Huaca Gallinazo (Millaire and Eastaugh 2014), where the environmental conditions are the same, there is a clear difference in the quality of the

results (Figure 4.35). It is noteworthy that the survey conducted at Huaca Gallinazo was done after the area had been shovel shinned. The topsoil was removed, which would have removed an abundance of eroded material, increasing the visibility of near-surface

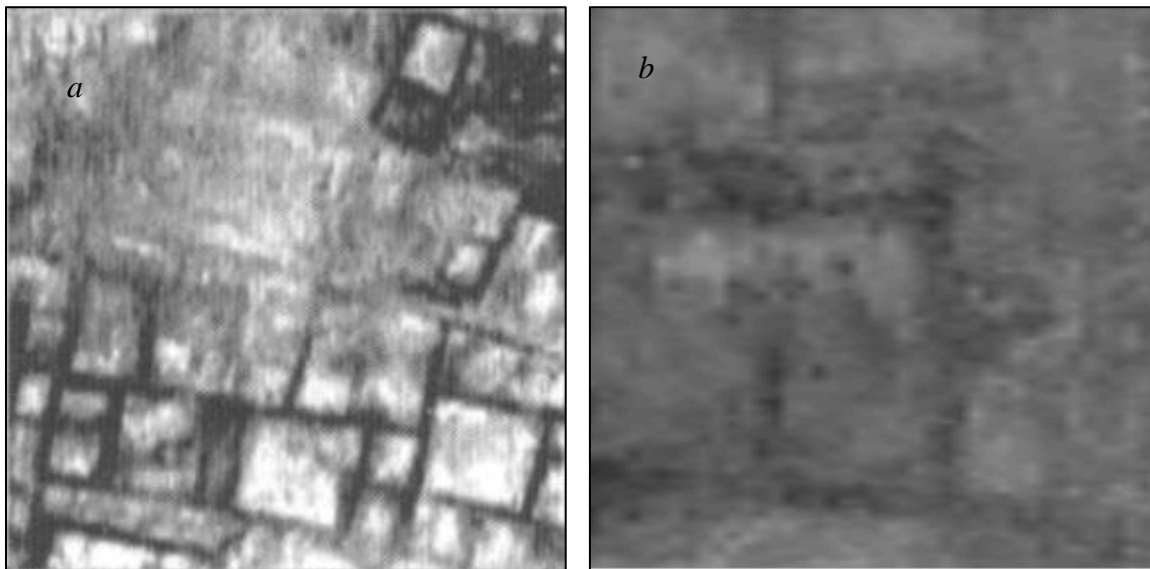


Figure 4.35: (a) GPR results from Huaca Gallinazo (Millaire and Eastaugh 2014); (b) GPR results from Las Colmenas features.

This survey provided an opportunity to test GPR results after clearing vegetation. Grid 11 corresponds to an area previously covered in large plant growth (Figure 4.36). Despite having removed the plant growth, moisture retention and most likely buried portions of the plant still affected the visibility of features buried below.

While there are definite factors influencing the success of the GPR results, this data set still provides an ample amount of information from 0-25cm. The results are moderately clear, but once digitized, numerous rooms could be clearly defined. The final map reveals an intricate system of walls following mostly the same orientation.

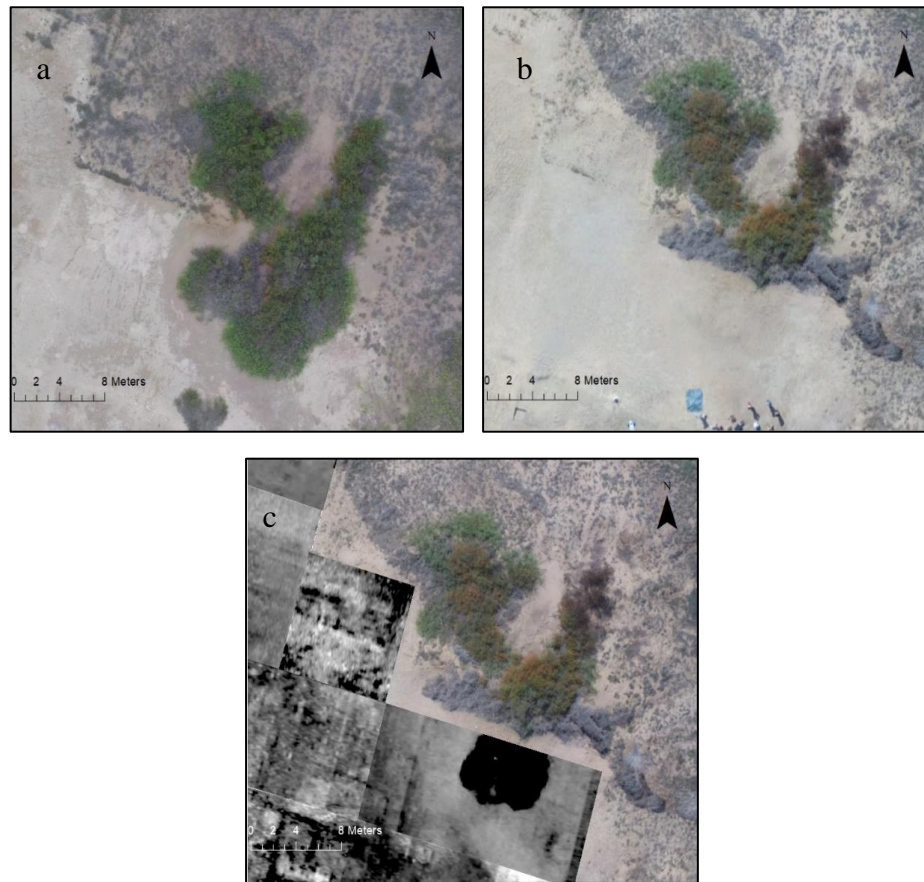


Figure 4.36: (a) area prior to vegetation removal (2018); (b) after vegetation removal (2019); (c) GPR results (2018)

5 Discussion

In recent years, archaeological prospection has seen significant advancements in the variety and resolution of remote sensing instrumentation. The tools continue to improve in speed and quality, making them more popular throughout archaeological practice. With these advances, attention has been given to the integration of multiple remote sensing techniques in order to limit issues associated with individual techniques. This thesis aimed to demonstrate the benefits of integrating results from multiple remote sensing sources at multiple scales. The project addressed two research questions: (1) What technique(s) worked best to identify the buried features at Las Colmenas? (2) What combinations of techniques proved to be most optimal for identifying buried features, and what are the benefits and limitations of using an integrated approach?

This chapter is separated into two sections that address each of the research questions. Question one assesses the techniques individually, with side-by-side comparisons, a common practice in remote sensing work. This allows for an understanding of what techniques worked best in a given environment. Question two moves to an integrated analysis that combines the surveys into one map to understand what techniques revealed confirmatory, complementary, or new information. Confirmatory data is consistent across multiple methods; thus, the additional method would confirm the presence of these features. Complementary data provides additional data that complements existing data. Lastly, new data is data that is entirely different from data obtained through other methods and does not combine with the existing data. An example of new data is a wall with an alignment that contrasts with surrounding walls. By integrating methods, we can make assumptions regarding the best combinations of techniques for assessing buried architecture at Las Colmenas.

5.1 Individual technique assessment

By assessing what features were identified by each technique and its limitations, we can suggest what remote sensing techniques work best in this dry, sandy-silty environment. Individually, each technique provided useful information regarding the

subterranean structures at Las Colmenas. The optical UAV survey revealed an array of walls across the northern portion of the site, with most identification in vegetated areas. The DEM from this survey outlined raised structures across the site. The thermal UAV survey outlined walls throughout both vegetated and soil-covered areas. The close-interval magnetic susceptibility survey identified buried features across its survey area, including rooms. The broad-scale magnetic susceptibility survey suggested increased occupation on the northern portion of the site. The magnetometer identified possible hearths, and the ground-penetrating radar documented an intricate system of rooms and walls. However, none of the techniques identified every anomaly identified by the other methods. This suggests the use of multiple remote sensing techniques increases the chance of identifying features in a given environment.

When comparing the aerial surveys, we can identify which of these two macro-scale surveys worked best to identify subsurface features at Las Colmenas (Figure 5.1). The thermal imaging detected more features than the optical imagery (Figure 5.2); this is in part due to the fact the thermal imagery can detect more features in soil-covered areas (Figure 5.3). There is minimal surface evidence of the buried adobe structures throughout soil-covered areas; this makes the detection of these features with optical imagery difficult or impossible to detect. While the DEM produced from the optical imagery shows increased details of the elevated features, a DEM can also be produced from Thermal imagery. Overall, of the two aerial surveys, the thermal imagery was more successful at identifying subsurface features at Las Colmenas.

Each of the ground-based remote sensing techniques offered insight regarding the buried features. When comparing the results of these three techniques (Figure 5.4), it is evident that each provided a different kind of information due to the different aspects of physical properties that each technique assesses. The GPR survey and close-interval magnetic

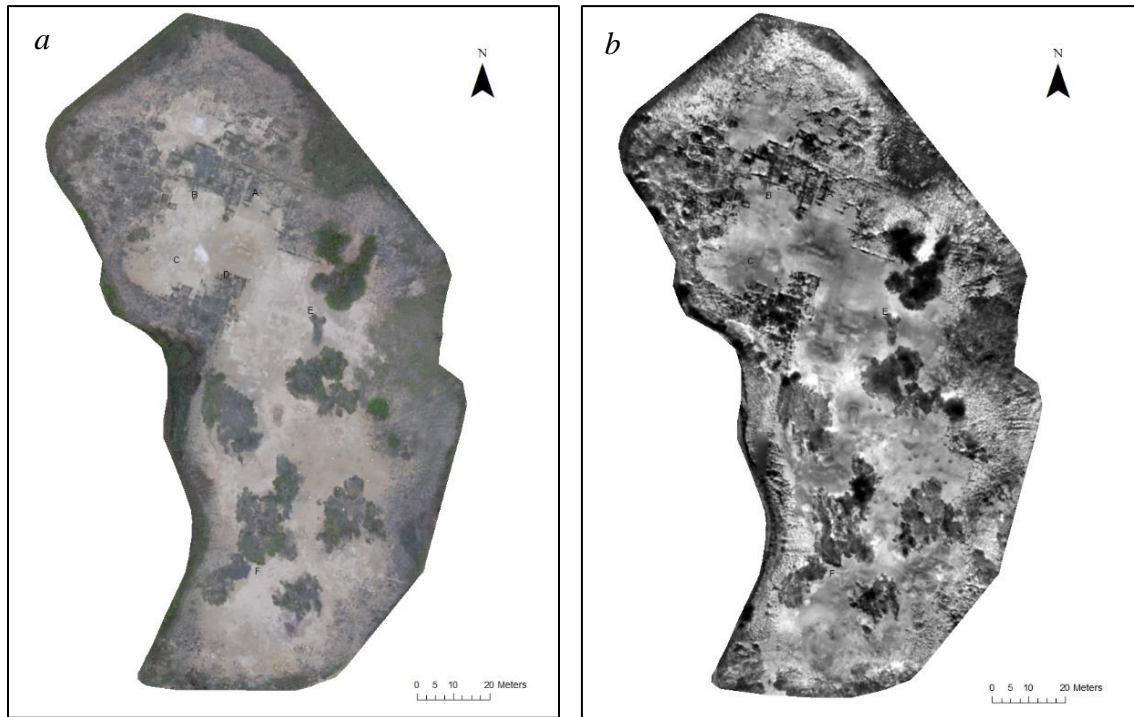


Figure 5.1: (a) Optical UAV survey; (b) Thermal UAV survey



Figure 5.2: Aerial survey digitization comparison. (a) Optical UAV survey; (b) Thermal UAV survey



Figure 5.3: Aerial survey comparison, vegetation versus soil. (a) Optical UAV survey; (b) Thermal UAV survey

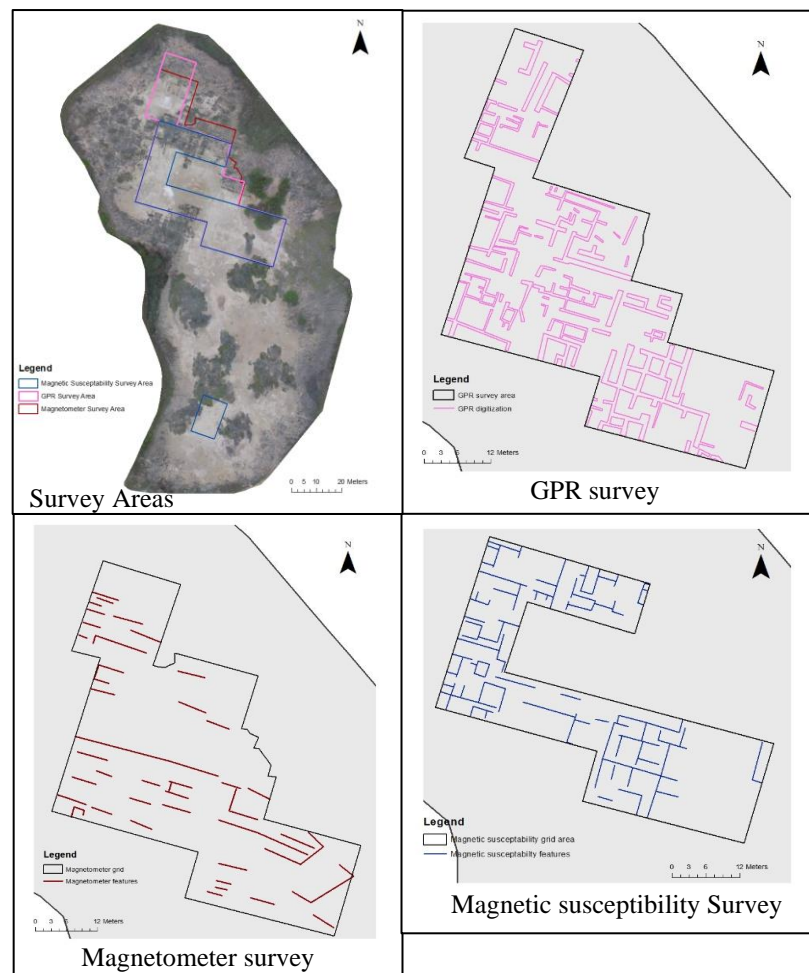


Figure 5.4: Comparison of ground-based remote sensing surveys

susceptibility survey show a similar number of features compared to the magnetometer, which revealed very few walls. However, the magnetometer did identify two potential hearth features, which were not identified in the other two ground-based methods and anomalies in the East, not identified by thermal or magnetic susceptibility surveys. This information is useful in determining the functional aspects of rooms. While the magnetometer survey determined the presence of archaeological features, the results yielded minimal information. The magnetic susceptibility close-interval survey revealed a substantial number of features. However, they cannot be defined as walls with one hundred percent certainty, versus space which included high susceptibility readings, such as a hearth or area of increased soil accumulation, such as the bottom of a knoll. Additionally, the width of the features can only be estimated. The broad-scale survey identified increased occupation on the northern portion of the site and defined the limits of the site. Of all ground-based techniques, the GPR proved to be the most useful, identifying an abundance of features and allowing for the production of a detailed map of the buried features.

Although the GPR appears to identify the greatest number of features amongst the ground-based remote sensing techniques and the thermal UAV survey amongst the aerial surveys, we cannot accurately determine which technique(s) identified more without considering the survey results over the same area. By doing so, we can assess the ability of each technique to document buried features in relation to another technique (Figure 5.5). Based on the previous discussion, GPR, magnetic susceptibility, and thermal imaging appear to be the three techniques that revealed the most information when comparing the techniques within their scale (aerial vs ground-based). However, by comparing each result within the same area, we can compare the capabilities of each technique between macro and micro-scale surveys. Figure 5.5 reveals the results of each technique over the same survey area. From this, it is clear that the thermal UAV, magnetic susceptibility, and GPR surveys remain the top techniques to reveal sub-surface features of this nature within in this environment. What is most clear is that the GPR gathered more information than any other technique within this area. However, there are still a few areas where features were not identified by the GPR but were picked up by another technique. Figure 5.6 offers a good example of this phenomenon, also showing

that features identified by the thermal UAV survey were missed by the magnetic susceptibility survey.

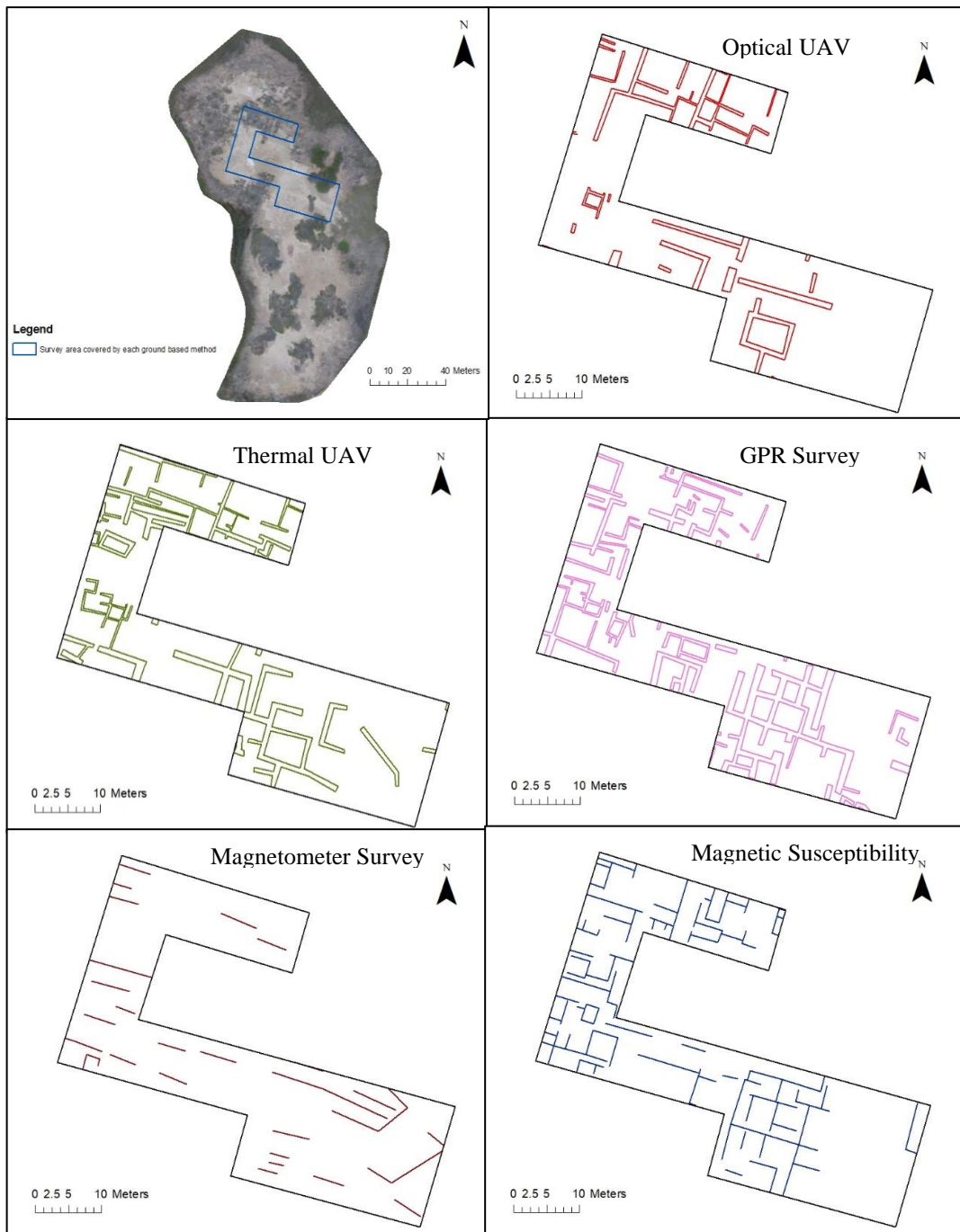


Figure 5.5: Comparison of all surveys over the same grid



Figure 5.6: Comparison of GPR, magnetic susceptibility, and thermal UAV survey results

The two surveys which yield little to no additional information regarding the buried features of Las Colmenas are the magnetometer and optical UAV surveys. While the magnetometer identified two features in Figure 5.5, as previously discussed (Section 4.2.5), these are most likely deposits of burnt material at the base of the knolls adjacent to each feature. Besides this anomaly, most features are identified by another technique. Likewise, the optical UAV survey provides little information in comparison to the thermal, GPR and magnetic susceptibility surveys. Nearly every feature within the optical UAV survey over this area is also documented in the thermal or GPR results.

Through this side-by-side comparison of each technique, as well as the individual results, it is clear that each method has its own merits, but they also have limitations. Table 5.1 identifies the strengths and weaknesses of the five remote sensing methods used in this project. No technique identified all walls in ground-truthing, but they did identify different aspects of the sub-surface features due to the physical properties they each assess. Having a comprehensive understanding of the strengths and weaknesses of each technique is important when considering what method would best suit a given project.

Table 5.1: Strengths and weaknesses of the remote sensing surveys techniques used in this project

Technique	All walls present in ground-truthing (Y/N)	Depth penetration at Las Colmenas	Strengths	Weaknesses
Optical UAV	N	0cm	<ul style="list-style-type: none"> •High-resolution data •Rapid assessment •Covers large area •Provides DEM •Identifies crop marks •Identification of large, continuous features 	<ul style="list-style-type: none"> •Difficulties identifying soil marks •Dependent on light and environmental conditions •Shallow depth features •Specialized software processing
Thermal UAV	N	50cm*	<ul style="list-style-type: none"> •High-resolution data •Rapid assessment •Covers large area •Provides DEM •Identifies crop and soil marks •Identification of large, continuous features 	<ul style="list-style-type: none"> •Variations in thermal emissivity between features •Specialized software processing •Dependent on light and environmental conditions
Magnetic Susceptibility	N	15cm	<ul style="list-style-type: none"> •Rapid assessment •Identify occupation extent •Identify burnt features and areas of increased burning •Can conduct different survey interval types (broad and close) 	<ul style="list-style-type: none"> •Near-surface anomalies only •Low-resolution, meaning no width of features can be determined
Magnetometer	N	1m	<ul style="list-style-type: none"> •Detection of burnt material and hearths •Increased survey depth 	<ul style="list-style-type: none"> •Heavily reliant on environmental conditions •Difficult to assess all features when at geomagnetic equator; no north-south anomalies •Sensitive to any metal objects •Need to keep sensors parallel to ground at all times •Width of features is not documented
Ground-penetrating Radar	N	25cm	<ul style="list-style-type: none"> •High resolution data •Provides stratigraphic images •Locates geomorphological features •Determine depth of features 	<ul style="list-style-type: none"> •Not ideal for all terrains; need flat ground surface •Specialized implementation and processing •Strongly affected by environmental and geological conditions •25cm depth

* Suggested depth penetration based on previous scholars work (Casana et al. 2017)

The use of various remote sensing methods can illuminate several different research goals, from archaeological potential to recording the extent and nature of an urban plan. An important aspect to consider when selecting a remote sensing method is the research goals and which remote sensing techniques are best suited to achieve those goals. Due to the fundamental variations in the physical properties which each method assess, each technique identified different types of features, as seen in Table 5.2. Therefore, while the GPR, thermal UAV, and magnetic susceptibility surveys identified more features, they still identified different features from each other. The magnetic susceptibility survey was able to identify areas of increased activity, areas of burning, as well as the limits of the

site. The magnetometer identified hearth features and that archaeology is present at this site. The GPR, while well suited to revealing the subsurface features, could not be used to determine the limits of the site due to the conditions required to complete a survey, such as immediate contact with the ground and smooth terrain. The GPR was also unable to identify hearths or burnt areas and could not determine areas of increased occupation. Thus, in order to select a tool to use, the goals of the project must be considered.

Table 5.2: Type of features identified by each method

Method	Type of archaeology it assesses	Identification of features at Las Colmenas
Optical UAV	<ul style="list-style-type: none"> •Near-surface features with crop or soil marks •Walls and floors 	<ul style="list-style-type: none"> •Areas of occupation • Large, long walls
Thermal UAV	<ul style="list-style-type: none"> •Near-surface features with variations in thermal emissivity •Walls and floors 	<ul style="list-style-type: none"> •Areas of occupation • Large, long walls • Few smaller walls • Potentially deeper walls than immediately at the surface
Magnetic Susceptibility	<ul style="list-style-type: none"> •Features within the top 15cm with fluctuations in induced magnetism •Walls with contrasting values •Rooms with contrasting values between walls and floors 	<ul style="list-style-type: none"> •Boundaries of magnetic susceptibility differences (e.g. walls and rooms)
Magnetometer	<ul style="list-style-type: none"> • Features up to a meter deep with fluctuations of induced and permanent magnetism •Hearths •Walls •Areas of increased burning 	<ul style="list-style-type: none"> •Potential hearths •Potentially identifying deeper buried walls
Ground-penetrating Radar	<ul style="list-style-type: none"> • Features up to a meter deep with differences in their dielectric constant (permability) •Walls and floors 	<ul style="list-style-type: none"> •Detailed smaller walls and rooms

While this research project explored the potential of a multifaceted approach of remote sensing within an archaeological context, it also identified limitations within the remote sensing techniques in this specific environment. These limitations are summarized in Table 5.1 and discussed below.

The optical UAV survey identified minimal walls in areas without vegetation cover. Even by enhancing the contrast between colours, it was challenging to determine buried structures from the soil in such areas. While the thermal UAV survey was not affected by this issue, it still failed to identify some walls. This is most likely due to variations in the thermal emissivity of the buried features. The magnetic susceptibility survey did not identify all buried walls; because it requires differences in susceptibility to identify boundaries. If a wall does not have a different susceptibility reading than the sounding soil, it cannot be identified. Additionally, a magnetic susceptibility survey cannot identify the width of the features due to the intervals used in this survey. The magnetometer had the most limitations at Las Colmenas, as it failed to identify features that followed a north-south orientation due to the minimal difference between the feature orientation and the orientation of the magnetic equator. Lastly, the GPR survey failed to identify any feature below 25cm due to the geomorphological conditions of the site. Likewise, there was minimal contrast between the adobe features and the background soil, producing results that were more difficult to interpret.

An additional issue faced within this research project was the site conditions, which limited the use of close-interval ground-based surveys on parts of the site. There was increased human disturbance (i.e. looters pits and beehives) on the southern portion of the site, making it impossible to conduct close-interval surveys across the site. The periphery of the site was a steep and undulating surface, making it inaccessible to the ground-based techniques.

Despite the limitations of each method, the remote sensing methods used within this project allowed for rapid and non-invasive imaging of the archaeological landscape of Las Colmenas. From this assessment, it is clear that the GPR, magnetic susceptibility, and thermal UAV methods identified the greatest number of features. There is the chance that a technique could perhaps provide purely confirmatory information and not provide any new information. As such, it is essential to not only provide a side-by-side analysis of each technique but integrate the methods to understand what each technique brings to the table. Likewise, the integration of multiple techniques can reduce these limitations.

5.2 Integrated technique assessment

The GPR, magnetic susceptibility, and thermal UAV surveys each provided important information about the buried features at Las Colmenas. We also just suggested that it is the integration of these methods that provide researchers with the richest and most nuanced datasets for assessing the ancient occupation of an archaeological site. This section integrates multiple sets of remote sensing data with GIS to produce continuous and complex visualizations of the buried features.

Given that the thermal UAV survey generated the largest amount of information, those results were usually used as the base map onto which other survey results were added. The following protocol was used when integrating the datasets:

- 1) All complimentary and confirmatory features were included in the final map.
- 2) New data was also included unless the new data present in one dataset contradicted complimentary or confirmatory data in another set; in this case, the confirmatory or complimentary data was given priority.
- 3) In cases where the method did not provide wall width (magnetometer and magnetic susceptibility), the wall width was estimated based on the thickness of nearby walls identified through another method.

One issue with the integration of this data is that it shows the features that are closest to the surface at any given point, irrespective of the erosion processes that took place. Indeed, given that the site of Las Colmenas is an eroded earthen mound, the features identified on the periphery of the site likely predate those identified on top of the mound, where little erosion occurred. Thus, one needs to be very careful when making inferences about the communities of people that lived in this location using information derived from this map alone.

The comparison of individual survey results identified the thermal UAV, GPR, and magnetic susceptibility surveys as the most successful surveys. Thus, maps with varying combinations of these techniques were created to ensure the production of maps with the most information. The maps focus on the northern portion of the site where there

was an abundance of data. By combining the magnetic susceptibility and the GPR results, a very detailed map of the surveyed area was created (Figure 5.7A). However, without including a macro-scale survey, the results are limited to a small region. The geophysical techniques increase our understanding of the smaller features within the structures providing a targeted and intensive survey. In contrast, the aerial surveys allowed for the assessment of the site at a grander scale, identifying larger and longer features that cross the entire site, providing the information required to recognize broadly distributed cultural patterns. However, it is useful to note that such a combination of surveys could not be extended to the surrounding survey area due to uneven topography of the site and to human disturbance. If a combination of techniques were to be used, a project would greatly benefit from the inclusion of a macro-scale survey and micro-scale survey.

By comparing the results of thermal UAV and GPR surveys (Figure 5.7B) with thermal UAV and magnetic susceptibility surveys (Figure 5.7C), it is evident that there are minor differences between the two integrated maps. However, the magnetic susceptibility results have to be taken with caution. Indeed, as previously mentioned, the magnetic susceptibility technique identifies boundaries between areas that are differently susceptible to being magnetized. Thus, while some boundaries could correspond to walls, they could also correspond to other types of sub-surface features. Nevertheless, the boundaries do appear to follow the same orientation as the walls in the thermal imaging, which suggests that they are indeed architectural. Between these two combinations, the results are relatively similar in the number of features identified, but they differed in what was identified. Figure 5.8a shows an area in which the GPR, in combination with the thermal imaging, allowed for more internal walls to be identified, whereas Figure 5.8b the magnetic susceptibility in combination with thermal imaging revealed more large external walls to be identified.

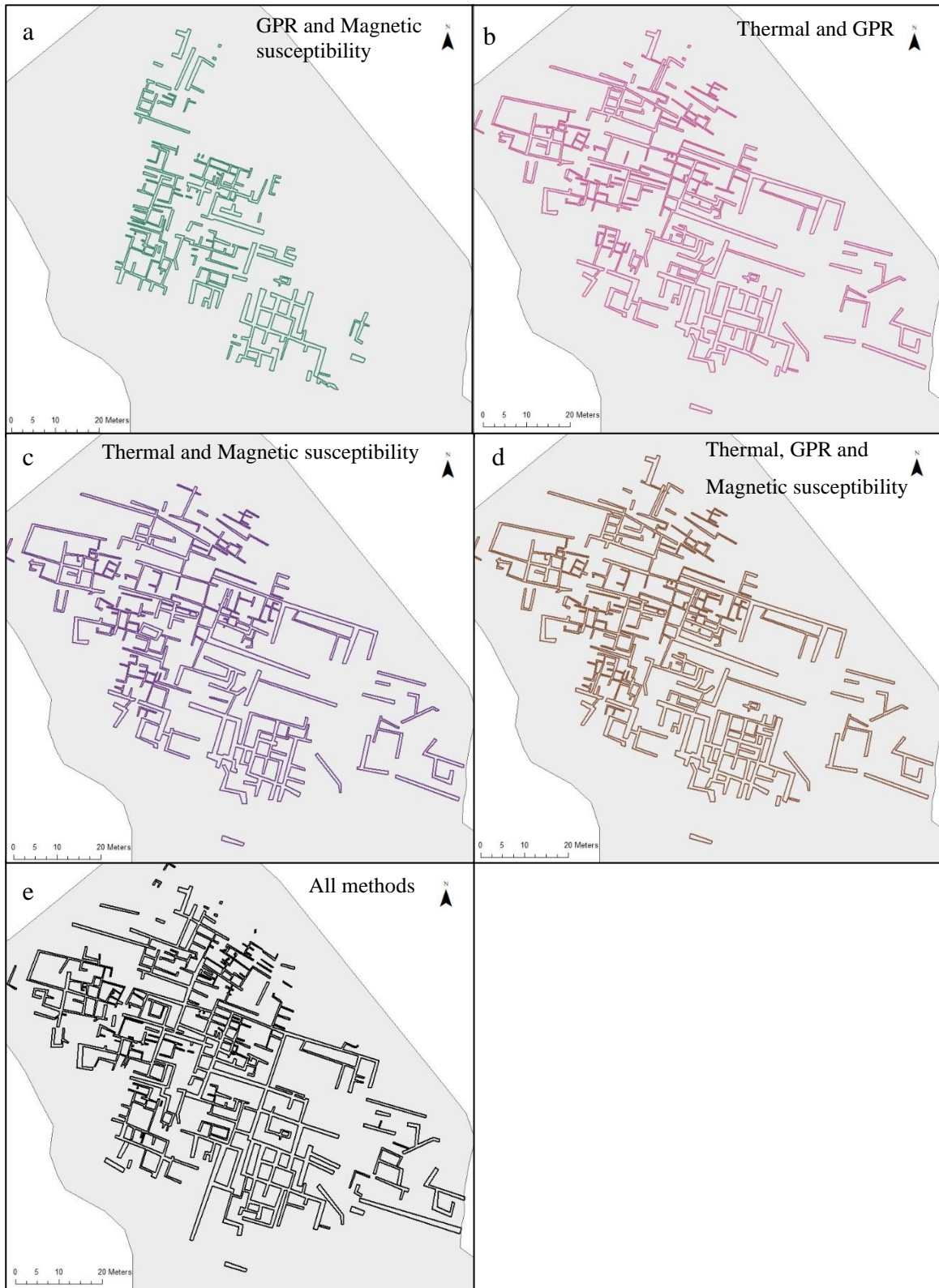


Figure 5.7: Various integrations of remote sensing results



Figure 5.8: (a) Comparison of thermal with GPR results; (b) thermal with magnetic susceptibility results.

The combination of thermal UAV, GPR, and magnetic susceptibility survey methods (Figure 5.7D) produces a dataset with numerous features across the entirety of the northern portion of the site, which integrated the large walls identified by the magnetic susceptibility survey, and the internal walls noted by the GPR survey. By comparing this map with Figure 5.7B and Figure 5.7C, it is clear that the more combinations of techniques added, the more detailed the map becomes. Throughout chapters 3 and 4, the geological conditions which each technique assesses are outlined. As such, each technique identifies different features due to the various aspects of the environment they assess, as outlined in Table 5.2. By having an understanding of the type of physical conditions each technique assesses, we can comment on the nature of the features that are identified. For example, some features identified through the magnetic susceptibility surveys suggested walls which have been burnt can lead to inferences regarding areas of cooking or perhaps leveling of structures prior to construction. Additionally, including more datasets provides increased opportunities for cross-validation (confirming the presence of a wall when it appeared in more than one set of results). This was especially helpful when the features identified by two distinct methods did not appear to follow the general orientation of the surrounding walls.

A combination of the five remote sensing techniques used throughout this project was incorporated into one single cohesive map (Figure 5.7E). The results show a complex system of rooms, compounds, plazas, and platforms. This map looks very similar to Figure 5.7D, which includes the thermal, GPR, and magnetic susceptibility surveys. Obviously, by incorporating two additional techniques — optical UAV and magnetometer — there are more features compared to the map incorporating three of the techniques. This indicates the additional techniques do not necessarily repeat the same features but are additive and provide more information regarding the subsurface features. However, the difference between the two maps is relatively minimal. Depending on the goal of the project, using three of the five techniques could provide enough information to address the research goals of the given project. Nevertheless, if the goal is to have a detailed map as possible, including these five techniques would be ideal.

Therefore, generally speaking, the more techniques used and combined, the more information ends up being collected. However, in the present case, the thermal imaging coupled with either the magnetic susceptibility or GPR survey provided the bulk of that information, which is something that needs to be considered when it comes to project design.

5.2.1 Benefits and limitations of a multifaceted remote sensing approach

One of the most attractive aspects of remote sensing work is its non-destructive nature. Remote sensing is a powerful non-destructive research method for the detection, mapping, and preservation of archaeology. The remote sensing surveys implemented in this project successfully provided information regarding the buried structures while leaving the structures intact and undisturbed. The only instance of invasive procedures was ground-truthing to compare results with known buried features. However, with respect to the size of the site, the two areas of shovel shining and small test units caused minimal ground disturbance. The map produced reveals a detailed urban plan for the northern portion of the site with only two small areas of ground disturbance versus having excavated the entire site.

The previous section has shown that increasing the number of sensors and including multiple scales as the investigation allows archaeologists to create increasingly more detailed maps of subsurface features which can be used to document specific anthropological questions, such as the nature of early urban planning. The largest benefit of a multifaceted approach to remote sensing is to provide confirmatory and complementary information and to generate new data. Confirmatory data helps cross-validate information provided by different remote sensing techniques, increasing the accuracy of our results and reducing the chance of false positives (identifying features that are not archaeological). Complementary data provides additional data that complements existing datasets. Finally, new data brings new information to the table that was not provided by other methods because of the specificity of a given sensor. Indeed, each sensor addresses a different aspect of geomorphological characteristics of the site, allowing for the identification of different features and phenomena (e.g. areas of burning, areas of occupation, raised buildings/platforms, etc.). Incorporating these different types of data provides a holistic and informative dataset.

An additional benefit of including multiple sensors is what could be defined as a double assurance plan. When a method does not work as part of field research, it can have a significant impact on the outcome of a project. Including multiple methods of data acquisition, therefore, increases the likelihood that at least one method will work and that the field research will be successful. This is especially important with geophysical analysis, given that sites with apparently ideal physical and geological conditions for the survey might not yield as much as expected. Another important aspect to consider is that equipment has a tendency to malfunction or break unexpectedly. Ensuring multiple sensors are used in given survey can minimize the impact an equipment failure and increase the chances that the field project will yield results.

While the techniques used in this project generated, for the most part, exquisite datasets, a number of limitations were noted that could affect the decisions of researchers when designing a multifaceted approach in other contexts. This includes geomorphological and environmental conditions, expertise, cost, and time required to

conduct the surveys, and the portability of the equipment. Each of these is discussed in the following sections.

5.2.1.1 Geomorphological and environmental conditions

While this is not strictly an issue with a multifaceted approach, as it is also a concern with remote sensing in general, the impact of geomorphological and environmental conditions must be considered. Throughout the methods section associated with each technique, we pointed out how each method could be affected by geological phenomena and physical conditions of the site. Whether it was an increase in salt concentration, a lack of differentiation between anomalies and background soil, or an increase in water saturation, the techniques might not record subsurface features anomalies. While aerial remote sensing techniques are less affected by geological anomalies, the three ground-based remote sensing techniques are reliant on ideal soil conditions.

Aerial surveys and ground-based surveys are also limited by environmental conditions. Areas that have dense vegetation cover obviously prevent aerial surveys, and uneven terrain prohibits the use of certain ground-based techniques. In addition, areas with no vegetation mean that no crop marks will be visible.

Resolution and depth are often an issue, especially when features are located deep below the surface. As was mentioned when describing the GPR survey, a decrease in resolution was noted with depth due to a high noise-to-feature ratio. The attenuation of the radar waves bouncing off salt crystals in the soil resulted in too much noise to view the archaeological features. The environmental and geological characteristics of a site, therefore, need to be considered before a decision is made regarding which remote sensing techniques will be used. Given that all archaeological sites are different, and no one technique is suited to address every situation, it is therefore essential for archaeologists to consider geological and environmental conditions as part of the research design. But, due to the physical properties which can hinder remote sensing results, multiple techniques are suggested to increase the likelihood of having results.

5.2.1.2 Expertise

Remote sensing is instrumentation-, software-, and interpretation-intensive. Each survey technique requires knowledge about the physics involved and the geological and environmental conditions that could potentially affect the results. This means that archaeologists who become surveyors usually have a steep learning curve ahead of them to obtain the kind of know-how that will allow them to obtain optimal results during fieldwork. Additionally, extensive expertise and experience are needed to determine if anomalies identified by remote sensing are, in fact, archaeological features or caused by other factors. Interpretation of the results is also tricky, as one is restricted to interpreting based on known structures and archaeological features. Thus, expertise regarding the types of archaeology in the area is extremely important when it comes to interpreting the results. The requirement of expertise leads to an additional issue, which has to do with the cost of paying for an expert if the surveyor does not have the required expertise and experience.

5.2.1.3 Cost and Time

Additional issues associated with the use of remote sensing techniques have to do with time and/or funding constraints. Purchasing equipment and software or hiring a specialist is often costly and can be prohibitive for archaeologists. A basic cost and time breakdown for each technique used in this project helps provide a holistic assessment of each technique. Table 5.3 presents the estimated cost of the equipment and software for each type of survey, which were used as part of this research project (in Canadian dollars before tax), but does not consider spare parts, such as batteries or propellers.

The prices for the equipment and software combos in 2020 range from \$4,755 to \$24,500: a remarkable range of \$20,000. The GPR and thermal UAV are similar in price, at the top of the scale, and the results of these surveys were by far the best. The thermal camera and drone estimates used for this cost analysis are based on the DJI Mavic 200 with the H20T thermal camera. However, the camera and drone used for the thermal and optical UAV surveys are no longer in production today, which points to another issue

Table 5.3: Cost analysis of remote sensing techniques employed in this project

Technique	Approximate Equipment cost * ¹	Processing software * ⁴	Total	Cost of equipment
Optical UAV * ²	6,873.00	5,610.00	12,483.00	Medium
Thermal UAV * ³	17,815.00	5,610.00	23,425.00	High
Magnetic Susceptibility	4,755.00	0.00	4,755.00	Lowest
Magnetometer	13,465.00	0.00 * ⁵	13,465.00	Medium
Ground-Penetrating Radar	20,500.00	4,000.00	24,500.00	Highest

*1 Average cost of available equipment in CAD.

*2 Cost of camera and drone similar to one used in this project. Cheaper but lower quality cameras are available.

*3 Cost of camera and drone similar to one used this project. Cheaper but lower quality cameras are available.

*4 Excluding cost of GIS software needed to digitize each result data set, in CAD

*5 This is based on the free Snuffle software. Can purchase software, such as Geoplot and Terrasurveyor, but that is at the discretion of the purchaser.

with those technologies: equipment becomes obsolete quickly, replaced with models that are more powerful and sometimes cheaper. For example, drones with increased accuracy and flight time are already available on the market, and the prices keep going down.

In relation to budget, another aspect to consider is the cost of infield personnel. Personnel costs are affected by the survey size used and the number of people required for each survey type. Additionally, the cost difference between an expert and a technician needs to be considered. However, for the purpose of this estimated assessment, this is not included. Post-field expenses, such as data processing, were also not included in this analysis. Such time and expenses were excluded due to non-measurable aspects of analysis and the accumulation of numerous variables, such as computer requirements, and expert knowledge of the software.

Table 5.4: Time to complete surveys for each remote sensing technique employed in this project

Technique	Minutes per 200m ² * ¹	Persons required	Minutes per 200m ² based on persons required	Speed
Optical UAV	0.0521	1	0.0521	Fastest
Thermal UAV	0.0681	1	0.0681	Faster
Magnetic Susceptibility: broad-interval	10	1	10	Fast
Magnetic Susceptibility: close interval	20	2	40	Slow
Magnetometer	20	3	60	Slower
Ground-Penetrating Radar	60	2	120	Slowest

*1 time for implementation of survey only, not setup.

Table 5.4 presents the time it took each for each technique to complete a survey over an area of 200m². This does not consider the time it took to set up the surveys. However, the ground-based surveys would have a longer set up, as a grid is required in most cases. Since two different methods were employed for the magnetic susceptibility survey, both are considered as separate methods here due to differences in the number of people and time required to conduct the survey. Based on time in the field and people required, the most cost-effective methods are the UAV surveys. The time variation between the two aerial techniques is minimal. However, thermal imaging takes more time as the UAV must be flown closer to the surface of the site. There is a large contrast between the time required to complete the UAV surveys and the GPR surveys. The GPR took the longest, as the grid intervals required are smaller, and at least two people are required.

Table 5.5 combines the results of the previous two tables, with an estimate in the quality of results based on the need for a map of the subsurface features. Generally speaking, higher quality survey methods come at the highest price. However, the magnetic susceptibility surveys provide informative results at a relatively low cost. In fact, both types of surveys can be conducted with only one piece of equipment, making them the most cost-effective solution for archaeologists who wish to enter the field of remote sensing. The optical UAV survey also proved to be a relatively cost-effective survey method that yielded respectable results.

Table 5.5: Comparison of speed, cost and quality of results for each remote sensing technique employed in this project

Technique	Speed by people minutes	Cost of equipment	Quality of results
Optical UAV	Fastest	Medium	Good
Thermal UAV	Faster	Highest	Best
Magnetic Susceptibility: broad-interval	Fast	Lowest	OK
Magnetic Susceptibility: close interval	Slow	Lowest	Very good
Magnetometer	Slower	Medium	Poor
Ground-penetrating Radar	Slowest	High	Best

An additional cost not included here, but essential to consider is the cost of spare parts. The flight time for each UAV battery used within this project was low, which forced us to purchase six batteries for the UAVs, increasing equipment costs, and increasing survey time because of the need to periodically change the battery. For UAVs, another issue has to do with the need to carry spare blades, as these tend to break easily during the survey.

5.2.1.4 Portability

A significant issue not often considered when purchasing equipment is portability. If travelling with equipment, individuals must be aware of airline restrictions. For instance, bringing multiple pieces of equipment on a plane can become prohibitive. Batteries can also be challenging when it comes to air travel. For instance, during this project, the GPR battery was not allowed on the plane, and we had to purchase an additional battery once in Peru. The weight of the equipment can also be an issue when travelling with specific weight restrictions, such as small aircraft travelling to the Arctic. Travel to and from the archaeological site with the equipment is another important variable to consider. Indeed, if the survey site is not accessible by vehicle, one must be prepared to carry the equipment on foot. Carrying multiple pieces of equipment to a remote location can be difficult: for example, previous fieldwork in the Moche Valley and upper Virú Valley revealed how cumbersome it was to carry a GPR and large drone up mountains, leading our team to rapidly revise our survey protocol.

5.2.2 Conclusion

There are clearly many obstacles in working with remote sensing and multiple sets of equipment. However, in this project, the benefits of using an integrated approach greatly outweighed those obstacles. We found that the thermal UAV, GPR, and magnetic susceptibility surveys worked best to identify the buried structures at Las Colmenas. Additionally, we noted the importance of integrating multiple techniques across two different scales to produce the best results. The complete suite of the five remote sensing techniques —thermal UAV, optical UAV, magnetic susceptibility, magnetometer, and

GPR surveys— each in its own right helped produce a detailed map of the subsurface archaeological features at the site. However, it was noted that a smaller combination of techniques could produce similar results, something which would inevitably translate into time and cost savings in any given context.

6 Conclusion

The primary aim of this thesis was to assess the use of a suite of remote sensing techniques in specific environmental conditions at the site of Las Colmenas (V-157), on the north coast of Peru. The secondary aim was to integrate various combinations of remote sensing techniques to assess the benefit of using multiple techniques in this specific archaeological context. The ultimate goal of the study was to assess the benefits and limitations of using an integrated, multifaceted approach to map sub-surface features in the context of an early urban environment.

The results of each technique made it clear that the thermal UAV, magnetic susceptibility, and GPR surveys were the most informative of the five methods used. These three methods highlighted a large portion of the features on the northern part of the site. When compared side-by-side, these methods identified numerous features, but it is difficult to determine whether these three techniques are producing confirmatory or complementary data or if they identified new features. When compared to the ground-truthing results, however, none of the techniques could locate all the buried features, pointing to the importance of a multifaceted approach to remote sensing for enhancing the quality of the survey work.

The integration of the thermal UAV, magnetic susceptibility, and GPR surveys into various maps highlighted three different trends. Firstly, restricting the analysis to a single scale risks a loss of information; incorporating these two scales into a single dataset ensured that smaller features and site-wide features are being considered. A second trend highlighted is that each method helps identify new and complementary data. Each technique assesses different aspects of the buried features, between changes in velocity, burnt, or decomposing material, to voids in surface vegetation and discoloration of soil. Since each technique relies on a specific set of physical parameters, they each contribute unique and differing perspectives on the buried structure, something that can be exploited through a multifaceted approach to produce a more refined and holistic understanding of the features. This leads to the third trend: the fact that the more datasets

that are integrated into a single map, the more information is revealed about the subsurface features.

While multi-sensor and multi-scale methodologies have proven useful in the identification of features, as we have seen, it is not always feasible to opt for such a range of methods due to environmental, financial, time, expertise, and portability constraints. Remote sensing methods are strongly dependent on the ideal environmental and geomorphological conditions of the study site. However, these issues can be overcome by considering the proper techniques based on the conditions of the site and integrating a wide range of methods to overcome limitations. Expertise, cost and time are all major aspects to consider when incorporating multiple techniques. However, the outcomes are incredibly positive. This thesis provided a basic cost analysis of each method, in reference to the quality of results to show archaeologists the various options available which may fit within the budget of the project. However, one issue that should be considered before using multiple, or even a single remote sensing technique, is the portability of the equipment. Throughout this project, as well as other projects in the Moche Valley and Upper Virú Valley, the transportation of equipment to field sites was a major concern for the team and one that often ended up determining which combination of methods would be used in a given environment.

Despite these limitations, this thesis concludes that combining different remote sensing methods contributes to a better-supported dataset and stronger interpretations of subsurface features. Indeed, each method individually allows for the acquisition of limited information on sub-surface features, and therefore usually can only partially help address specific research questions, such as to document the ancient urban morphology of an ancient Andean site. By integrating the results from multiple techniques, however, a detailed map was produced, allowing the team to make important inferences regarding the nature of the urban design at Las Colmenas, a neighbourhood of an early city. Put differently, in remote sensing, the whole is greater than the individual parts: each method contributes a unique set of information, helping archaeologists to produce more accurate and unambiguous visualizations of buried structures.

Which method should I choose? The answer obviously depends on the research goals. Researchers need to take into consideration the particular case study and environmental characteristics of the site, including the size and topography of the area, and the material of the archaeological features they wish to identify. That being said, given that no single remote sensing technique is suited for every archaeological context, it is recommended that researchers use a combination of techniques suited for a particular environment so that different datasets can be integrated into a composite map that includes as many features as possible.

6.1 Future research

Future investigations are necessary to validate our conclusions. By further studying the implementation of multiple remote sensing techniques at various sites with different geology and archaeological material, we can fully understand the benefits of an integrated remote sensing approach. Since different environments and archaeological features offer different characteristics that affect remote sensing analysis, it is necessary to continue integrated remote sensing projects within different environments.

One aspect which requires further investigation is the ideal time of day to conduct thermal UAV surveys to maximize data collection. The fact that some features were missed by the thermal surveys is most likely due to variations in thermal emissivity of different sized adobes. In this case, the goal would be to find the most optimal time of day to increase the number of features identified (the time when adobes have a heat signature that differs significantly from the surrounding soil)

The introduction and background chapter discussed the larger project directed by Jean-François Millaire at the Gallinazo Group. This project fits within this framework by documenting urbanization and the urban morphology of a suspected neighbourhood within this great city. The next step following this research project is to use the final map produced from the techniques implemented in this project (Figure 5.7E) to document various aspects of urban design, such as urban layout, patios, public spaces, ceremonial centers, and other elements of urban living. The analysis of these features will reveal

essential aspects of incipient urbanism, contributing to a greater understanding of the Gallinazo Group, and life on the north coast of Peru during the Early Intermediate Period.

References

- Annan, A. P.
2005 11. Ground-Penetrating Radar. *In* Near-surface geophysics. Dwain K. Butler, ed. Pp. 357–438. Investigations in geophysics, 13. Tulsa, Okla.: Society of Exploration Geophysicists.
- Aspinall, Arnold, Christopher F. Gaffney, and Armin Schmidt
2009 Magnetometry for archaeologists. Geophysical methods for archaeology, Volume 2. Lanham: AltaMira Press.
- Abu-Hamdeh, Nidal H. and Randall C. Reeder
2000 Soil Thermal Conductivity Effects of Density, Moisture, Salt Concentration, and Organic Matter. *Soil Science Society of America Journal*, 64(4):1285–1290.
- Bennett, Wendell
1939 Archaeology of the North coast of Peru; an account of exploration and excavation in Virú and Lambayeque valleys. *Anthropological papers of the AMNH*; v. 37, pt. 1: New York, American Museum of Natural History,
<http://digitallibrary.amnh.org/bitstream/2246/230/1/v2/dspace/ingest/pdfSource/ant/A037a01.pdf>.
- Bennett, Wendell C.
1950 The Gallinazo group, Virú Valley, Peru. New Haven Connecticut: Yale University Press.
- Campbell, James and Randolph Wynne
2011 Introduction to Remote Sensing, Fifth Edition. New York: Guilford Publications,
<http://gbv.ebib.com/patron/FullRecord.aspx?p=843851>.
- Capizzi, P., P. L. Cosentino, G. Fiandaca, R. Martorana, P. Messina, and S. Vassallo
2007 Geophysical investigations at the Himera archaeological site, northern Sicily. *Near Surface Geophysics*, 5(6):417–426.
- Casana, Jesse, Jason T. Herrmann, and Aaron Fogel
2008 Deep subsurface geophysical prospection at Tell Qarqur, Syria. *Archaeological Prospection*, 15(3):207–225.
- Casana, Jesse, Adam Wiewel, Autumn Cool, Austin Chad Hill, Kevin D. Fisher, and Elise J. Laugier
2017 Archaeological Aerial Thermography in Theory and Practice. *Advances in Archaeological Practice*, 5(4):310–327
- Clark, Anthony J.
2003 Seeing beneath the soil. Prospecting methods in archaeology. London: Routledge,
<http://search.ebscohost.com/login.aspx?direct=true&scope=site&db=nlebk&db=nlabk&AN=97390>.

Conyers, Lawrence B.

2009 Ground-Penetrating Radar. *In* Remote Sensing in Archaeology. An Explicitly North American Perspective. Jay K. Johnson, Marco Giardino, Kenneth L.

Kvamme, R. Berle Clay, Thomas J. Green, Rinita A. Dalan, Michael L. Hargrave, Bryan S. Haley, Jami J. Lockhart, Lewis Somers, and Lawrence B. Conyers, eds. Pp. 131–159. Tuscaloosa: University of Alabama Press.

2016 Interpreting ground-penetrating radar for archaeology. London: Routledge.

Daniels, David J.

2005 Ground Penetrating Radar. *In* Encyclopedia of RF and microwave engineering. Kai Chang, ed. P. 9. Hoboken, NJ: Wiley-Interscience.

Downey, Jordan T.

2014 Statecraft in the Virú Valley, Peru, in the First Millennium A.D. Ph.D., University of Western Ontario, London, Ontario.

Drahor, Mahmut G.

2006 Integrated geophysical studies in the upper part of Sardis archaeological site, Turkey. *Journal of Applied Geophysics*, 59(3):205–223.

Drahor, Mahmut G., Meriç A. Berge, Caner Öztürk, Nuray Alpaslan, and Gamze Ergene

2009 Integrated usage of geophysical prospection techniques in Höyük (tepe, tell)-type archaeological settlements. *ArchéoSciences*(33 (suppl.)):291–293.

Eppelbaum, Lev V., Boris E. Khesin, and Sonya E. Itkis

2001 Prompt magnetic investigations of archaeological remains in areas of infrastructure development: Israeli experience. *Archaeological Prospection*, 8(3):163–185

ESRI

2019 Stretch function—Help | Documentation. Electronic document, <https://desktop.arcgis.com/en/arcmap/latest/manage-data/raster-and-images/stretch-function.htm>, accessed March 24, 2020.

Federman, A., M. Santana Quintero, S. Kretz, J. Gregg, M. Lengies, C. Ouimet, and J. Laliberte

2017 UAV Photogrammetric Workflows: A Best Practice Guideline. *ISPRS - International Archives of the Photogrammetry, Remote Sensing and Spatial Information Sciences*, XLII-2/W5:237–244.

Fassbinder, J. W., H. Stanjek, and H. Vali

1990 Occurrence of magnetic bacteria in soil. *Nature*, 343(6254):161–163.

Fassbinder, Jörg W. E. and Tomasz H. Gorka

2011 Magnetometry near to the geomagnetic equator. *In* Archaeological Prospection. M. G. Drahor and Meric A. Berge, eds. Pp. 45–48. Izmir, Turkey: Archaeology and Art Publications.

- Fassbinder, Jörg W.E.
2015 Seeing beneath the farmland, steppe and desert soil: magnetic prospecting and soil magnetism. *Journal of Archaeological Science*, 56:85–95.
- Fiandaca, Gianluca
2010 The MYG methodology to carry out 3D Electrical Resistivity Tomography on media covered by vulnerable surfaces of artistic value. *Il Nuovo Cimento B*, 125(5-6):711–718.
- Fitzpatrick, R. W. and J. Le Roux
1975 Pedogenic and solid solution studies on iron-titanium minerals. *Proc. Int. Clay Conf*, 585:599.
- Fogel, Heidi
1993 *Settlements in Time: A study of Social and Political Development During the Gallinazo Occupation of the North coast of Peru*. Ph.D., Yale University, New Haven.
- Gaffney, Christopher F. and John A. Gater
2003 *Revealing the buried Past: Geophysics for Archaeologists*. Stroud, England: Tempus Publishing.
- Gaffney, V., H. Patterson, S. Piro, D. Goodman, and Y. Nishimura
2004 Multimethodological approach to study and characterize Forum Novum (Vescovio, central Italy). *Archaeological Prospection*, 11(4):201–212.
- Games, K. P.
1977 The magnitude of the palaeomagnetic field: A new nonthermal, nondetrital method using sun-dried bricks. *Geophysical journal of the Royal Astronomical Society*, 48:315–330.
- Graham, K. P. and I. Scollar
1976 Limitations on magnetic prospection in archaeology imposed by soil properties. *Archaeo-Physika*, 6:1–124.
- Hodgetts, Lisa, Peter Dawson, and Edward Eastaugh
2011 Archaeological magnetometry in an Arctic setting: a case study from Maguse Lake, Nunavut. *Journal of Archaeological Science*, 38(7):1754–1762.
- Hodgetts, Lisa, Jean-François Millaire, Edward Eastaugh, and Claude Chapdelaine
2016 The Untapped Potential of Magnetic Survey in the Identification of Precontact Archaeological Sites in Wooded Areas. *Advances in Archaeological Practice*, 4(1):41–54.
- Jensen, John R.
2005 *Introductory digital image processing. A remote sensing perspective*. Prentice Hall series in geographic information science. Upper Saddle River, NJ: Pearson/Prentice Hall.
- Johnson, Jay K., Marco Giardano, Kenneth L. Kvamme, R. B. Clay, Thomas J. Green, Rinita A. Dalan, Michael L. Hargrave, Bryan S. Haley, Jami J. Lockhart, Lewis

- Somers, and Lawrence B. Conyers, eds.
2009 *Remote Sensing in Archaeology. An Explicitly North American Perspective.* Tuscaloosa: University of Alabama Press.
- Khorram, Siamak, Frank H. Koch, Cynthia F. van der Wiele, and Stacy A.C. Nelson
2012 *Remote Sensing.* Springer Briefs in Space Development. s.l.: Springer-Verlag, <http://site.ebrary.com/lib/alltitles/docDetail.action?docID=10538824>.
- Le Borgne, E.
1955 Susceptibilite magnetique anormale du sol superficiel. *Annales de Geophysique*, 11:399–419.
1960 Influence du feu sur proprietes magnetique du sol et du granite. *Annales de Geophysique*, 16:159–195.
- Leucci, Giovanni, Lara de Giorgi, and Giuseppe Scardozzi
2014 Geophysical prospecting and remote sensing for the study of the San Rossore area in Pisa (Tuscany, Italy). *Journal of Archaeological Science*, 52:256–276.
- Lillesand, Thomas M. and Ralph W. Kiefer
1994 *Remote sensing and image interpretation.* New York: Wiley.
- Lillesand, Thomas M., Ralph W. Kiefer, and Jonathan W. Chipman
2015 *Remote sensing and image interpretation.* Hoboken: Wiley.
- Linford, N. T.
2004 Magnetic ghosts: mineral magnetic measurements on Roman and Anglo-Saxon graves. *Archaeological Prospection*, 11(3):167–180.
- Maher, Barbara A. and Reginald M. Taylor
1988 Formation of ultrafine-grained magnetite in soils. *Nature*, 336(6197):368–370.
- Maki, David
2005 Lightning strikes and prehistoric ovens: Determining the source of magnetic anomalies using techniques of environmental magnetism. *Geoarchaeology*, 20(5):449–459.
- Mastelic, Toni, Josip Lorincz, Ivan Ivandic, and Matea Boban
2020 Aerial Imagery Based on Commercial Flights as Remote Sensing Platform. *Sensors (Basel, Switzerland)*, 20(6).
- Millaire, Jean-François
2010 Primary State Formation in the Virú Valley, North coast of Peru, 107(14):6186–6191.
2020 Dating the occupation of Cerro Arena: A defensive Salinar-phase settlement in the Moche Valley, Peru. *Journal of Anthropological Archaeology*, 57:101142.
- Millaire, Jean-François and Edward Eastaugh
2011 Ancient urban morphology in the Virú Valley, Peru: Remote sensing work at the Gallinazo Group (100 B.C.–A.D. 700). *Journal of Field Archaeology*, 36(4):289–297.

- 2014 Geophysical Survey on the Coast of Peru: The Early Prehispanic City of Gallinazo Group in the Virú Valley. *Latin American Antiquity*, 25(03):239–255.
- Millaire, Jean-François, Kayla Golay Lausanne, and Edward Eastaugh
2018 Drone survey at the Gallinazo Group site in the Virú Valley, Peru: Reconstructing an ancient urbanscape through aerial photogrammetry and thermography. 58th Annual Meeting of the Institute of Andean Studies.
- Myers, J. W. and E. E. Myers
1995 Low-Altitude Photography. *American Journal of Archaeology*, 99:85–87.
- Nagata, Takesi
1971 Introductory notes on shock remanent magnetization and shock demagnetization of igneous rocks. *Pure and Applied Geophysics PAGEOPH*, 89(1):159–177.
- Nex, Francesco and Fabio Remondion
2014 UAV for 3D Mapping Applications: A Review. *Applied Geomatics*, 6(1):1–15.
- Nor, mm and N. B.M. Noor
2014 Urban morphology analysis by remote sensing and GIS technique, case study: Georgetown, Penang. *In 35th Asian Conference on Remote Sensing 2014, ACRS*.
- Olsen, Nils
2016 Earth's Magnetic Field. *In Space weather fundamentals*. Georgiæi Vladimirovich Khazanov, ed. Pp. 35–45. Boca Raton: CRC Press.
- Opdyke, Neil D. and James E.T. Channell
1996 Magnetization Processes and Magnetic Properties of Sediments. *In Magnetic stratigraphy*. Neil D. Opdyke and James E. T. Channell, eds. Pp. 26–48. International geophysics series, 64. San Diego: Academic Press.
- Powlesland, Dominic, James Lyall, Guy Hopkinson, Danny Donoghue, Maria Beck, Aidan Harte, and David Stott
2006 Beneath the sand—remote sensing, archaeology, aggregates and sustainability: a case study from Heslerton, the Vale of Pickering, North Yorkshire, UK. *Archaeological Prospection*, 13(4):291–299, <https://onlinelibrary.wiley.com/doi/pdf/10.1002/arp.297>.
- Richards, John A.
2013 Remote sensing digital image analysis. An introduction. Berlin: Springer, <http://site.ebrary.com/lib/alltitles/docDetail.action?docID=10656656>.
- Saarenketo, Timo
1998 Electrical properties of water in clay and silty soils. *Journal of Applied Geophysics*, 40(1-3):73–88.
- Schwertmann, U. and H. Fechter
1984 The Influence of Aluminum on Iron Oxides: XI. Aluminum-Substituted

- Maghemite in Soils and Its Formation. *Soil Science Society of America Journal*, 48(6):1462–1463.
- Schwertmann, U. and R. M. Taylor
1979 Natural and synthetic poorly crystallized lepidocrocite. *Clay Minerals*, 14(4):285–293.
- Sever, T. L.
1995 Remote Sensing. *American Journal of Archaeology*(99):83–84.
- Slater, Lee D. and David Lesmes
2002 IP interpretation in environmental investigations. *GEOPHYSICS*, 67(1):77–88.
- Smith, Michael E.
2007 Form and Meaning in the Earliest Cities: A New Approach to Ancient Urban Planning. *Journal of Planning History*, 6(1):3–47.
- Tikoo, Sonia M., Jérôme Gattacceca, Nicholas L. Swanson-Hysell, Benjamin P. Weiss, Clément Suavet, and Cécile Cournède
2015 Preservation and detectability of shock-induced magnetization. *Journal of Geophysical Research: Planets*, 120(9):1461–1475.
- Tite, M. S.
1972 The Influence of Geology on the Magnetic Susceptibility of Soils on Archaeological Sites. *Archaeometry*, 14(2):229–236.
- Tite M. S. and R. E. Linington
1975 Effect of climate on the magnetic susceptibility of soils. *Nature*, 256(5518):565–566.
- Tite M. S. and C. Mullins
1971 Enhancement of the Magnetic Susceptibility of soils on Archaeological Sites. *Archaeometry*, 13(2):209–219.
- Van der Marel, H. W.
1951 Gamma ferric oxide in sediments. *Journal of Sedimentary Petrology*, 21:12–21.
- Weston, D. G.
2002 Soil and susceptibility: aspects of thermally induced magnetism within the dynamic pedological system. *Archaeological Prospection*, 9(4):207–215.
2004 The influence of waterlogging and variations in pedology and ignition upon resultant susceptibilities: a series of laboratory reconstructions. *Archaeological Prospection*, 11(2):107–120
- Weymouth, John W.
1986 Geophysical Methods of Archaeological Site Surveying. *Advances in Archaeological Method and Theory*, 9:311–395.
- Willey, Gordon R.
1953 Prehistoric Settlement Patterns in the Virú Valley, Perú. *Smithsonian*

Institution Bureau of American Ethnology Bulletin, 155. Washington D.C.:
Smithsonian Institution

Wiltschko, R. and W. Wiltschko

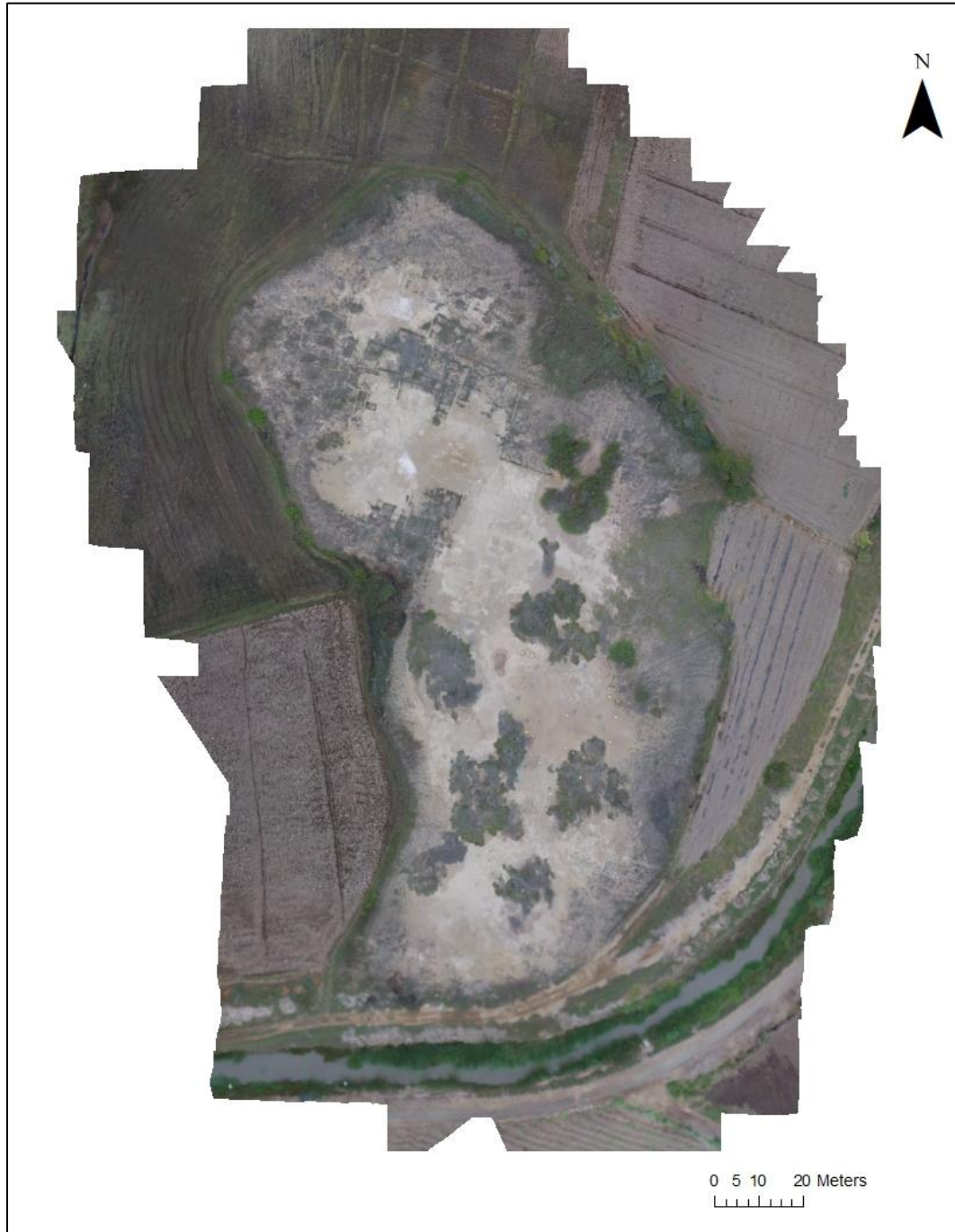
1995 Magnetic orientation in animals. *Zoophysiology*, v. 33. Berlin: Springer.

Winterbottom, S. J. and T. Dawson

2005 Airborne multi-spectral prospection for buried archaeology in mobile sand dominated systems. *Archaeological Prospection*, 12(4):205–219

Appendices

Appendix 1: Optical Survey 2018-14:20



Appendix 2: Optical Survey 2018-9:30



Appendix 3: Optical Survey 2019-14:30



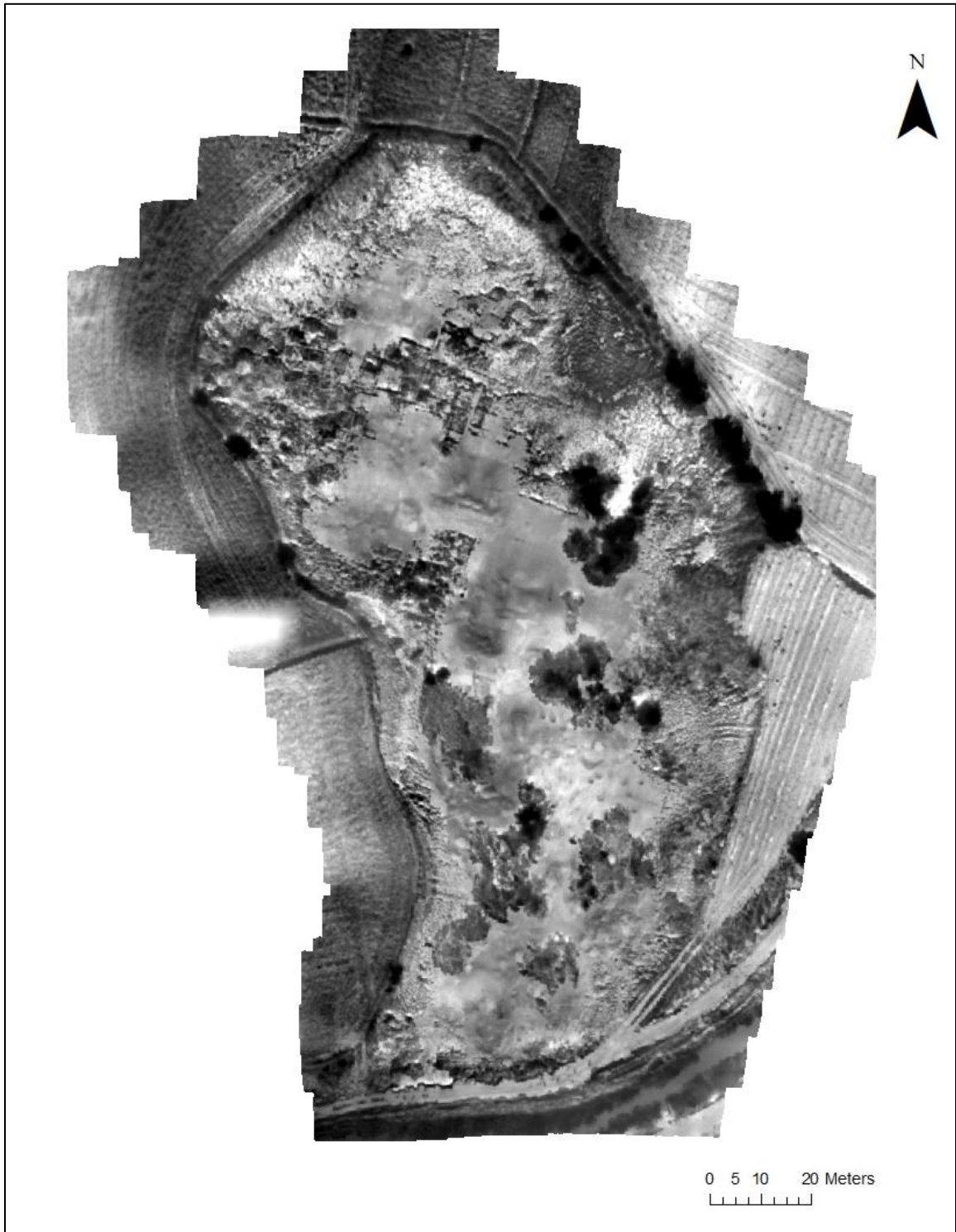
Appendix 4: Crops growing along buried walls, HP-1



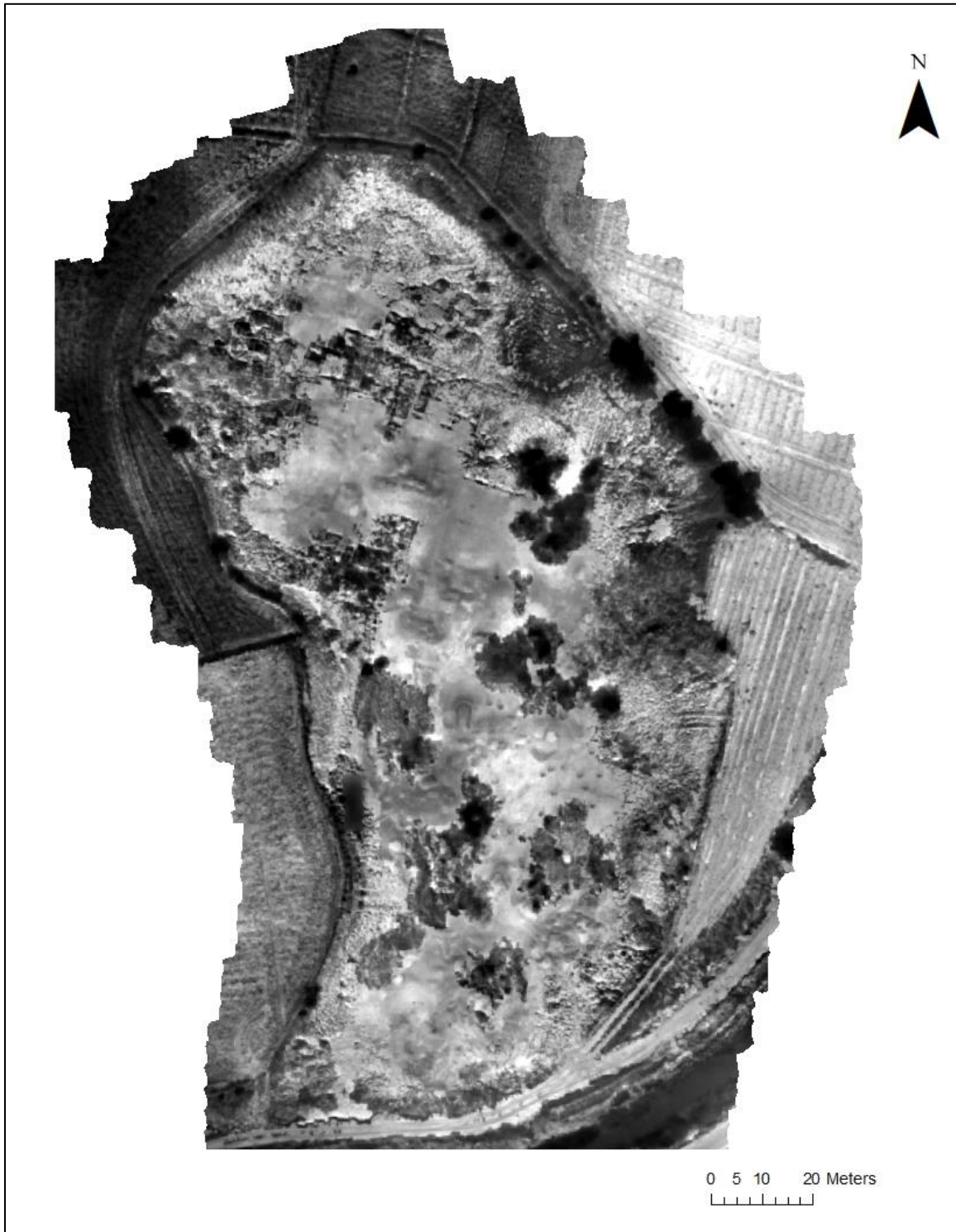
Appendix 5: Salt in the field beside Las Colmenas



Appendix 6: Thermal survey 2018-10:45



Appendix 7: Thermal survey 2018-13:00



Curriculum Vitae

Name: Kayla Golay Lausanne

Post-secondary Education and Degrees: University of Western Ontario
London, Ontario, Canada
2014-2018 B.A.

Honours and Awards

Social Science and Humanities Research Council (SSHRC)
Master's award
2018-2020

Province of Ontario Graduate Scholarship
2019-2020

Social Science and Humanities Research Council (SSHRC)
Doctoral Fellowship
2020-2023

Related Work Experience

Curatorial Assistant
University of Western Ontario
2016-2017

Archaeological Field Technician
Timmins Martelle Heritage Consultants
2017-2018

Research Assistant
University of Western Ontario
2017-2018

Research Assistant
University of Western Ontario
2018-2019

Teaching Assistant
University of Western Ontario
2019-2020

Publications:

Golay Lausanne K. (2018). Mapping the Invisible: Using aerial photogrammetry, thermography, and 3D modelling to map the urban structures of Las Colmenas. N/A. GIS Day, London, Canada, Conference Date: 2018/11 Poster

Golay Lausanne K. (2018). Geophysics on the Peruvian Coast -Locating Archaeological Structures with Geophysical Techniques. N/A. Western Anthropology Undergraduate Research Showcase, Conference Date: 2018/3 Poster

Millaire J, Golay Lausanne K, Eastaugh E. (2018). Drone survey at the Gallinazo Group site in the Virú Valley, Peru: Reconstructing an ancient urbanscape through aerial photogrammetry and thermography. 58th Annual Meeting of the Institute of Andean Studies. 58th Annual Meeting of the Institute of Andean Studies, Conference Date: 2018/1 Paper

Golay Lausanne K. (2019). The Gourds of Huaca Santa Clara. Millaire J, Downey J. Huaca Santa Clara: An Ancient Settlement in the Virú Valley. Submitted, American Museum of Natural History

Golay Lausanne K, Millaire J (2020). Understanding the Urban Devolvment of Las Colmenas through an Integrated Remote Sensing Approach. 60th Annual Meeting of the Institute of Andean Studies. 60th Annual Meeting of the Institute of Andean Studies, Conference Date: 2018/1 Paper